ISEL

INSTITUTO SUPERIOR DE ENGENHARIA DE LISBOA

ÁREA DEPARTAMENTAL DE ENGENHARIA QUÍMICA

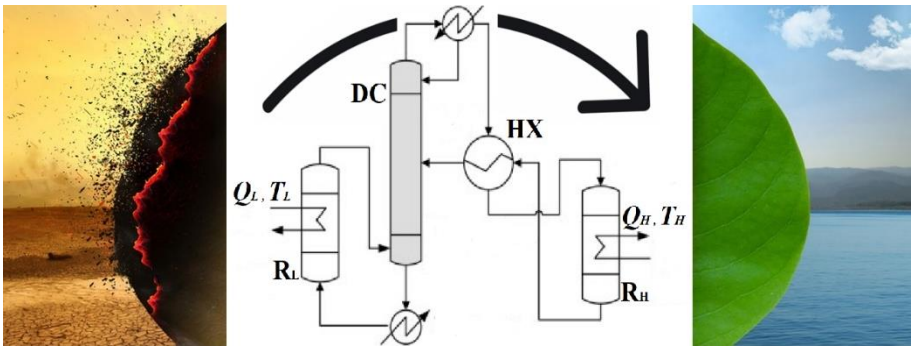

PROMOTING EXCESS HEAT USING CHEMICAL REACTIONS - CASE STUDY

LUIS ANTÓNIO PINELA DA SILVA

(Licenciado em Engenharia Química e Biológica)

Trabalho Final de Mestrado para obtenção do Grau de
Mestre em Engenharia Química e Biológica

Orientadores:

Professor Doutor João Miguel Alves da Silva
Professora Doutora Isabel Maria da Silva João

Júri:

Presidente:	Professor Doutor João Fernando Pereira Gomes
Vogais:	Professor Doutor José Valério do Nascimento Palmeira
	Professor Doutor João Miguel Alves da Silva

Julho de 2021

INSTITUTO SUPERIOR DE ENGENHARIA DE LISBOA

Área Departamental de Engenharia Química

PROMOTING EXCESS HEAT USING CHEMICAL REACTIONS - CASE STUDY

Luis António Pinela da Silva

Orientadores: Professor Doutor João Miguel Alves da Silva

Professora Doutora Isabel Maria da Silva João

Julho de 2021

Acknowledgments

I would like to thank my supervisors, Professor João Silva and Professor Isabel João, for their continued support throughout this work. Their guidance and feedback were instrumental in carrying out this work and their constructive criticism was invaluable in elevating the written document's quality.

To my family, who allowed me to pursue this MSc with a calm mind, my deepest appreciation for their comprehension, patience, and support.

And to my girlfriend, for all the moments I spent away, for all of the critical thinking moments where I made no sense, for all the times when I just needed to vent. For everything, my earnest and most heartfelt thank you!

Abstract

Heat recovery and promotion is an invaluable asset on the road to decarbonization and organic reaction chemical heat pumps present sufficient arguments to become a successful solution if proper politico-economic support and incentives are established. This technology's ability to recover low-temperature heat and promote it to usable temperatures allows savings regarding energy costs and significant decreases in greenhouse gas emissions.

This work focused on the study and optimization of the isopropanol/acetone/hydrogen (IAH) and the *tert*-butanol/isobutene/water (*t*B/iB) systems regarding their performance and economic competitiveness (EComp).

The main studies found that the IAH and the *t*B/iB systems reached performances of around 71% and 56%, respectively, however, their EComp left much to be desired. On this note, the IAH system underwent further experimentation focusing on i) the excess hydrogen in circulation, ii) the reactors' operating pressures, and iii) the use of a distillation column as the system's separation equipment. The first led to a decrease of 10% in the system's performance, but its EComp improved around 20%. The second did not alter the system's performance significantly, but resulted in an enhancement of its EComp by around 8%. The third resulted in an increase in the system's heat capacity, since the column's reboiler can be fed the same low-temperature heat as the endothermic reactor, which created a scenario for which the payback period can be determined. Unfortunately, the best value found was of 14 years, however, if implemented, this solution prevents the emission of approximately 7500 ton CO_2/year.

This work found that these systems are both technically and economically feasible, but suffer from poor economic performance. Despite this, their potential and relatively early stage of investigation should serve as motivation to improve upon this technology's existing foundations, whether through the catalysts employed, reactive distillation solutions, or the development of entirely new systems.

Keywords: Chemical heat pump, Reversible organic reactions, Excess-heat recovery and upgrade, Aspen HYSYS, Design of experiments, Isopropanol/Acetone/Hydrogen, *Tert*-butanol/Isobutene/Water, Enthalpy efficiency, Entransy efficiency, Economic analysis.

Resumo

A recuperação e promoção de excesso de calor é uma das áreas de investigação mais importantes da atualidade, dentro da qual as bombas de calor químicas exibem potencial no que toca à melhoria da eficiência energética de um vasto leque de indústrias e na prevenção da emissão de grandes quantidades de gases com efeito de estufa. Esta tecnologia tem o potencial de se tornar numa solução de sucesso se receber incentivos político-económicos adequados.

Além dos pontos mencionados, esta tecnologia apresenta ainda as vantagens de utilizarem quantidades desprezáveis de trabalho mecânico ou energia elétrica, as reações envolvidas poderem ocorrer a elevadas temperaturas e em maiores intervalos, ocuparem volumes relativamente pequenos, não carecerem de isolamento térmico significativo uma vez que a energia é armazenada nas ligações químicas, e da maioria dos sistemas existentes se basearem em reações bastante comuns e presentes em vários sectores industriais.

No que diz respeito ao funcionamento desta tecnologia, o esquema base é composto por um reator endotérmico, onde é fornecido calor de baixa temperatura para promover a reação endotérmica, e um reator exotérmico, onde é libertado calor de alta temperatura resultante da reação exotérmica. Além destes, é ainda utilizado algum equipamento de separação e um permutador de calor responsável por pré-aquecer a corrente de entrada do reator exotérmico.

Este trabalho propôs-se a estudar dois sistemas, o isopropanol/acetona/hidrogénio (IAH) e o *tert*-butanol/isobuteno/água (*t*B/iB), a nível de performance e competitividade económica.

A performance foi avaliada através da eficiência entálpica, dada pela *effectiveness*, e da eficiência entrópica, dada pela *entransy efficiency*. A competitividade económica dos sistemas em estudo foi determinada por comparação com o custo de utilização de gás natural para produção da mesma quantidade de calor de alta temperatura.

Os estudos principais deste trabalho foram realizados com recurso à metodologia de desenho de experiências que assenta na construção de um planeamento experimental, ou seja, a definição de uma estratégia que permite maximizar a aprendizagem sobre um qualquer sistema, minimizando, simultaneamente, os recursos necessários. Esta metodologia permite a identificação das interações existentes entre as diversas variáveis, algo fundamental uma vez que são inúmeras as situações em que os efeitos das interações se revelam mais relevantes do que os efeitos dos fatores individuais.

Começando pelo sistema IAH, o primeiro passo consistiu na construção do seu *flowsheet* no simulador de processos *Aspen HYSYS*, sendo que o resultado final se assemelhou bastante ao esquema genérico, com a exceção de que se utilizou um separador flash uma vez que que a diferença de temperatura entre os pontos de ebulição do isopropanol e da acetona o permite. Concluído este passo, foram identificados todos os fatores passíveis de manipulação e realizadas sete experiências.

As experiências realizadas produziram um volume significativo de informação, do qual se devem salientar as ações da temperatura de reação e da pressão de operação do reator endotérmico na capacidade do sistema para absorver calor de baixa temperatura, e da temperatura de reação do reator exotérmico na produção de calor de alta temperatura. Relativamente ao custo do sistema, é de destacar a influência, ainda que indireta, da pressão de operação do reator exotérmico sobre o compressor, equipamento de onde surgem as parcelas de custo mais significativas. O resultado final deste estudo consistiu na produção de uma solução capaz de atingir eficiências de aproximadamente 31% e 71% em termos entálpicos e entrópicos, respetivamente. No entanto, esta mesma solução é cerca de duas vezes mais cara que utilizar gás natural, sendo necessário continuar o estudo e otimização deste sistema.

O segundo estudo debruçou-se sobre a manipulação do excesso de hidrogénio em circulação no sistema através da comparação da situação base com três outros cenários. Como seria de esperar, a diminuição da quantidade de matéria em circulação levou a uma diminuição da performance do sistema e a um aumento da sua competitividade económica, pelo que se torna importante atingir um equilíbrio entre estes parâmetros. Aquela que se considerou como a melhor solução apresentou performances de 26% (entálpicas) e 61% (entrópica), no entanto, e apesar de se registar uma melhoria relativamente ao estudo base, esta solução é ainda cerca de 30% mais cara do que utilizar gás natural.

O terceiro estudo focou-se nas pressões de funcionamento de ambos os reatores. As grandes observações deste estudo foram que i) maiores pressões no reator endotérmico levam a melhores resultados em termos de custo e performance, mas piores a nível de capacidade energética e competitividade económica, e ii) maiores pressões a nível do reator exotérmico levam a melhores resultados em termos de performance e capacidade energética, mas piores a nível de custo e competitividade económica. Estes resultados levaram a que, tal como sucedido anteriormente, se procurasse atingir um equilíbrio entre as várias respostas, sendo que pressões de 2.1/2.2 atm ofereceram as soluções mais equilibradas.

O último estudo centrou-se no equipamento de separação utilizado. Como supramencionado, tem vindo a utilizar-se um separador flash, no entanto é interessante tentar perceber qual o efeito de utilização de uma coluna de destilação no seu lugar uma vez que, apesar do incremento de custo, a maior eficiência de separação, bem como o aumento da capacidade energética do sistema, podem conduzir a soluções mais competitivas. Como esperado, os resultados deste estudo revelaram um aumento do custo total do sistema, no entanto, o aumento da capacidade energética, efeito da absorção de calor de baixa temperatura por parte do ebulidor da coluna, levou ao surgimento de duas soluções cujo custo é inferior ao de utilizar gás natural, permitindo que se calcule o tempo de retorno de investimento das mesmas. Infelizmente, obtiveram-se valores muito elevados, 14 e 16 anos, respetivamente, para taxas internas de retorno muito baixas (3% e 5%), no entanto, é fundamental ressalvar que a melhor solução deste sistema é, ainda assim, muito prometedora, e capaz de evitar a emissão de cerca de 7500 ton CO_2/ano, uma quantidade extremamente significativa e que deve servir de inspiração e motivação para continuar os esforços de investigação que têm vindo a ser desenvolvidos sobre este sistema e outros que se lhe assemelhem. Relativamente à performance deste sistema, a utilização de uma coluna de destilação teve uma consequência bastante interessante, a maior eficiência energética da mesma levou a um aumento da eficiência entálpica, para cerca de 38%, mas a maior entropia, natural deste equipamento, levou a uma diminuição da eficiência entrópica, para cerca de 54%.

Passando ao sistema *t*B/iB, a formação de um azeótropo binário entre o *tert*-butanol e a água levou a que fosse necessário adicionar uma coluna de destilação azeotrópica e um pré-concentrador ao esquema base, o que aumentou significativamente a complexidade do seu *flowsheet*. Assim como no caso anterior, identificaram-se todas as variáveis passíveis de otimização e procedeu-se à realização de cinco experiências baseadas em planeamentos experimentais de diferentes *designs*.

Para este sistema, além de se salientar novamente a influência da pressão de funcionamento do reator exotérmico sobre o custo, é ainda de assinalar o aumento dos custos relacionados com utilidades, consequência do maior número de equipamentos existentes no processo. Relativamente à sua performance, é interessante assinalar a existência de valores superiores a 100%. Esta aparente impossibilidade advém do facto de uma das equações utilizadas no cálculo da *effectiveness* não considerar a entrada de calor de baixa temperatura através do ebulidor da coluna. Sintetizando, o estudo deste sistema produziu informação muito semelhante ao estudo do primeiro sistema, até em termos de competitividade económica, sendo que a melhor solução obtida após este primeiro estudo é também cerca de duas vezes

mais cara que utilizar gás natural. Já a sua performance entrópica é ligeiramente superior à do primeiro sistema, registando um valor de cerca de 56%.

O segundo estudo abordou as pressões de funcionamento de ambos os reatores. Este foi muito claro no que tocou à identificação das melhores condições, no entanto estas originaram uma solução apenas marginalmente melhor que a obtida a partir do estudo base (apresentou uma performance de cerca de 58%), sendo que a sua competitividade económica relativamente à utilização de gás natural regista uma melhoria de apenas 1% relativamente à solução encontrada anteriormente.

Este trabalho mostrou que é possível otimizar significativamente o sistema IAH. Ademais, verificou-se que os estudos focados no excesso de hidrogénio em circulação e na utilização da coluna de destilação foram os que mais impactaram a sua competitividade económica.

O futuro desta tecnologia passará pelo desenvolvimento dos catalisadores utilizados e pela investigação de soluções baseadas em destilação reativa, sendo que o desenvolvimento e aplicação de novos sistemas deve ser uma constante.

Palavras-chave: Bomba de calor química, Reações orgânicas reversíveis, Recuperação e promoção de excesso de calor, *Aspen HYSYS*, Desenho de experiências, Isopropanol/Acetona/Hidrogénio, *Tert*-butanol/Isobuteno/Água, Eficiência entálpicas, Eficiência entrópica, Análise económica.

List of Abbreviations

ACF	Accumulated Cash Flow
ADC	Azeotropic Distillation Column
AGT	Average Global Temperature
AHP	Absorption Heat Pump
ANOVA	Analysis of Variance
APEA	Aspen Process Economic Analyzer
Bz/Cy	Benzene/Cyclohexane/Hydrogen system
C&P	Chemical & Petrochemical industrial sector
CC	Composite Curves
CCS	Carbon Capture and Storage
CH_4	Methane
CHP	Chemical Heat Pump
CHP_{Ccost}	Chemical Heat Pump system's capital cost
CHP_{Ocost}	Chemical Heat Pump system's operating cost
CHP_{Tcost}	Chemical Heat Pump system's total cost
CO_2	Carbon Dioxide
CT	Carbon Tax
DE	Designed Experiments
DF	Degrees of Freedom
DoE	Design of Experiments
EComp	Economic Competitiveness
ECst	Excess Cost
EHP	Excess-Heat Potential
EU	European Union
FB&T	Food, Beverage & Tobacco industrial sector
FE	Factorial Experiments
FFD	Fractional Factorial Design

FS	Flash Separator
GCC	Grand Composite Curves
GHG	Greenhouse Gas
GWP	Global Warming Potential
HEN	Heat Exchanger Network
HP	Heat Pump
IAH	Isopropanol/Acetone/Hydrogen system
JRC	Joint Research Centre
MHP	Mechanical Heat Pump
MS	Mean Square
NM	Non-metallic Minerals industrial sector
N_2O	Nitrous Oxide
NG	Natural Gas
NG_{cost}	Natural Gas' acquisition cost
ORC	Organic Rankine Cycle
ORCHP	Organic Reaction Chemical Heat Pump
PM	Primary Metals industrial sector
PP&P	Paper, Pulp & Printing industrial sector
PA	Pinch Analysis
PCA	Paris Climate Agreement
R&D	Research & Development
RA	Residual Analysis
RSM	Response Surface Model
SA	Sensitivity Analysis
SAsc	Steepest Ascent
SDsc	Steepest Descent
SS	Sum of Squares
*t*B/*i*B	*tert*-Butanol/Isobutene/Water system
TES	Thermal Energy Storage
UCF	Updated Cash Flow

UK	United Kingdom
VCHP	Vapor Compression Heat Pump
WHP	Waste-Heat Potential
WHO	World Health Organization
YCF	Yearly Cash Flow

Symbols

ΔH	Reaction Enthalpy/Heat		
ΔT_{min}	Minimum Temperature Approach		
C	Concentration		
DC	Distillation Column		
E_a	Activation Energy		
e	Residuals		
ϵ	Random error component		
G*	Entransy Efficiency		
HX	Heat Exchanger		
K	Adsorption Equilibrium Constant		
K_0	Pre-exponential Factor for K		
K_C	Chemical Equilibrium constant		
k	Rate constant		
k_0	Pre-exponential Factor for k		
P	Pressure		
Q_H	High-temperature heat		
Q_L	Low-temperature heat		
Q_R	Heat supplied to the reboiler		
R	Ideal Gas constant (= 8.314)	$[J\ mol^{-1}\ K^{-1}]$	
R_H	Exothermic reactor		
R_L	Endothermic reactor		
r	Reaction Rate		
T	Temperature	[K], unless otherwise specified	

T_0	Ambient temperature
T_C	Condenser temperature
T_H	High temperature
T_L	Low temperature
T_R	Reboiler temperature
y	Response's experimental value
$\hat{y}$	Response's estimated value

Greek symbols

E	Exergy
η	Enthalpy efficiency
η_{max}	Maximum theoretical enthalpy efficiency
η (ε)	Exergy efficiency
ξ	Effectiveness

Subscripts

A	Acetone
dH	Dehydrogenation
dW	Dehydration
E	Error
Evap	Evaporator
Gen	Generator
H	Hydrogen
hH	Hydrogenation
hW	Hydration
iB	Isobutene
NS	Non-significant
*t*B	*tert*-Butanol
W	Water

Index

List of Figures

List of Tables

I – INTRODUCTION

1. Energy, Greenhouse gases, and Climate change

Earth. ”Our” little blue marble in the middle of nowhere has been home to the human race since our first ancestors, and though we may look towards the stars in search of a solution to the over-population, over-extraction, over-consumption, and general over-indulgence in this planet’s finite resources, which undoubtedly pushed us towards the climate-shifting, global fauna/flora threatening and potentially devastating reality that we live in today, one thing is certain, our species’ only path to salvation is to nurse the environment that surrounds us back to full health in a straightforward manner, as swiftly and aggressively as possible!

The main driver behind our planet’s climate predicament is the massive amounts of carbon dioxide (CO_2) and other greenhouse gases (GHG), such as methane (CH_4) and nitrous oxide (N_2O), released to the atmosphere every year. Atmospheric CO_2 concentrations prior to the industrial revolution were about 280 ppm.[1–5] Recent data shows an increase of about 45% to a concentration close to 410 ppm.[6–8] This is, by far, the highest value of the last 800,000 years, and, quite possibly, of the last 20 million years.[3,8–10] Although GHG emissions have slowed, this did not occur naturally and was only possible through a large effort to shift toward less carbon-intensive technologies and activities.[11] This is easily proven when one compares the renewable energy share in 2018 and 2019’s energy mixes (18% and 19.7%, respectively) *versus* 2004’s (8.5%).[12,13] Despite this decrease, these abnormally high atmospheric GHG concentrations still result in a series of problems, some very well-know, such as atmospheric pollution and global warming,[14,15] some undoubtedly less visible, such as ocean acidification,[3,6,8] and others that may not be immediately linked to bigger problems, such as a higher intensity and frequency in wildfires, floods, droughts, storms, etc.[16,17] The increasingly more severe, and frequent, “natural” disasters, all reaching sizes never seen prior to the last decade, undeniably caused by the large, and fundamentally unsustainable, anthropogenic development of the past 250 years, result in progressively heavier capital cost and human life endangerment. Floods, wildfires, storms, and droughts were responsible for 93% of the $ 131.7 billion lost worldwide in 2018 alone![18] These 4 categories were also responsible for 94% of the 68.5 million people affected that year.[18] In addition to this, a World Health Organization (WHO) report found that air pollution was responsible for the death of 7 million people worldwide in 2012.[19]

Perhaps the most well-known metric, the average global temperature (AGT) is used worldwide on all levels of discussion and decision-making, however, it is important to understand that behavioral changes that may lead to an AGT variation will only result in such after many years,

mostly due to our planet's size and the complex heat transfer mechanisms involved. This delay between our actions and their consequences should only intensify our pursuit for greater and faster decarbonization, especially considering that end-of-century projections indicate an atmospheric CO_2 concentration of 800 ppm[3] and a global warming trend upwards of 3 °C.[20,21] 2015's Paris Climate Agreement's (PCA) most important objective consists of "Holding the increase in the global average temperature to well below 2 °C above pre-industrial levels and pursuing efforts to limit the temperature increase to 1.5 °C above pre-industrial levels".[20,22–27] Well, recent data shows that global warming is already at the halfway point (1.0 °C) of its least ambitious goal,[28] with Europe already registering a 1.6 °C increase.[29] To further emphasize what is at stake, past ice ages were triggered by changes of only 6/7 °C.[30]

While many nations have developed strong political and economic efforts towards the reduction of GHG emissions, be it through a shift towards a greater renewable energy share in the overall mix, or the development and deployment of carbon capture and storage (CCS), and other atmospheric CO_2 abatement technologies (*e.g.* afforestation), the truth is that there is only one path capable of leading to PCA's goals, and that is to focus, and rely, not only on one type, or family, of technologies, but on the synergistic effect only attainable through the implementation of a wide scope of solutions. In addition to environmental and energy-focused measures, a greater incorporation of sustainable development practices within countries and the industries therein will surely also contribute towards a greener and brighter future. On a side note, this need for several, fundamentally different, strategies, which target different areas of operation, while aiming for a singular goal, should be more than enough to give even the most inexperienced reader a good sense of the urgency, and magnitude of the problem(s) at hand.

Given the world's current state, there is one absolute certainty, the world must turn away from raw energy consumption, intensifying its focus on efficient utilization and recovery/reuse as the industrialized nations find it increasingly arduous to maintain their past rates of energy consumption, both due to the rising prices of fossil fuels and to the critical levels of greenhouse gas emissions.[31–33] Well, this work's focus, excess-heat recovery and upgrade, opens up an interesting and exciting path in terms of addressing the problems presented above. Seeing as how most GHG emissions originate from energy production and consumption,[34] a technology capable of "recycling" energy is extremely appealing to industries worldwide, including food and beverages, paper and pulp, and chemical and petrochemical.[35,36]

By recovering, and reusing, energy that would otherwise be wasted, a chemical process, for instance, is able to reduce their primary energy consumption, decreasing the expense with energy acquisition,[37,38] can improve its overall energy efficiency,[38,39] given the amount of

energy used per unit input will be higher, will reduce its GHG emissions and their associated overhead costs (regarding environmental taxes, for example),[36,37] among other improvements. Adding to these benefits and given the current political status observed throughout the world, an excess heat recovery approach may just be what companies and industries need in order to meet the intense and ever-pressing eco-friendly demands of government and public alike, and may result in decreased energy demand and CO_2 emissions, and, perhaps most importantly, an economic gain from decreased expenses. These aspects highlight the excess heat's potential and they do not include considerations regarding cooperative implementation, which will only augment existing arguments in favor of its development and implementation, both in number and in strength.

2. Heat recovery towards carbon neutrality

Industrial excess-heat recovery, often referred as waste-heat[a] recovery in the literature, represents one of the most valuable research topics in energy utilization,[40,41] on par with improving the overall energy efficiency.[42] It is well-known that sizeable amounts of thermal energy are released to the environment as low-temperature excess heat, mainly in the forms of water or gas, at temperatures that range from the ambient to around 200 °C, however, this low-grade heat must be upgraded to useful thermal levels before it can reused.[31,43–47] Thus, it has been recognized that efficient use, through retrieval and regeneration, of excess-heat generated from conventional energy sources should be seriously considered in parallel with the development of new and alternative energy sources.[44] Moreover, the recovery and reuse of excess-heat is of paramount importance to such an extent that it is almost impossible to improve the energetic efficiency of industries around the globe, and, consequently, of the overall productive system, until an economic energy upgrading solution allows for the recovery of this enormous quantity of energy, thus reinforcing the global significance associated with the development and implementation of the technology necessary to achieve the aforementioned heat recovery.[42,43,45] In addition to improving the energy-efficiency associated with all types of industries, the recovery of low-grade excess-heat may introduce new and exciting possibilities regarding the integration between district energy infrastructures and nearby industrial energy systems.[42,48–50]

[a] The term waste-heat will be herein replaced by excess-heat to highlight the need to take advantage of this energy source, and not consider it as waste.

Adopting innovative and advanced systems, such as chemical heat pumps (CHPs), organic rankine cycles (ORCs), among others, to upgrade low-temperature heat to more useful levels (*i.e.* higher temperatures), can provide considerable energy savings, efficiency increase, and greenhouse gas emissions reductions in several industries, solely from fossil fuel displacement.[47,51–53] Papapetrou *et al.* found that there is an estimated 300 TWh/year waste-heat potential (WHP; hereafter referred to as excess heat potential (EHP)) in Europe, with close to 33% of this heat corresponding to temperatures below 200 °C, *i.e.* low-temperature excess heat.[54] Kosmadakis also estimated the EHP in Europe, with a focus towards two specific temperature bands (100 – 150 °C and 150 – 200 °C), in which he determined these bands' total potential to be of about 21 TWh/year.[55] A preliminary study by Panayiotou *et al.* estimated the theoretical and applicable, or Carnot, EHP in Europe to be about 370 and 175 TWh/year, respectively.[56] This study was built upon by Bianchi *et al.* who, using the same methodology, but through higher data accuracy, obtained EHP values of 920 TWh/year (theoretical) and 279 TWh/year (Carnot's), with low-temperature (<200 °C) heat comprising 51.1% (*i.e.* ~470 TWh/year) and 23.2% (*i.e.* ~65 TWh/year), respectively.[57] Moving from Europe to a global frame, Forman *et al.* estimated the total theoretical, and Carnot, excess heat potentials to be about 68 and 13 PWh/year, respectively. Of these, low-temperature heat represents 60% and 21%, respectively.[58] These shares of low-temperature heat are roughly the same as those obtained by Bianchi *et al.*, which is to be expected considering that the latter utilized the methodology developed by the former. Although encouraging toward the present work, the studies presented are all relatively outdated, which is why it was decided to conduct a relatively simple update utilizing the most recent data available (2018) pertaining to the European Union (EU). Applying the methodology presented in the work of Papapetrou *et al.*,[54] while also updating the terms that needed such attention, in conjunction with Eurostat's "Energy data – 2020 edition" statistical book,[59] which collects and presents data concerning the calendar year of 2018, an EHP of nearly 1250 PJ (about 347 TWh/year) was obtained, of which about 60% (approximately 735 PJ, or around 204 TWh/year) corresponds to low-temperature heat.

Even though the existence of excess-heat is undeniable and its properties are well-documented (temperature at which it occurs and amount available), its recovery is only as interesting as it is feasible, which is why such a line of work is extremely pertinent to the present work. Therefore, it is important to bring attention to the works of Karaca *et al.*,[60] Spoelstra *et al.*,[61] Ajah *et al.*,[62] Demir *et al.*,[63] and Xu *et al.*,[64] who conducted economic analysis, mostly concerning the isopropanol-acetone-hydrogen (IAH) system, having found that this system is both technically and economically feasible, given that sufficient excess-heat is available, and more suitable for greater high-temperature heat duties.

Several studies have found that excess-heat recovery leads to an energy efficiency increase,[65,66] GHG emissions reduction,[51] among other very beneficial findings. Aside from the conventional industrial low-grade heat, other sources, such as renewable energies, can also be harnessed. This point becomes even more important considering their falling prices, which, associated with the surge registered for crude oil, results in an increase in the attractiveness associated with energy efficiency through a higher focus on clean energy sources, which may explain the growth in eco-friendly investments that many firms have adopted.[67,68] Apart from the obvious economic advantages presented by the recovery of excess-heat, there are also some environmental benefits that must not be disregarded given the current state of affairs on our planet, such as a decrease in harmful emissions from the consumption of primary fuels.[51,52]

3. Thesis goals

Heat recovery and promotion has the potential to be one of our societies' cornerstones on the road to the much ambitioned, and even more needed, carbon neutrality. Thus, this work entails several objectives within a larger goal of determining whether or not these solutions prove themselves capable of attaining economically competitive levels.

First, it is important to identify chemical systems capable of carrying out the desired heat recovery/promotion, as well as their main operating conditions, namely the heat input/output temperatures.

Second, it is necessary to design and build the system within the simulation software. This process, alongside the system's optimization, conducted through design of experiments, will allow the identification of the main challenges involved in its operation, as well as each equipment's sensitivity.

Lastly, it is absolutely paramount to evaluate the various solutions' economic competitiveness (EComp) through their comparison with one another and, more importantly, with existing, conventional solutions.

4. Thesis outline

Chapter I – INTRODUCTION: The current chapter briefly introduce the great environmental problematic that afflicts the world, which coincides with the author's motivation, and how the technology in discussion may play a key role in improving our current predicament. It also presents the work's goals and overall structure adopted for the present document.

Chapter II – HEAT PUMPS: This chapter presents a brief overview of the history of heat pumps and how these operate, how their performance is assessed, and where they may be implemented, as well as the criteria to consider in an implementation study.

Chapter III – DESIGN OF EXPERIMENTS: This chapter concerns itself with the process of designing successful experiments and how the resulting data should be processed and analyzed.

Chapter IV – STEADY STATE SIMULATION AND OPTIMIZATION: This chapter explains the systems' assembly in the simulation software and follows the optimization path chosen for each system in great detail.

Chapter V – CONCLUSIONS AND FUTURE WORK: This chapter condenses the knowledge acquired throughout this work, discusses the technology's potential, and presents some likely paths for further investigation.

The last two chapters present this work's REFERENCES and APPENDICES, from which Appendix G should be highlighted. This appendix contains the abstract[69] accepted for the 24th International Congress of Chemical and Process Engineering, CHISA 2021 Virtually, where this work was presented in the form of an oral communication. Furthermore, said presentation was selected be submitted as a paper in the congress' special issue Chemical Engineering & Technology and is currently pending acceptance.[70]

II – HEAT PUMPS

5. A brief history of heat pumps

Given the massive amounts of low-temperature excess-heat available in almost every industrial sector (chemical and petrochemical, food and beverage, pulp and paper, among others), it comes with no surprise that devices for its recovery and reuse were heavily investigated and developed. Today, these systems are known as heat pumps (HPs).

Although there are several classifications, the two main groups into which we can separate these systems are the mechanical and chemical heat pumps. Despite fulfilling the same role, the mechanisms adopted are what distinguishes them. Whereas mechanical heat pumps (MHPs) rely on the input of mechanical work to achieve the desired outcome,[71] CHPs only require thermal energy to achieve the same exact outcome. Even though these can improve the overall energy efficiency in a given industrial process, their capital and operation costs should always be taken into consideration, as with any other investment,[72] in order to meet any situation with the solution that best suits both those with a direct interest and the world around us.

Regarding MHPs, it is important to note that, even nowadays, the most advanced solutions can only deliver upgraded thermal energy at a maximum of 110 °C, which is too low for most existing industrial requests.[43,45] As such, new devices are necessary. Among them, the CHP presented itself as an attractive alternative that can recover low-level thermal energy for different purposes, such as heating, cooling, and storage/transportation, as well as heat upgrading.[43,44] It is interesting to note that the idea behind these CHP systems can be traced to the 19th century (1824, to be precise), when the English scientist Michael Faraday suggested the development of a refrigerating unit based on a reaction between NH_3 and AgCl.[73,74]

Although the proposal of novel organic CHP systems for heat upgrading can be traced to 1980/1987 (IAH system first proposed by Prévost *et al.* in 1980,[75,76] but worked upon and advanced by Saito *et al.*, in 1987)[76,77] and 1991 (*tert*-butanol/isobutene/water (*t*B/*i*B) system proposed by Kato *et al.*),[78–80] to state a few, some earlier studies, which focused on relatively simple reactions, such as the EVA-ADAMS pair and some inorganic reaction sets, had already begun making use of, and developing, the core principles that underline all these systems, both for the storage of solar[74,81] and recovery of low-level industrial[31] thermal energy.

Focusing now on the CHP, this type of system can upgrade heat from various sources (industrial, solar, geothermal, among others), to higher temperatures by taking advantage of reversible coupled endo-exothermic chemical reaction cycles, with the added benefits of requiring almost no mechanical work or electrical energy inputs.[31,44,45,71,82] Apart from these economical and technical advantages, the chemical reactions used in these systems can also occur in a much higher and broader temperature range, which allows for a higher flexibility and adaptability to the operating conditions necessary to meet user requests.[41,83]

As aforementioned, CHPs rely on reversible chemical reactions, meaning the energy is stored in the chemical bond, allowing for its release when needed. Because of this, the chemical species involved can be easily stored without heavy insulation, since there aren't any significant heat losses due to temperature differences with the environment.[38,44,84] In addition, owing to the much greater energy density in the working media, when compared with other types of heat pumps, the system's volume will be particularly small (when considering similar heat capacity values), a characteristic that becomes very important when spatial and/or transportation considerations arise.[43] Both these features contribute heavily for the reduction of the solution's total cost. Another strong point in favor of these heat pumps is the fact that most potentially exploitable reactions are fairly common in the commercial chemical industries.[73]

All the advantages associated with CHPs resulted in a heightened attentiveness by the scientific community, especially areas concerning energy research and management, which translated into an increase in literature works (papers published, patents registered, etc.) related to the world of CHPs (figure 1), whether they focus on system design, performance assessment, catalytic studies, or other, more specific, areas of study.

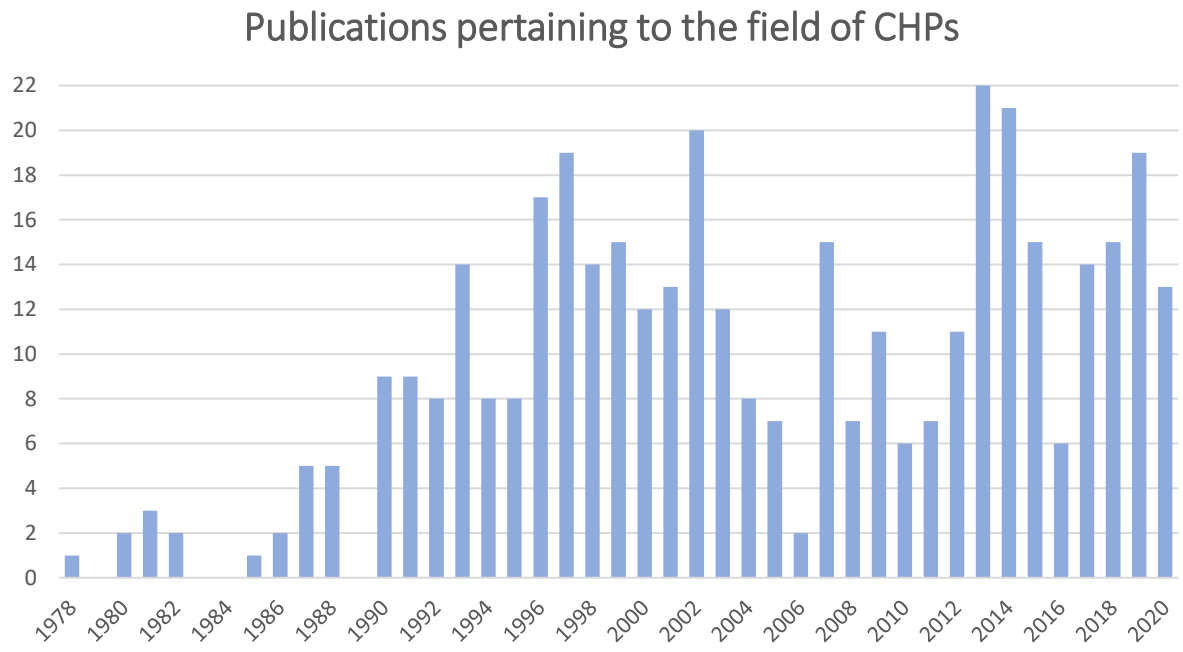

Figure 1 - Publication trend for CHPs over the years
[Source: Author's elaboration from data obtained through the Web of Science[b]]

As can be seen in figure 1, the number of publications grew considerably in the 90's and, even though the annual values may fluctuate, the last three decades have registered almost the same total number of publications each, which indicates a firm investigation effort regarding the topic of CHPs and all their operating details.

[b] Web of Science: https://www.webofknowledge.com/
[b] Keywords: "Chemical Heat Pump" OR Reversible Reaction Chemical Heat Pump, excluding 2021

6. Major systems and working principles

This section aims to provide a short yet broad review of the existing heat pump systems and their working principles so that later analysis and discussion can be made upon the basis of this knowledge.

6.1. Mechanical heat pumps

The first, and therefore oldest and most well-known, type of system employed in heat recovery is the MHP (also known as vapor compression heat pump, VCHP).[43,85] This system's operation is based on a pressurization/decompression cycle in which a working fluid, commonly known as refrigerant, flows between an evaporator, to which the low-temperature heat is fed, and a condenser, from which the high-temperature heat is recovered (figure 2).[51,53,86–88] The fluid circulation mentioned above is carried out through the action of a compressor, which produces mechanical/shaft work from an energy input, usually in the form of electricity.[42,53,89]

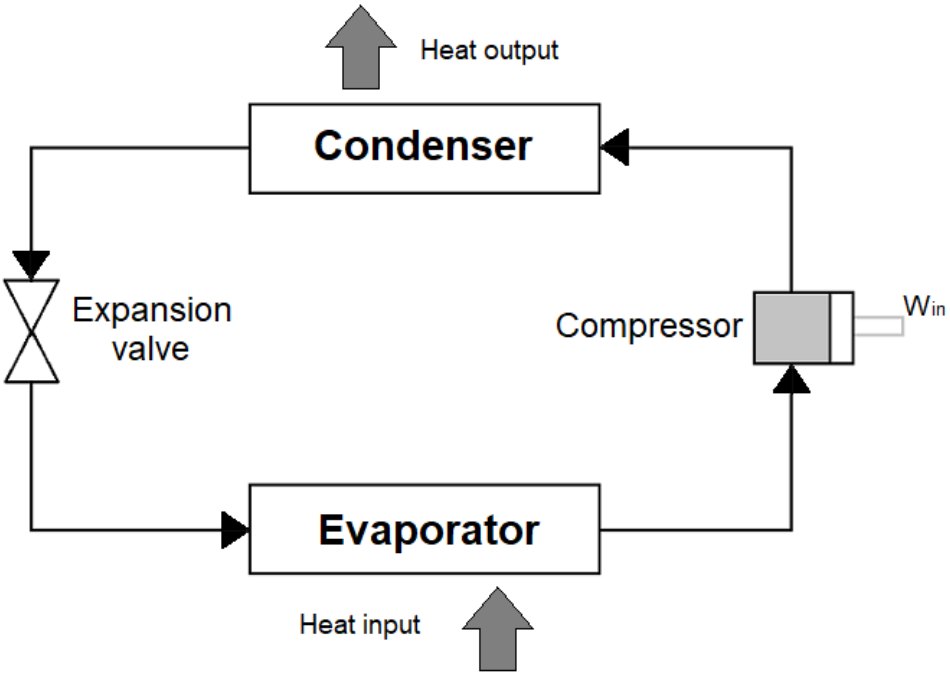

Figure 2 - Mechanical heat pump [Author's elaboration]

Besides relying on a high-quality electrical input to function, MHPs also suffer from high costs (capital and operating) and low efficiencies.[42,44,85,86,89] These also present environmental disadvantages, such as the use of refrigerants whose Global Warming Potential (GWP) values cannot be disregarded given that, even though there have been considerable efforts in developing new working substances with reduced GWP values, an operation based on a phase change of the working fluid, as is the case, increases the chances of gas leaks to the atmosphere, meaning this parameter must always be taken into consideration.[44,53,79,90]

6.2. Chemical heat pumps

CHP systems can be divided in distinct categories depending on the working fluids, operation mode and purpose (table 1), among others. Given this subject's extensive scope, this work will focus its efforts on the study of two continuous, liquid-gas, heat upgrading systems: the isopropanol/acetone/hydrogen system, and the *tert*-butanol/isobutene/water system.

Although the systems listed above will garner the entirety of this work's practical focus, it is significant to understand the other system types' operations, as well as their similarities and differences, which is why each shall be lightly reviewed before addressing this work's main topic, the organic reaction chemical heat pumps (ORCHPs).

Table 1 - Some CHP classifications[91,92]

Chemical Heat Pumps (CHPs)		
Working fluids	**Operation mode**	**Solution purpose**
➢ Solid-Gas	➢ Batch	➢ Immediate upgrade
➢ Liquid-Gas	➢ Continuous	➢ Storage/transportation

6.2.1. Solid-Gas (adsorption) systems

To facilitate the reader's comprehension on the topic, the first system to address shall be the solid-gas. Being part of the CHP family, these utilize reversible endo-exothermic reactions, however these occur between a gas and a solid, usually a salt, inside a single reactor. This unit also comprises a condenser-evaporator.[71] These systems may also utilize metal hydrides which operate through the adsorption/desorption of hydrogen. Apart from a CHP-oriented operation, these systems can manage large amounts of hydrogen gas, meaning their potential as hydrogen storage is very noteworthy.[91]

It is important to note that this system is not suitable for continuous operation as it utilizes two distinct sequential phases, both occurring within the same equipment, as illustrated in figure 3.[91,93]

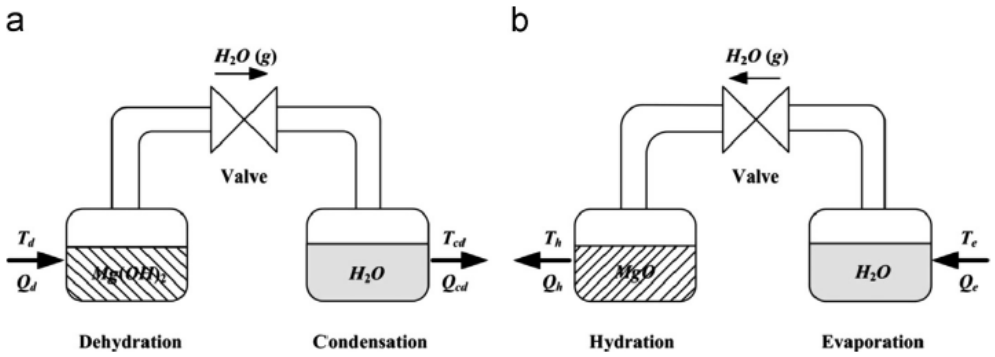

Figure 3 - Solid-Gas heat pump (a – decomposition; b – heat production)[93]

6.2.2. Liquid-Gas (absorption) systems

Next, we will address the liquid-gas absorption system, also known as absorption heat pumps (AHPs). This type of CHP can operate in two distinct modes, depending on the desired output: cold/heat production at low/mid temperatures (heat pump) or heat upgrading to higher temperature (heat transformer).[91,94] Contrarily to other CHPs, these are not based on the existence of chemical reactions, relying instead on absorption phenomena.

6.2.2.1. Heat pump mode

Before addressing this system's operation, it is interesting to take a closer look at figure 4 and note that these heat pumps can be designed to supply either heating or cooling.[33,94]

Focusing on this system's cycle, the working fluid circulates in a closed-loop solution circuit consisting of a generator, an absorber, a solution pump, an expansion valve, and, in most cases, an economizer, and its compression is considered to be achieved by thermal means since the mechanical input through the pump is negligible when compared to th high-grade energy input through the generator. and. Low-grade heat is provided to the evaporator where the working fluid is evaporated at low-pressure, which is then absorbed by the absorbent, generating heat at medium temperature. The resulting solution is then pumped to the generator, which functions at a higher pressure, where the working fluid (or absorbate) is boiled off through the supply of external high-temperature heat. The working fluid is then condensed and the absorbent passes through the expansion valve and returns to the absorber. The economizer helps the recovery of heat from the absorbate poor stream. The mechanical energy input is negligible when compared with the high-grade energy fed to the generator. The most common working pair for this type of system is water (absorbate) and lithium bromide (absorbent).[51,87,94–98]

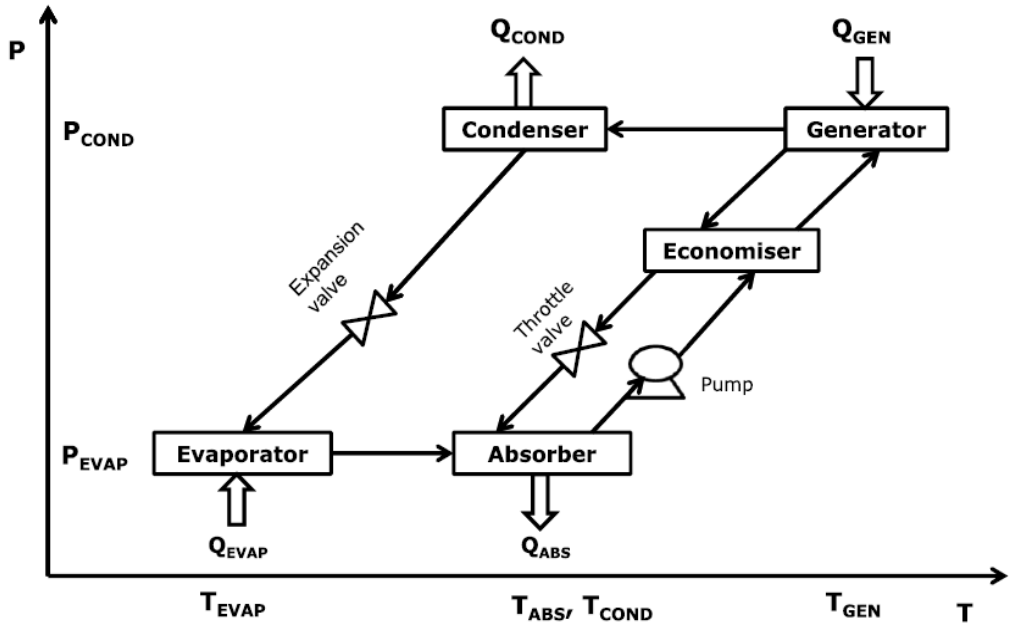

Figure 4 - Liquid-Gas heat pump (heat pump mode)[51]

6.2.2.2. Heat transformer mode

Examining now the heat transformer mode (figure 5) whose function is more in line with the present work, the similarities with the previous system are obvious, namely the fact that both utilize the same main components, however, the operating conditions of these are reversed, with the evaporator and absorber running at high pressure while the condenser and generator function at low pressure. The working fluid is partially vaporized in the generator, through the addition of excess heat at T_{Gen}, before being sent to the condenser, where its condensation will release part of the excess-heat supplied to the generator at a relatively low temperature. The condenser outlet is pumped to the higher-pressure zone, to the evaporator, where the working fluid is once again vaporized through the addition of excess-heat, whose source is typically the same as the excess-heat supplied to the generator, at an intermediate temperature, T_{Evap}. The resulting stream enters the absorber where high-temperature heat is generated by the absorption of the absorbate by the absorbent, which came from the generator mentioned earlier, after the initial vaporization of the working fluid. After this, the resulting mixture passes through the economizer before being decompressed and sent to generator, closing the cycle. As was the case in the previous system, the economizer helps the recovery of heat and increases the system's overall performance, however, contrarily to what occurs in that system, the absorbate rich stream is now the one that possesses excess heat.[33,46,51,52,95,96,99–101]

This type of system can be operated with residual heat at medium temperature to obtain a quantity of useful heat at higher temperature by using a negligible amount of primary energy,[96,99] meaning they are, conceptually, the closest to the ORCHP, which is the focus of the present work.

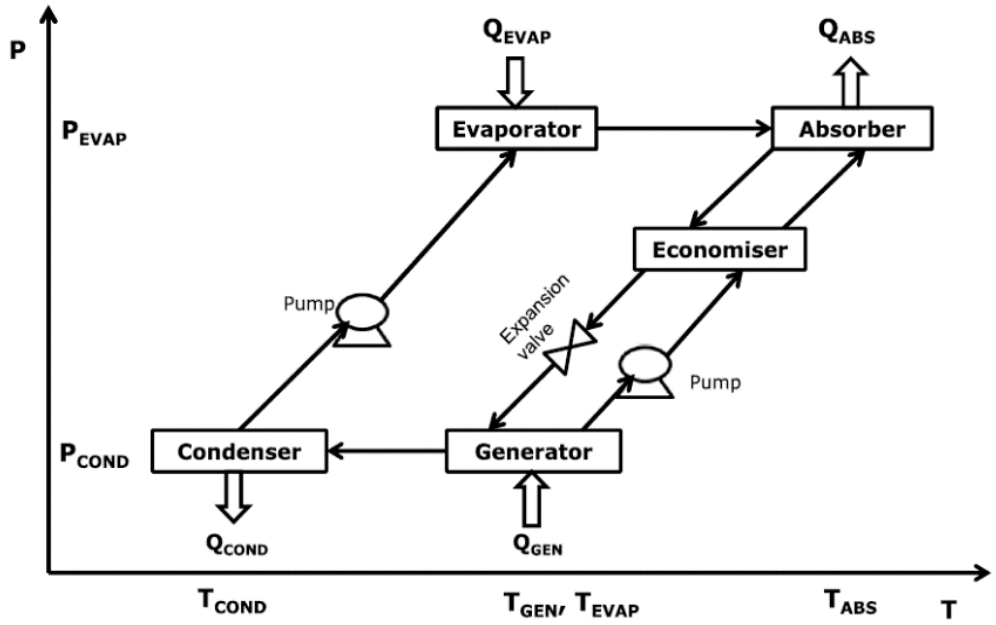

Figure 5 - Liquid-Gas heat pump (heat transformer mode)[51]

6.2.3. Organic reaction chemical heat pumps

The last type of system that shall be addressed is the liquid-gas chemical heat pump based on reversible organic reactions, also known as an ORCHP, which is the focus of the present work. The general reaction that takes place in these systems is of the form:

$$A \rightleftharpoons B + C$$

where the forward and backwards reactions occur at two different temperatures, thus enabling the upgrade of excess-heat to a higher temperature.[38,91,102] Most research developed in this field has been devoted to the study of the IAH, *t*B/*i*B, and benzene/cyclohexane/hydrogen (Bz/Cy) systems.[102] Although the general process is fairly simple, it is important to elucidate each system's reaction pair (table *2*) and give one working example, so, considering the most well-known system, IAH, the heat-upgrade procedure is: isopropanol is decomposed into acetone and hydrogen (forward/endothermic reaction; table 2) and the reaction between these two compounds will yield isopropanol (backwards/exothermic reaction; table 2). The forward reaction is endothermic and proceeds through the addition of low-temperature heat (Q_L), be it from excess-heat or other source, whereas the backward hydrogenation reaction is exothermic, thus liberating heat at higher temperature (Q_H), resulting in the intended heat

upgrade.[91,102] These alternating reactions, in conjunction with the closed-loop design, allow this type of chemical heat pump to operate continuously.[102]

Table 2 - Reactions for the three main CHP systems[102]

System	Reaction pair
IAH	$(CH_3)_2CHOH \rightleftharpoons (CH_3)_2CO + H_2$
*t*B/*i*B	$(CH_3)_3COH \rightleftharpoons (CH_3)_2CCH_2 + H_2O$
Bz/Cy	$C_6H_{12} \rightleftharpoons C_6H_6 + 3\ H_2$

As can be easily understood, the most critical components in an ORCHP are the reactors where chemical reaction, and heat and mass transfer occur. However, these systems also include other essential components such as distillation column, condenser and reboiler, and heat exchanger. Although an ORCHP will almost always be composed by the elements listed above, these can be connected in two different ways, while maintaining their desired function of heat upgrading, the continuous and the storage[c] type.[77,102] The selection of component assembly stems largely from the existence, or not, of time or quantity dependent discrepancies in the supply of the excess-heat and the necessities of the upgraded heat.[77] It is, therefore, important to understand the actual working intricacies associated with each operation mode.

6.2.3.1. Continuous type

Regarding the continuous mode (figure 6), the first step is the liquid-phase endothermic reaction, which occurs at low temperature (T_L). The mixture of unconverted reactant and products flows from the endothermic reactor (R_L) to the distillation column (DC) where the components are separated according to their volatilities. After this, the liquid reactant is sent back to the endothermic reactor whereas the gaseous products exit through the top of the column and are fed to the exothermic reactor (R_H), after passing through a heat exchanger

[c] The storage type CHP can be utilized for thermochemical energy storage, which is part of a larger field known as thermal energy storage (TES), which will not be discussed here. For this reason, we recommend the works of Pardo *et al.*,[160] Sarbu & Sebarchievici,[161] and Stengler & Linder,[162] as well as the EU's Joint Research Centre's (JRC) report.[163]

(HX). The recombination of the gaseous mixture will yield the initial reactant, in gas-phase, while releasing high-temperature (T_H) reaction heat that can be harnessed for any desired suitable application. The resulting gas-phase mixture is passed through the heat exchanger mentioned earlier, where it will preheat the exothermic reactor's feed stream, before returning to the distillation column, thus completing the cycle.[77,102]

In this type of system, part of the recovered excess-heat is used to promote the endothermic reaction and the remaining heat is used as an energy source for the distillation process, which is the driving-force for the organic liquid-gas CHP.[45,77,102]

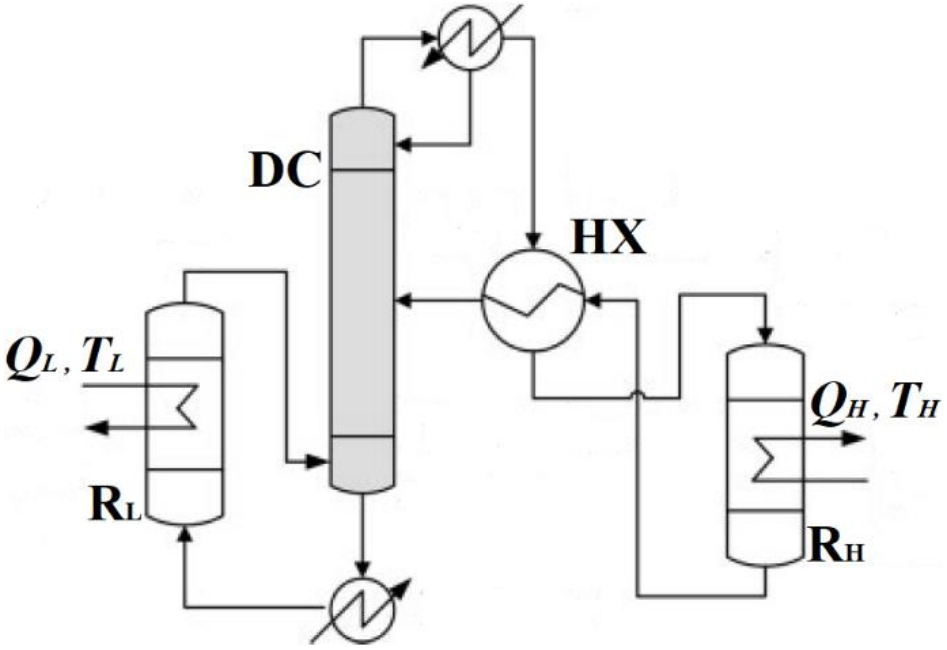

Figure 6 - Continuous mode CHP [Adapted from Cai et al.[102]]

6.2.3.2. Storage type

Concerning the storage mode (figure 7), its operation is extremely similar to the previous one, with the difference that the components in the distillation column's top stream are separated immediately after passing through the condenser. Considering the IAH system, acetone and hydrogen pass through a separator and the former is sent to a storage tank whereas the latter is sent, at condenser temperature (T_c), to a metal hydride reactor where it is stored at atmospheric pressure. High-pressure heat is regenerated by heating the metal hydride at T_L. This releases the hydrogen which then flows to the exothermic reactor, passing through the acetone storage tank, and the heat exchanger, in the same manner as earlier, however, after

pre-heating the exothermic reactor's feed stream, the reaction mixture is sent to a second separator where hydrogen is recirculated back to the reactor. After this separation, the liquid-phase species are passed through a pressure-relief valve and fed to the distillation column, thus completing the cycle.[77,102,103]

As in the previous mode, the excess-heat used in this system will promote both the endothermic reaction and the distillation process, while also functioning as a heat source for the heat regeneration step in the metal hydride reactor, which may lead to lower overall enthalpy efficiencies.[77,102,103]

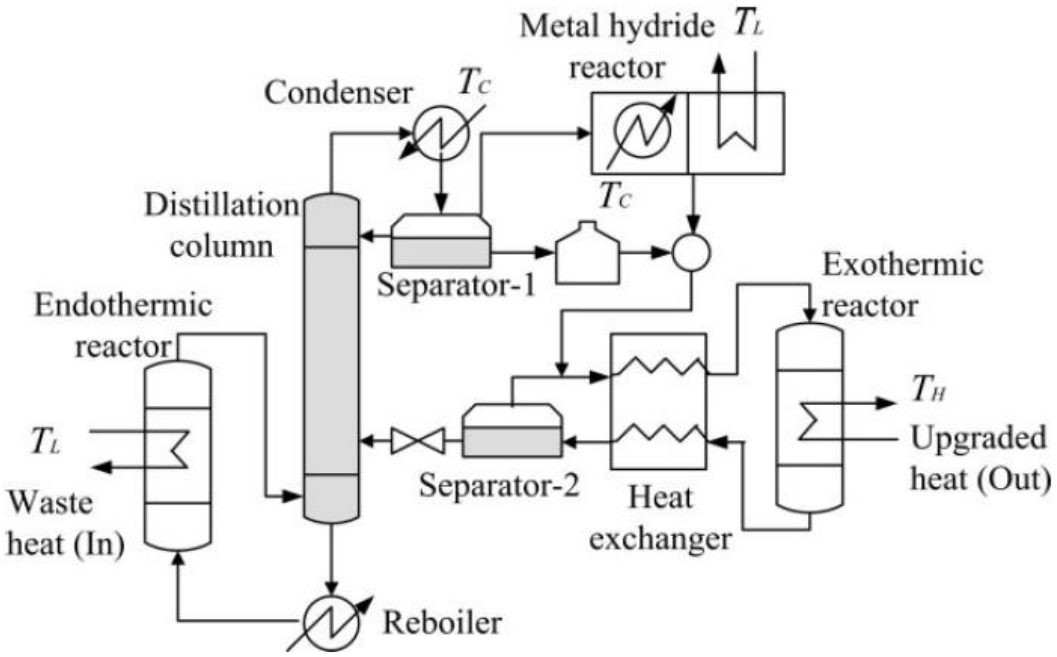

Figure 7 - Storage mode CHP[102]

6.2.3.3. Reactive distillation type

Although both system arrangements discussed thus far can produce reliable and satisfactory results, they still have some limitations due to the chemical reaction sets involved.

As has been shown, the IAH system's endothermic reaction produces acetone and hydrogen from isopropanol. Well, it is known that the acetone produced in this step is a strong dehydrogenation inhibitor given its competitive adsorption on the catalyst's active sites.[75,76,102,104,105] Regarding the *t*B/*i*B system, the problem lies with the endothermic reaction once again. In this case, it is the water produced from the *tert*-butanol dehydration that will

severely inhibit the reaction rate.[79,102,106–108] Both these effects severely limit their respective system's thermodynamic performance.

To answer these shortcomings, Gastauer *et al.*, advanced a proposal where an intricately designed vapor-phase dehydrogenation reactor was to be used, however, this system's distillation column's internal structure was quite elaborate, which, associated with the rigid overall pressure balance, rendered the proposal non-alluring.[109] Five years later, Gaspillo *et al.*, proposed a simpler design which incorporated a process intensification technology known as reactive distillation.[40] This technology combines two, normally separate components, chemical reaction and fractional distillation, into one processing equipment (figure 8). The catalyst section, which can also be called reaction field, is located inside the distillation column. This technology allows for the continuous separation of products and reactant, thus decreasing the inhibitory impacts described above.[40,102,104,108–110]

Given there are no azeotropic mixtures regarding the IAH system, the use of reactive distillation can facilitate the complete conversion of isopropanol under certain conditions, thus overcoming the flaws stated earlier and improving this system's overall performance.[76,104]

Although a reactive distillation arrangement may also benefit the *t*B/iB system,[108] this solution must be carefully evaluated since *tert*-butanol and water form an azeotropic mixture,[111,112] meaning one of two outcomes is likely: i) obtain the azeotrope and deal with this in some other suitable equipment, or, ii) apply some azeotrope breaking technique in the reactive distillation column, considerably increasing the equipment's complexity.

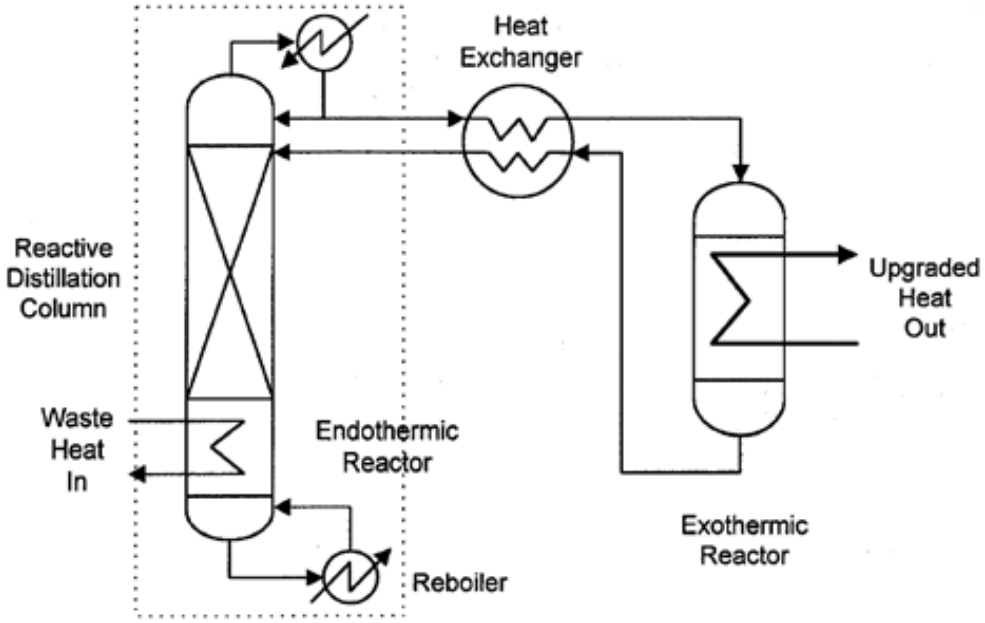

Figure 8 - Reactive distillation mode CHP[83]

7. System Performance

Now that the various systems' operation principles and general designs have been presented, it is time to understand just how their performances can be determined and compared. A particularly important aspect is that they function under different conditions, which means this comparison must be independent from any given operational scope. To this end, there are several metrics available to characterize a CHP's performance, such as actual upgrading temperature, coefficient of performance (COP), effectiveness (ξ), exergy efficiency (η(ε)) and entransy efficiency (G*).[91,102,113–115] Among these, COP and exergy efficiency are the most established since they correlate to the first and second laws of thermodynamics, respectively, and allow for the comparison among several CHPs and between chemical and mechanical heat pumps.

7.1. Actual upgrading temperature

The actual upgrading temperature is, as the name indicates, the temperature gain obtained from the lower (T_L) to the higher (T_H) level.[91]

7.2. Coefficient of Performance

The coefficient of performance (COP; also known as enthalpy efficiency) correlates to the 1st law of thermodynamics as these are both defined as the ratio of heat released at higher temperature to that absorbed at a lower temperature level, as expressed by equation 1, however this means the focus is solely aimed at the quantity of heat recovered but not its quality.[45,52,60,64,99,101,114]

$$COP = \frac{Q_H}{Q_L + Q_r} \quad (1)$$

where,

Q_H – High-temperature heat recovered from the exothermic reaction

Q_L – Low-temperature heat supplied to the endothermic reactor

Q_r – Low-temperature heat supplied to the reboiler

7.3. Effectiveness

Although the COP is a useful parameter when comparing different heat pumps, a system's effectiveness (equation 2) is, from an engineering standpoint, more pertinent as it expresses how near said system's efficiency is to its maximum through the COP (equation 3) and the theoretical maximum COP (equation 4).[60,101,113]

$$\xi = \frac{\eta}{\eta_{max}} \tag{2}$$

where,

$$\eta = COP \tag{3}$$

$$\eta_{max} = \frac{1 - \left[{}^{T_c}/_{T_L}\right]}{1 - \left[{}^{T_c}/_{T_H}\right]} \tag{4}$$

and,

T_c – Temperature of the fluid leaving the distillation column's condenser

T_L – Temperature of the low-T heat supplied to the system

T_H – Temperature of the high-T heat recovered from the exothermic reactor

7.4. Exergy efficiency

The exergy efficiency, also known as second-law efficiency, is very useful since it complements the somewhat narrow perspective provided by the COP through the added consideration of the released heat's quality, *i.e.* the temperature to which it is upgraded. As stated earlier, this metric correlates to the 2nd law of thermodynamics, as can be seen through equation 5.[64,99,102,114,116]

$$\eta\,(\varepsilon) = \frac{Q_H \times (1 - T_0/T_H)}{Q_L \times (1 - T_0/T_L) + Q_R \times (1 - T_0/T_R)} \quad (5)$$

where,

Q_H – High-temperature heat recovered from the exothermic reaction

T_0 – Ambient temperature surrounding the CHP system

T_H – Temperature of the high-T heat recovered from the exothermic reactor

Q_L – Low-temperature heat supplied to the endothermic reactor

T_L – Temperature of the low-T heat supplied to the system

Q_r – Low-temperature heat supplied to the reboiler

T_R – Temperature of the low-T heat supplied to the reboiler (equal to T_L)

7.5. Entransy efficiency

Lastly, the entransy efficiency[d] can replace the concept of exergy when it comes to describing the second law of thermodynamics as it is more suitable for heat transfer processes without heat-work conversion,[115,117] as is the case in the present work. Furthermore, this metric is more succinct than exergy efficiency since it does not introduce an additional factor (environmental temperature), as shown in equation 6.[64,115]

$$G^* = \frac{Q_H \times T_H}{Q_L \times T_L + Q_r \times T_r} \quad (6)$$

where,

Q_H – High-temperature heat recovered from the exothermic reaction

T_H – Temperature of the high-T heat recovered from the exothermic reactor

Q_L – Low-temperature heat supplied to the endothermic reactor

T_L – Temperature of the low-T heat supplied to the system

Q_r – Low-temperature heat supplied to the reboiler

T_R – Temperature of the low-T heat supplied to the reboiler (equal to T_L)

[d] As the study of this performance metric is not the focus of the present work, we recommend the works of Guo *et al.*,[164] Xu,[165] and Chen *et al.*[166] as further reading material on this topic.

8. Chemical Heat Pumps - Systems, Applications, and Implementation

This section aims to give the reader a simple understanding of the main CHP systems' operating details, as well as where and how this technology may be applied.

8.1. System requirements and operating details

To best utilize low-temperature excess heat, it is extremely important that a suitable solution is chosen, that is, a system fitting for the quality and quantity of the source. As a long-term, closed-loop structure, the ORCHP must satisfy a series of especially thorough requirements which result in the establishment of several criteria that must be met when selecting a reaction system, such as:

- Desired reactions have good reversibility as well as considerably high conversion and selectivity;[89,102]
- Few compounds are involved, and reactant(s) and product(s) are easily separated;[89,102]
- Exothermic reaction should have a large reaction heat and all chemical species should be thermally stable.[89]

In addition to the requirements mentioned above, the excess-heat source/reaction system combination plays a paramount role concerning the overall performance associated with the CHP solution, which means it is crucial to be familiar with the different systems' operating conditions (table 3), namely reaction temperatures (T), pressures (P), and enthalpies (ΔH).

Table 3 - Organic reaction system's operating conditions[64,78–80,82,102,106,108,114,116,118]

Reaction system		IAH	*t*B/*i*B	Bz/Cy
Endothermic reaction	Temperature [°C]	~80	~70	~200
	Pressure [atm]	~1	~1	~1
Exothermic reaction	Temperature [°C]	~200	~200	~350
	Pressure [atm]	~1	~13	~19
Reaction heat [kJ/mol]		100.4	56.6	207.0

8.2. Potential applications

One of the most important aspects in energy recovery/upgrade is the identification of a system's potential, that is, where can a given technology provide an adequate solution to an existing problem or shortcoming.

In view of the large information available concerning the EU, and considering that the technology discussed in the present work is to be mainly used in industrial applications, we shall narrow our discussion to the several industrial sectors in Europe.

As briefly addressed, a CHP's potential is only as significant as the excess-heat available. This means that an EHP assessment is extremely important to determine this technology's viability, and, although some groups have conducted such studies (see 1), the data used is somewhat outdated, which is why we decided to update the work of Papapetrou *et al.*[54] with Eurostat's most recent data pertaining to the EU's heat consumption and energy intensities.[59] Their work's methodology is based on an investigation of the technically available excess-heat estimated from 425 industrial sites in the United Kingdom (UK) between 2000 and 2003.[54,119] By determining the excess-heat fraction linked to each sector and temperature band, they determined the same index for other countries.

By applying the methodology described in Papapetrou *et al.*,[54] we found that the EU consumed about 11000 PJ of energy in 2018, with the 15 largest consumers (which will be focused henceforth) representing over 92% of said consumption (about 10200 PJ). Due to constraints stemming from the original work, only 5 industrial sectors were studied regarding their EHP, however, they represent approximately 80% of the energy consumption recorded for the 15 largest consumers, which we considered to be sufficiently representative for the intended discussion. The aforementioned consumers represent over 96% of the total EHP for the EU in 2018, with a value of 1200 PJ.

Even though the low EHP found, which amounts to around 11% of the total energy consumption registered, is a clear indicator of the extensive research and development (R&D) efforts carried out regarding heat recovery and optimization, a more detailed analysis should be conducted given the data's wide scope of countries and industrial sectors.

To begin, it would be expected that larger countries, with greater industrial sectors and energy consumption, would present greater EHPs, however this is not always the case as Finland and Sweden are the 8th and 9th largest energy consumers but present the 5th and 3rd highest EHP,

respectively (figure 9). This is an indication that these two countries most likely present several heat recovery opportunities. A very important aspect concerning energy consumption and EHP is that these must considered as a whole and as the parts of the whole. This is very well illustrated by comparing Germany and Portugal. The former is the largest energy consumer in the EU (approximately 2400 PJ in 2018), and its EHP only amounts to about 12% of that value (about 284 PJ), and the latter appears in 14th, with a consumption of 190 PJ, and registered an EHP slightly greater than 25% of that expenditure (slightly above 48 PJ). This scenario could lead many to disregard Germany's 12% as optimized, but the truth is that those 12% are almost six times larger than Portugal's 25%, meaning the more developed country still presents the greater number of opportunities for excess heat recovery. On the other hand, it is essential that Portugal be given proper attention, especially considering that 48 PJ are roughly equivalent to 1.33x10^{7} MW!

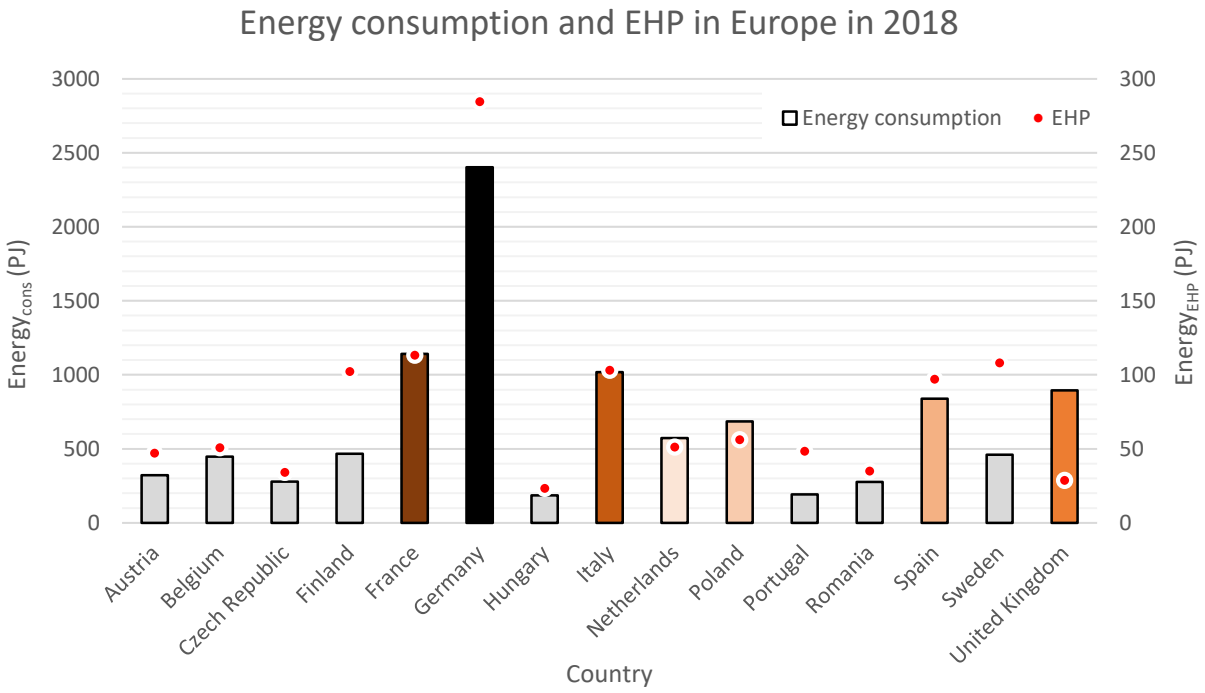

Figure 9 - Energy consumption and EHP in Europe in 2018 for the 15 largest users (Total ≈ 7243 PJ) [Source: Author's elaboration and update from Papapetrou *et al.*[54]]

Regarding the several industrial sectors included in this analysis, it is with no surprise that the Chemical and Petrochemical (C. & P.) industry consumes the most energy with over 2200 PJ in 2018 (figure 10). What is noteworthy is the fact that this industry presents the lowest EHP, both in absolute values (just under 62 PJ) and as a percentage (under 3%), which clearly

illustrates the extensive R&D efforts and investment that have been devoted to energy optimization. However, a low EHP should never discourage further investigation, especially since currently implemented solutions may be surpassed as knowledge, expertise, and technology continues to evolve, and progress, leading to the development of newer and enhanced solutions.

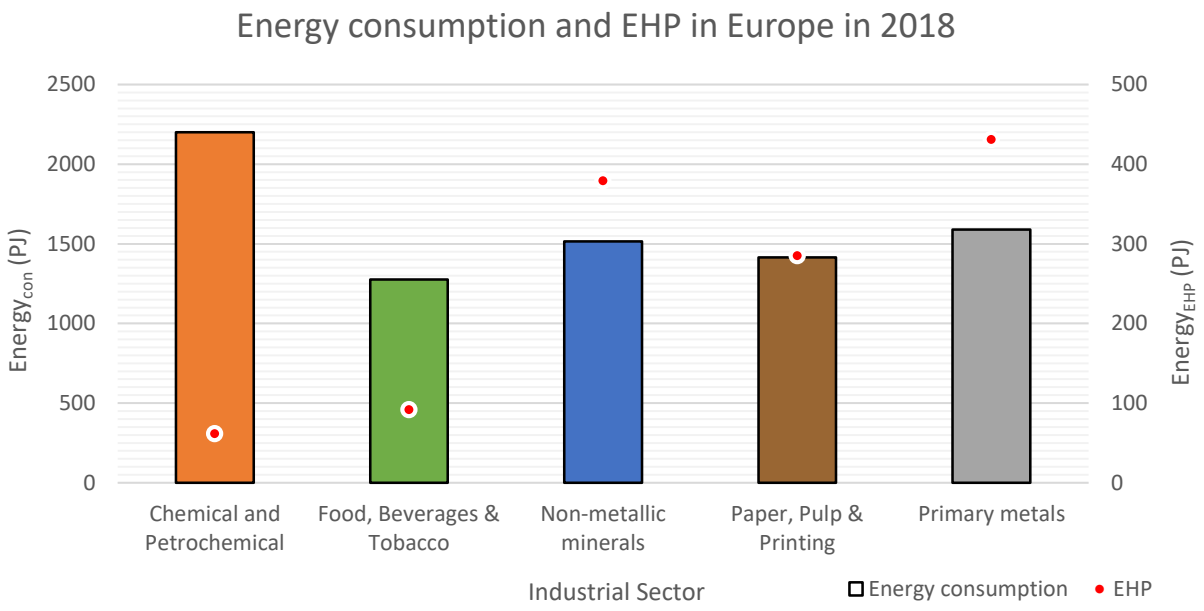

Figure 10 - Energy consumption and EHP in Europe in 2018 for the 5 largest industrial sectors [Source: Author's elaboration and update from Papapetrou *et al.*[54]]

Perhaps the most interesting aspect, considering the present work, is the temperatures at which the excess-heat being discussed is available. Thus, figure 11 presents the EHP distribution considering seven temperature bands (under 100 °C, 100 – 200 °C, 200 – 300 °C, 300 – 400 °C, 400 – 500 °C, 500 – 1000 °C, and above 1000 °C).

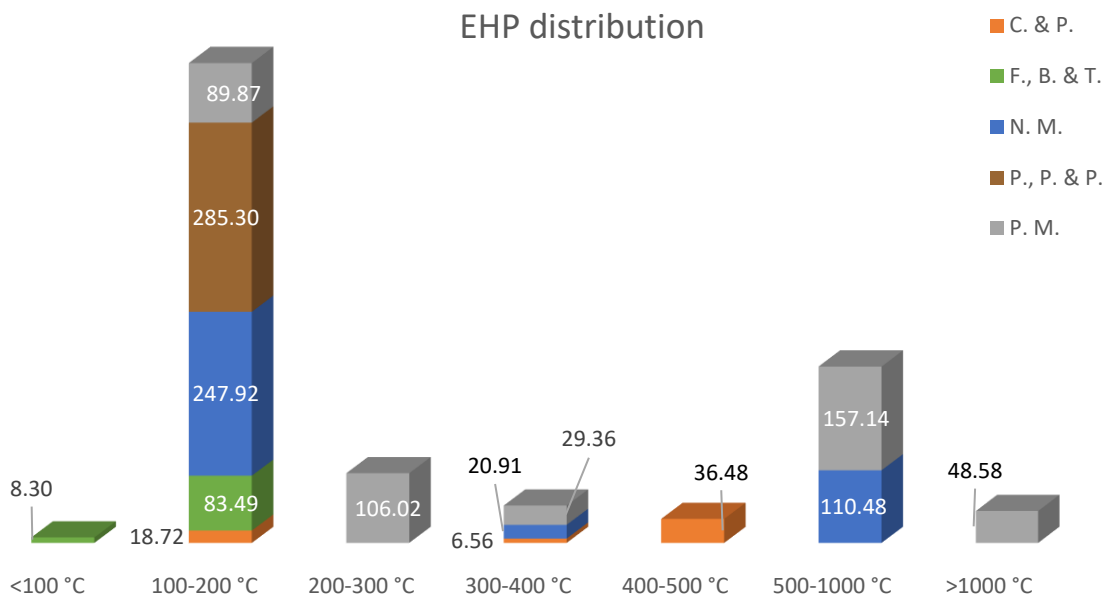

Figure 11 - Main industrial sectors' EHP distribution, in PJ, among the considered temperature ranges [Source: Author's elaboration and update from Papapetrou *et al.*[54]]

This analysis' highlight is the significantly larger bar in the 100 – 200 °C band, which was expected and confirms that most excess-heat is available at low-temperature (< 200 °C). Again, it can be seen that the Chemical and Petrochemical (C. & P.) industry presents the lowest EHP, closely followed by the Food, Beverages, and Tobacco (F., B. & T.) industry. Focusing on the 100 – 200 °C band, it can be seen that the Paper, Pulp, and Printing (P., P. & P.) industry possesses the highest amount of excess-heat available, which suggests this industry might present some interesting opportunities for heat pump implementation.

Appendix A contains detailed information regarding the EHP distribution by industrial sector within the 15 largest users (figure 72) and among the different temperature ranges within the five industrial sectors herein considered (figures 73 to 77).

8.3. Implementing a Chemical Heat Pump

Since there are, to the best of our knowledge, no established guidelines nor methods specifically designed for the implementation of CHPs in industrial settings, this section aims to understand the general ideas behind heat pump implementation and adapt these to the case of a CHP. Through this, we hope to give the reader a rational notion of the most important steps and considerations to bear in mind during a CHP viability/feasibility study.

Given the complexity inherent to any given chemical process, it is best to subdivide it into smaller, easier to approach, subsystems when conducting optimization studies.[120] The onion model (figure 12) is a well-established and systematic approach to the problematic of industrial process' energy efficiency optimization.[32,121] This model also represents the energy hierarchy of a chemical process.[120,121]

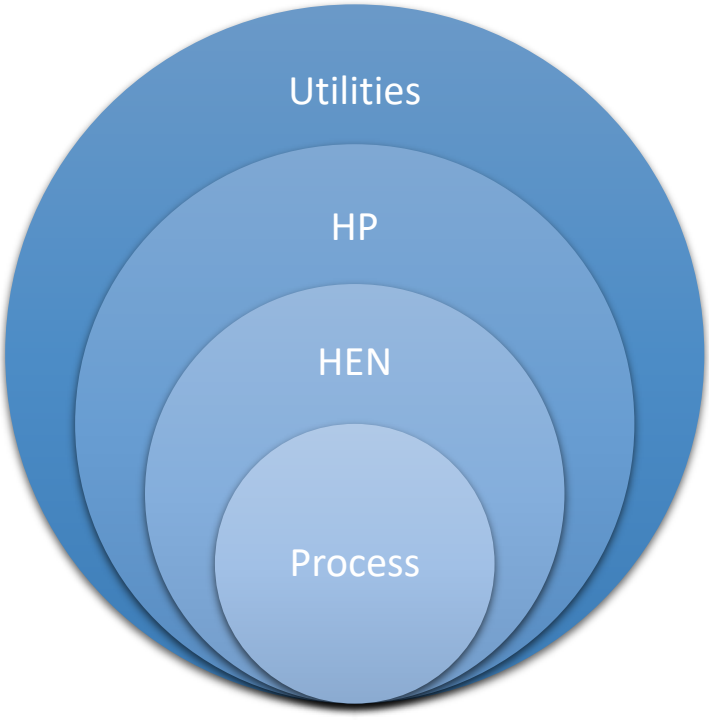

Figure 12 - Onion model for energy efficiency improvement [Adapted from Bruinsma et al.[32]]

The first stage's focus is directed towards the more energy-intensive equipment (reactors, separators, compressors, among others) and the approach to optimization is highly reliant on

a balance between annualized costs, both from an investment and an operating standpoint, *versus* resulting benefits, for each equipment.[32]

The second stage concerns itself with heat integration, mainly through the introduction of heat exchangers, and implementation of a heat exchanger network (HEN), allowing the transfer/recovery of heat from hot to cold streams, which ultimately decreases total hot and cold utility consumption, however, these require a driving-force (temperature difference (ΔT) between hot and cold fluids), meaning there is a limit to what can be achieved in this stage.[32]

The third stage, and most relevant for the present work, is responsible for determining how attractive a heat pump solution may be for a given industrial process, eventually carrying out its development and implementation.[32] This device's heat upgrading capabilities mean it will be able to promote would-be excess-heat to higher temperature, allowing further heat recovery, and added utilities savings.[32]

In a new project design scenario, this onion-model approach, in which each layer is studied and integrated with the next, presents little challenges in terms of deployment limitations since everything is projected, and revised many, many times, before proceeding to the next stages, however, i) there are little new projects nowadays, and ii) most facilities have already undergone some kind of retrofitting action, for the most part aimed towards overall plant cost reduction through enhanced heat recovery. These constraints indicate most chemical heat pumps will be implemented in established sites, which means a deep understanding of the existent HEN is imperative. The most accepted methodology towards understanding, and optimizing, the HEN is Pinch Analysis (PA). First introduced by Linnhoff in 1977,[122] this methodology was further advanced into the form in which it is known today by Linnhoff and Townsend in 1983.[123,124]

PA is mostly used for heat integration through development and/or optimization of the HEN. This methodology can use two depictions, i) two composite curves (CC), and ii) a grand composite curve (GCC), to represent the hot and cold streams in a process. Both representations allow the determination of the heat that can be exchanged between process streams (wallin1994), the identification of the pinch-temperature, and the minimum hot and cold utility requirements,[32,86,98,125,126] depending on the minimum temperature approach (ΔT_{min}) intended. The GCC also aids the determination of the best types of utilities to apply. Both CC and GCC representations can be used for HP integration though using the CC's diagram presents the advantage of easier HEN redesign after HP integration.[98]

The development of heat integration has led to a fundamental rule: “Heat should never be transferred across the pinch temperature”.[32,86,120] Breaking this rule results in a double penalty where both hot and cold utility requirements will register an increase equal to the amount of heat exchanged across the pinch.[86,126]

However, given a heat pump’s operation, these must be arranged in a way that enables heat transfer across the pinch, enabling heat upgrade from below (where there is an excess) to above the pinch (where there is a necessity), thus reducing both hot and cold utility requirements.[123,125,127] This new cross pinch rule is widely accepted and has been successfully implemented in several studies.[127]

After ascertaining how to integrate a HP into both new and existing HENs, it is critical to understand there are a number of topics that must be addressed before deeming such a solution as effective and, most importantly, appealing from both economic and energetic standpoints. Considering the specific case of a CHP, these are:[32]

- Plant/process ΔT_{min} and major enthalpy balance;
- Plant pinch temperature and overall flexibility;
- Temperature lift required;
- System configuration and existing operational constraints;
- Chemical reaction cycle and global efficiency;
- Available utilities;
- Annualized capital costs vs utility costs;
- Total investment costs (heat pump, and, if necessary, HEN retrofitting) vs Payback period.

III – DESIGN OF EXPERIMENTS

9. Optimization through designed experiments

The concept of optimization is a global tool. This process can be applied to staff and time management, delivery and transportation routes, manufacturing and production output, among many others, however, the goal is almost always the same: cut expenses, increase revenue, and ultimately reach a higher profit margin, attaining larger profits.

Generally speaking, an optimization process consists in minimizing or maximizing a given function (*e.g.* cost and performance, respectively), in order to achieve an optimal solution. The functions involved are frequently characterized by their high complexity and large number of variables (*i.e.* control factors). Given this intricacy, an OFAT (one factor at a time) approach, in which only one factor varies at time, while the others remain fixed, is not recommended due to its narrow scope and inability to identify the interactions between process variables.[128–130] Design of experiments (DoE) is more effective than an OFAT method to determine the impact of two or more factors on a response variable because it requires less resources (*e.g.* material, time, among others), which is extremely important when these are limited, as is frequent, particularly considering the monetary and time aspects (*i.e.* experiments can be very expensive and time consuming).[129,130]

Multivariant systems analysis approaches are absolutely vital[131] due to the increasing complexity associated with chemical processes, which stems from a greater intricacy of the actual processes, and from the rise in beneficial inter-process integrations. In addition, computer-aided investigation is an indispensable tool when studying and/or optimizing any given facility. Simulation software (*e.g. Aspen HYSYS*, *CHEMCAD*, *Pro/II*) capable of handling the extensive mathematical load involved are invaluable due to their ability to provide instantaneous and precise information on how a certain variation might affect the output, and the changes induced throughout the process. Aside from this, most software packages are capable of estimating a project's costs through dedicated "sub-programs" such as *Aspen Process Economic Analyzer* (APEA).[132,133]

The growing complexity of real-world scenarios, especially their increasingly more time/resource consuming aspects, has led to the development of methods focused on generating clear and objective experiments through which a process' study may be conducted (*e.g.* design of experiments) and although DoE was developed for real-world scenarios, there are a number of instances in the literature where it has been used successfully in tandem with process simulation software.[75,134–137]

DoE is a method by which an experiment, or set of experiments, is planned in order to assure appropriate data collection, followed by proper statistical analysis, thus guaranteeing valid, impartial, and focused conclusions. Given its focus on planning, it is possible to project assays which yield the desired results while minimizing the resources involved, both human and process/product related.

A deep and broad understating of the process in study is fundamental when designing an experiment. Knowledge of which variables will be affected when certain changes are made, and in what magnitude, greatly facilitates the development of "targeted" experiments, meaning the researchers will expend less effort and time to reach the desired goals.

This method may seem simple, however, it is important to possess a clear vision of the problem/situation in question, which variables will be manipulated, and their respective ranges, how the data will be collected and processed, and most importantly, the experiment's final goal.[128–130] This procedure is carried out step-by-step, as illustrated by figure 13.

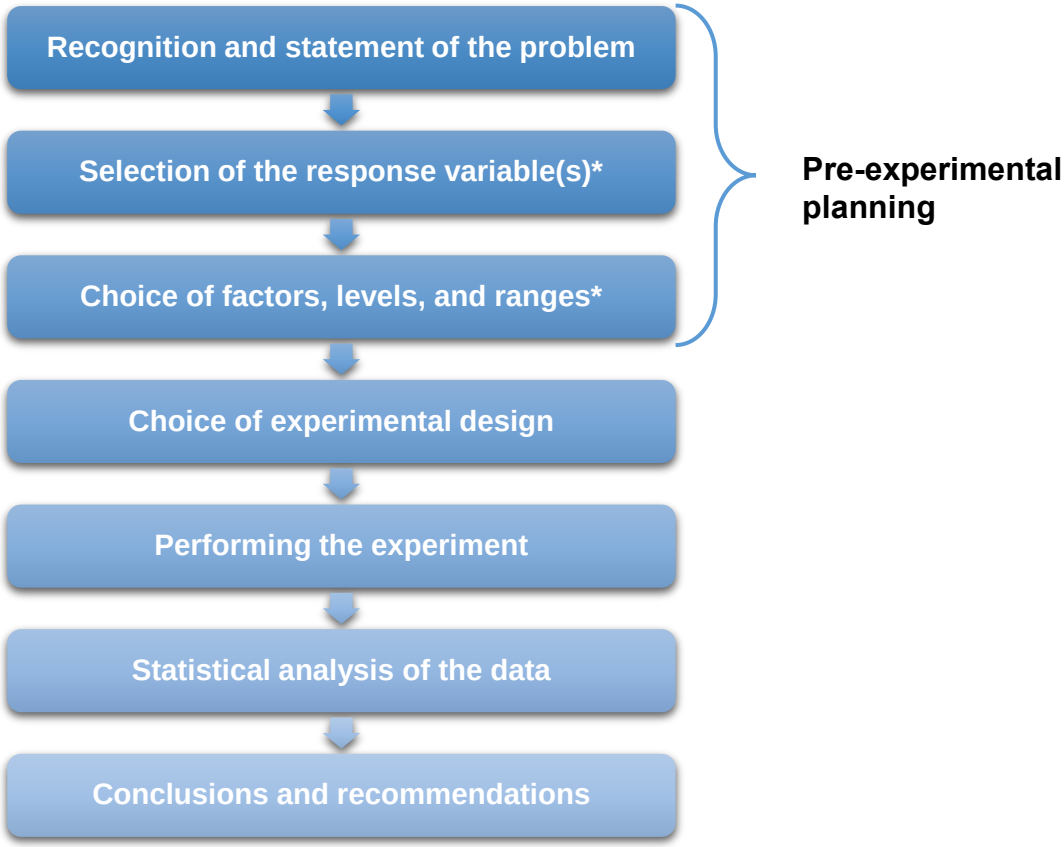

Figure 13 - Procedure/guidelines for designing an experiment[129,130]
(*Can be done simultaneously or in reverse order)

Each of the steps mentioned above are vital for the process of designing an experiment. As such, a brief explanation of each one is provided, however, we highly recommend consulting the works of Montgomery for a deeper explanation of this process.[129,130]

Step 1. Recognizing and stating the problem

This step is crucial in the sense that a clear identification of the problem, which is often challenging on its own, as well as the experiment's objective(s), may contribute substantially to a superior process understanding. Listing the questions the experiment is meant to address is often helpful in identifying the underlying problem. The objective is to establish a cause-and-effect relationship between a number of independent variables and a dependent variable of interest.

Step 2. Selecting the response variable(s)

The response variable will serve as the basis for the study's conclusion(s), therefore, a careful selection should be made. The experimenter(s) should be certain that this variable conveys useful information about the process in study, thus guaranteeing that all factor effects can be appropriately investigated. It is very important, both in this step and the next, that everyone involved avoids being influenced by past experiments/studies.

Step 3. Choosing the experiment's factors and their respective levels

A deep, and broad, process knowledge is of paramount importance in this step. A better selection of the factors (*i.e.* independent variables), their levels (*i.e.*, the factors' values), variation ranges, and units of measurement, increases the efficiency surrounding the experimentation process, leading to the solutions being reached quicker, thus decreasing the resources invested, however, it is important to understand that all factors must be investigated thoroughly. This step is also responsible for identifying and deciding how "noise" factors, controllable or not, are to be addressed, if at all.

Step 4. Choosing an experimental design

Sample size (number of replicates), suitable run order, and if/which randomization constraints are to be applied, are some of the considerations involved in this step. Choosing an appropriate experimental design is relatively easy if the previous steps were done correctly.

Factorial experiments (FE) are the most common techniques. These should be used when a relatively large number of factors are being considered, which is true for most cases. Of these, fractional factorial designs (FFDs) should be highlighted for their role in decreasing the number of experiment that have to be performed.

Instead of changing one factor at a time, the different factors' levels are systematically varied, resulting in a final data set in which all combinations were tested. This approach means that all interactions are analyzed and taken into account, which is a vital resource since it is quite often that all factors influence the process simultaneously.

The most commonly used factorial design, 2^k, is extremely useful in early experiment stages since it provides useful information for studying *k* factors at two levels (low level (-1) and high level (+1)). As the number of factors in a 2^k design increases, the number of runs also increases substantially. For example, studying a total of six factors (2^6) requires a total of 64 experiments without replication. FFDs are very useful in reducing this huge number of experiments. These are largely employed in factor screening experiments where the main objective is to identify a relatively few significant factors, from a larger number of factors, through the smallest possible number of runs.

One important aspect regarding FE is the possibility to fractionate the experiment. This is typically employed when a large number of factors is being considered, which would exponentially increase the amount of runs in the experiment, and/or when the experimenter(s) wish to identify/quantify the most impactful factors, most commonly referred to as screening experiments. FFDs are an excellent choice when resources are limited since they use fewer runs than the full factorial design. The successful use of these designs is based on three key concepts:

i. The sparsity of effects principle, which states that most systems are dominated by some of their main effects and low-order interactions, *i.e.*, it is possible to assume that certain high-order interactions are negligible and combine their mean squares to estimate the error;

ii. The projection property, which states that any 2^{k-1}, for example, fractional designs, can be projected into stronger 2^{k-p} designs in subsets which will only contain significant factors, which can itself be collapsed further, so long as there are sufficient factors to allow it;

iii. And the sequential experimentation concept, which states that FFDs can be combined to construct a larger design to estimate the factors'/interactions' effects of interest.

One of the first decisions made when running a fractionated experiments is the number of main factors to be considered. This is essential and must be carefully addressed since it will influence the experiments' sample size and the design's resolution, which directly influences the factors' aliases patterns.

The designs' resolutions describe the extent to which the effects in an FFD are aliased with one another. This means the confounded, or aliased, effects cannot be estimated separately from each other. The main objective is to use an FFD with the highest possible resolution for the amount of fractionation required. The three main design resolutions are briefly described:

- Resolution III

  Main effects (*i.e.* factors) are aliased with two-factor interactions, which may be aliased among each other.

- Resolution IV

  Two-factor interactions are aliased with each other and main effects are aliased with three-factor interactions. This resolution provides excellent information regarding main effects and some useful information on two-factor interactions due to the fact that these are not confounded with each other.

- Resolution V

  Three-factor interactions are aliased with two-factor interactions and main effects are aliased with four-factor interactions.

Factor screening experiments regularly utilize resolution III or IV designs due to their remarkably convenient aliasing structures. Screening designs are usually of resolution III due to its ability to explore many factors' effects through an efficient number of runs. Despite being more time and cost expensive, resolution IV designs are sometimes used due to their advantages from a confounding perspective.

Step 5. Performing the experiment

Although this may appear simple and easy to execute, errors in this stage destroy the experiment's validity more often than naught, which means closely monitoring the experiment is absolutely paramount.

Step 6. Analyzing the data

Data analysis should be conducted through statistical methods (*e.g.* analysis of variance (ANOVA)). These are relatively effortless to carry out (many software packages are available) while providing unbiased and clear results. Even though this step's automation and simplicity are undeniable, it is always important to conduct some sort of model validity assessment, such as a residual analysis (RA).

Step 7. Concluding

Unquestionably the most relevant step when decision-making is concerned, this stage relies heavily on graphical methods to transmit the experimenter(s)' concrete/objective findings. Future work recommendations are also expressed and confirmation testing should be performed when necessary.

10. Data processing in designed experiments

Before getting into the systems' optimization studies, it is important to understand how the data obtained from the experiments will be processed and analyzed. Thus, the procedure adopted when studying data obtained from DoE is:[129,130]

Step 1. Estimate the factors'/interactions' effects;
Step 2. Generate the preliminary model;
Step 3. Test all factors'/interactions' significance;
Step 4. Analyze residuals
Step 5. Refine the model
Step 6. Interpret results

A factor's effect translates how a response will vary as a result of changing said factor's level. If the difference in response between a factor's levels is not identical, for all levels of every other factor, then there is an interaction between the factors. These can be calculated through equations 7 (for complete factorial experiments) and 8 (for fractional factorial experiments). A factor's contrast essentially represents the difference between the response's values when said factor is at its high or low level. It can be determined by using a plus/minus table, however, this method becomes unnecessarily time-consuming as the number of factors increases. As such, equation 9[e] presents an alternate method in which each parenthesis' sign is negative if the factor is included in the effect and positive if not.

$$Effect_i = \frac{Contrast_i}{n \times 2^{(k-1)}} \tag{7}$$

$$Effect_i = \frac{Contrast_i}{n \times 2^{(k-p)-1}} \tag{8}$$

$$Contrast_i = (a \pm 1)(b \pm 1) \dots (m \pm 1) \tag{9}$$

[e] The expanded equation will yield a term equal to 1. This is replaced by (1) in the final expression.

where:

n – Number of replicates in an experiment (bearing in mind that this work is simulation-based, no replicates are carried out, meaning n is always equal to 1);

k – Number of factors involved in the experiment;

p – Number of design generators;

a, b, …, m – Coefficients of the factors involved in the experiment;

i = A, B, …, M.

The preliminary model is generated by fitting the data obtained, considering the significant factors/interactions, determined earlier, to a first-order equation. This is known as a first-order RSM (Response Surface Model) and given by equation 10.

$$y = \beta_0 + \sum_{i=1}^{m} \beta_i \cdot x_i + \sum_i \sum_j \beta_{ij} \cdot x_i \cdot x_j + \epsilon \quad (10)$$

where:

y – Response value obtained through experimentation;

β_0, β_i, β_j – Regression coefficients;

x_i ; x_j – Represents the codified level(s) of the i^{th} and j^{th} factors;

ϵ – Corresponds to the random error component of the model.

The factors'/interactions' significance towards the response considered in a given experiment can be ascertained through an analysis of variance. This is a tool frequently used in the field of statistical inference. This technique tests equality among several means by comparing variance between groups to the various within those groups (*i.e.*, their random error). The ANOVA relies on hypothesis testing to determine if a factor, or interaction, is significant towards the response (equation 11).

- H_0: $\lambda_i = 0$, for all i;
- H_1: at least one $\lambda_i \neq 0$. (11)

Considering that λ represents a deviation from the mean, if the null hypotheses (H_0) is true, then it can be stated that all observations are taken from a normal distribution, *i.e.*, changing the factor's level has no effect on the mean response, which means the factor in question is not significant towards the response.

This hypothesis test can be done through an F-test, in which the null hypotheses should be rejected, for a desired significance level α, if equation 12 is verified. This is true due to the fact that, under the alternative hypothesis, H_0 should be rejected if F_{0i}, in equation 13, is large, and that the expected value for the numerator is larger than the expected value for the denominator.[129,130]

- $F_{0i} > F_{\alpha,iDF,ErrorDF}$ (12)

where:

$$F_{0i} = \frac{MS_i}{MS_E} \tag{13}$$

and,

$$MS_i = \frac{SS_i}{DF_i} \tag{14}$$

$$MS_E = \frac{SS_E}{DF_E} \tag{15}$$

$$SS_i = \frac{(Contrast_i)^2}{n \cdot 2^k} \tag{16}$$

$$SS_i = \frac{(Contrast_i)^2}{n \cdot 2^{(k-p)}} \tag{17}$$

where:

MS – Effects' and error's mean squares;

DF – Effects' and error's, degrees of freedom (this will be 1 for the former and equal to the number of assays minus the number of significant effects for the error);

SS_i – Sum of squares for effect i.

Due to a constant desire to be more and more efficient, it is often the case that only one replicate of a 2^k design is run, typically known as unreplicated factorials, especially in screening experiments when there are usually many factors under consideration.

Since there is no way to estimate the "pure", or internal, error of unreplicated factorials, a different approach is needed. One solution is to appeal to the sparsity of effects principle which usually implies only about half of the existing effects will be active. Although this principle is valid, certain systems may present real high-order interactions, which is why Daniel[138] proposed a simple graphical method to visually grasp which are in fact negligible as these will tend to fall along a straight line in a normal probability plot of the estimates of the effects. This method will allow the preliminary model to contain all significant effects while combining the remaining effects as an estimate of error (equation 18).

$$SS_E = \sum SS_{NS} \tag{18}$$

or,

$$SS_E = SS_T - \left(\sum_i SS_i\right) \tag{19}$$

where:

SS_E – Error's sum of squares (NS: factors/interactions found not to be significant);

SS_T – Total sum of squares.

The ANOVA assumes, through the model errors, that the observations are distributed normally and independently with the same variance in each factor level, and that this variance, though unknown, is constant, however, this must be examined in order to establish the model's adequacy.

This can be done by examining the residuals (e, equation 20). These are defined as the difference between the actual experimental observations and the value which would be obtained from a least squares fit of the underlying ANOVA model to the sample data.

$$e = y - \hat{y} \tag{20}$$

where:

y – Response value obtained from the experiment;

$\hat{y}$ – Estimated value for the response.

The fitted regression model ($\hat{y}$; equation 21), from which the estimated value for the responses is obtained, is built through the ANOVA and only takes the factors found to be significant into account.

$$\hat{y} = \hat{\beta}_0 + \sum_{i=1}^{m} \hat{\beta}_i \cdot x_i + \sum_i \sum_j \hat{\beta}_{ij} \cdot x_i \cdot x_j \tag{21}$$

where:

$\hat{y}$ – Estimated values for the response;

$\hat{\beta}_0$ – Average value of all significant effects' responses;

$\hat{\beta}_i$, $\hat{\beta}_j$ – One-half of the corresponding main effect or interaction;

x_i, x_j – Represents the codified level(s) of the i^{th} factor.

The residuals analysis should be an automatic part of any ANOVA as they are fundamental in identifying any model inadequacies and/or violations of the underlying assumptions.

The normality assumption can be verified by plotting the residuals in a normal probability plot. If the ANOVA is robust towards this assumption, *i.e.*, if it respects said assumption, then the plot will resemble a straight line (greater emphasis should be placed on the plot's central values than on its extremes). In addition to this, the residuals' variability should not depend on the estimated value ($\hat{y}$); tested by plotting the residuals against these estimates. The independence assumption can be verified by plotting the residuals *versus* the order in which the experiment was carried out. In this case, the plot should not present any tendencies towards the formation of positive/negative residuals patterns. This last assumption is particularly troublesome as it is related to the randomization of the experiment, which means it will be very difficult to correct and prevention, *i.e.*, proper experiment randomization, should be assured early on. The last assumption can be verified by plotting the residuals against the estimated values, in which no special structures should be observed.

Now that the ANOVA, and its intricacies, have been outlined, it is important to identify, and choose, an adequate method through which to guide the optimization process. The method of steepest ascent (SAsc), or descent (SDsc), depending on if the desired outcome is to maximize, or minimize, the response, are very efficient procedures. These allow the experimenter(s) to proceed along the path of steepest ascent/descent, *i.e.*, to follow a straight line, normal to the fitted response surface contours, thus steadily approaching the response's maximum.

IV – STEADY STATE SIMULATION AND OPTIMIZATION

11. Isopropanol/Acetone/Hydrogen System

Given this technology's relatively early stage of development, all studied systems present the same generic, and widely accepted, design,[102] however, some authors modify certain sections according to the study they wish to carry out.[139] In light of this design freedom, we constructed a system based on the IAH reaction system. Its intricacies and operations are presented next.

Given this work's simulation foundation, an adequate property prediction model must be employed. After some literature research, the UNIQUAC – Virial model was found to be satisfactory for the systems in discussion.[76,108,110,118,139]

11.1. Implementation

As was explained earlier in this work (see 6.2.3), this system's endothermic reaction is responsible for the conversion of isopropanol into acetone and hydrogen, and the exothermic reaction is responsible for the conversion of acetone and hydrogen back into isopropanol. There are several ways to introduce these reactions' information when a simulation software is to be used, however, the easiest might be to implement the reactions' kinetics directly into whatever program is being used. Thus, a bibliographic research was conducted and the following kinetics for the endo (table 4) and exothermic (table 5) reactions were discovered:

Table 4 – Endothermic reaction's kinetic equation and parameters (IAH system)[110,118,140]

$$\boldsymbol{r_{dH} = \frac{k}{1 + K_A (C_A)^{0.5}}} \qquad \boldsymbol{\left[mol\ {g_{cat}}^{-1}\ h^{-1}\right]}$$

$k = k_0\, e^{-E_a/RT}$	$K_A = K_0\, e^{\Delta H/RT}$
$k_0 = 1.55 \times 10^{27}\ mol\ {g_{cat}}^{-1}\ h^{-1}$	$K_0 = 6.15 \times 10^{-45}\ m^{1.5}\ mol^{-0.5}$
$E_a = 191.89\ kJ\ mol^{-1}$	$\Delta H = 290.42\ kJ\ mol^{-1}$

Table 5 - Exothermic reaction's kinetic equation and parameters (IAH system)[118,141,142]

$$r_{hH} = \frac{k\,K_A\,P_A\,K_H\,P_H}{(1 + K_A\,P_A + K_H\,P_H)^2} \qquad \left[mol\ g_{cat}^{-1}\ h^{-1}\right]$$

$k = k_0\, e^{-E_a/RT}$	$K_A = K_0\, e^{\Delta H/RT}$	$K_H = K_0\, e^{\Delta H/RT}$
$k_0 = 1.71 \times 10^6\ mol\ g_{cat}^{-1}\ h^{-1}$	$K_0 = 2.90 \times 10^{-11}\ Pa^{-1}$	$K_0 = 1.94 \times 10^{-15}\ Pa^{-1}$
$E_a = -61.5\ kJ\ mol^{-1}$	$\Delta H = 54.4\ kJ\ mol^{-1}$	$\Delta H = 82.5\ kJ\ mol^{-1}$

where:

r – Reaction rate (dH – dehydrogenation, and hH – hydrogenation);

k – Rate constant;

k_0 – Pre-exponential factor for k;

K – Adsorption equilibrium constant (A – acetone and H - hydrogen);

K_0 – Pre-exponential factor for K;

C – Concentration [mol m^{-3}];

E_a – Activation energy;

R – Ideal gas constat (8.314 J mol^{-1} K^{-1}).

Although both equations, and respective parameters, were found, only the endothermic reaction's kinetics were actually implemented due to limitations regarding the software. Given the system's assembly, both reactions will present very similar molar conversions. This occurs due to the fact that the system is closed and no fresh feeds are utilized, as would be the optimal case with a real-world implementation of a CHP. Thus, the exothermic reaction was implemented as an equilibrium reaction with a specified 80% approach, so as to not limit the endothermic reaction's potential.

The concrete system was envisioned on the basis of needing only two reactors, a distillation column, and a heat exchanger. Thus, this assembly was put in place in the software (figure 14). First, the endothermic reactor was defined as a Continuously Stirred Tank Reactor (CSTR) with a volume of 10 m^3. After this came the distillation column, however, due to isopropanol and acetone's sufficiently distant boiling points, a flash separator (FS) was used instead. Lastly, the exothermic reactor was defined as an equilibrium reactor, which also possesses a volume of 10 m^3. A heat exchanger was added between the flash and the exothermic reactor in order to pre-heat the exothermic reactor's feed through the reuse of some excess-heat that the vapor stream leaving said reactor may still retain, which would, otherwise, be integrated into another section of the process, or, in a worst-case scenario, wasted. Other equipment, such as pumps, compressors, and heat exchangers, was used when/where necessary.

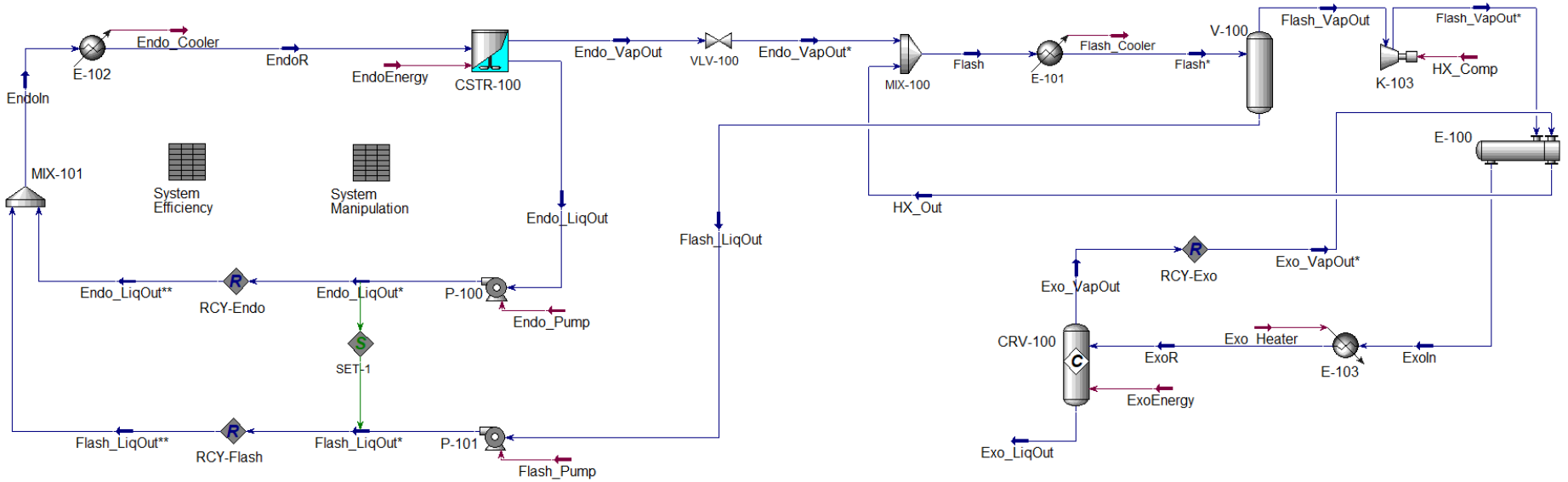

Figure 14 - IAH system's first design

Table 6 presents the initial convergence conditions (inlet and reaction temperatures, and pressures).

Table 6 - Initial convergence conditions for the IAH system

	Endothermic reactor	**Flash separator**	**Exothermic reactor**
Inlet Temperature [°C]	65	38.5	180
Reaction Temperature [°C]	75	-	180
Vessel Pressure [atm]	1.65	1.30	1.60

Table 7 presents the base molar flows of the different species in the system. The quantities shown relate to the recycled streams attached to the logical operations of the same name as the table's columns, and were used as the starting point for all studies carried out on this system.

Table 7 - Molar flows for the IAH system (in kgmole/h)

	RCY Endo	**RCY Flash**	**RCY Exo**
Isopropanol	100.5403	439.2385	514.2183
Acetone	11.0584	61.4472	287.8274
Hydrogen	0.0020	0.0296	2647.3402

Table 8 presents the pressure drops used throughout the system's heat exchangers.[143,144]

Table 8 - Pressure drops used in the heat exchangers

Phase change (evaporation/condensation)	0.10 atm
Gaseous mixtures	0.20 atm
Low viscosity liquids	0.35 atm

The recycle streams' process re-entry points were determined based on each component's molar flow. Thus, the liquid streams from the endothermic reactor and the flash separator, which are rich in isopropanol, are recycled to the aforementioned reactor, whereas the hydrogen-rich, gaseous stream from the exothermic reactor is recycled to the flash separator.

11.2. Optimization

Before moving on to the system's optimization, it is important to preface some considerations regarding both systems:

1. These systems' main goal is to upgrade energy (*i.e.*, promote excess-heat), which means each system's performance is just as important as its cost, even if the ultimate decision-making metric is the latter. Given this, three outputs were studied/optimized (cost, effectiveness, and entransy efficiency);

    a. The total cost, given by equation 22, translates the annual payments needed to repay a 20-year loan taken out to cover the system's capital costs (this gives the system's annual amortization costs), and its operating costs[f], which involve the equipment acquisition and installation, and hot, cold, and electrical utilities, respectively. This parameter is of the smaller better type;
    b. The performance metrics, effectiveness and entransy efficiency, given above by equations 2 and 6, respectively, are of the larger better type;

$$CHP_{Tcost} = \left(\frac{CHP_{Ccost}}{20\ years}\right) + CHP_{Ocost} \tag{22}$$

where,

CHP_{Tcost} – System's total cost [€/year]

CHP_{Ccost} – System's Capital cost [€]

CHP_{Ocost} – System's Operating cost [€/year]

[f] Both cost parcels are taken directly from Aspen HYSYS' APEA (Aspen Process Economic Analyzer) sub-program.

2. Regardless of a system's cost, the most important factor is its comparison with competing technologies; other HPs and natural gas. This means a fundamental question must be posed: "Are these systems competitive with other available technologies?"[g];

3. Taking the work's goals into consideration, and seeing as information regarding these systems' optimization is relatively scarce, it is important to set some guidelines regarding the studies that will be conducted;

    a. This system is too complex for a linear and/or rigid optimization path to be followed, so each new experiment will be designed as a result of carefully evaluating all measured responses. This will result in a more balanced approach, thus preventing the work from being ruled by a single response;

    b. Considering the systems' costs vs EComp nuance and the high number of variables involved in each system, it becomes extremely arduous to optimize both performance and cost simultaneously while guaranteeing that no competitive solutions were overlooked. In view of this, a compromise was made that the systems' performance would be the major optimization focus in this study's early stages, and their cost, while not completely disregarded, would only come into consideration later;

4. Due to the present work's nature, all purely statistical treatment-oriented information (ANOVA and RA) will only be presented in its main body for each system's first two experiments, being available in appendices C, for the first, and E, for the second, from then on. This will allow a more active and dynamic results-oriented approach, which enables a more adequate and engaging pacing, while also preventing reading fatigue;

5. In keeping with the same goal as the previous item, appendix B presents the matrices used to carry out the complete factorial experiments when considering 2, 3, 4, and 5 factors (tables 88, 89, 90, and 91, respectively).

[g] Given these systems' operating conditions, they will only be compared to the alternative of natural gas to produce the same amount of heat as measured in the exothermic reactor.

Before an optimization study can be carried out, it is important that any system be as “equipment efficient” as possible. Keeping this in mind, a new assembly was implemented (figure 15) in which only one pump is employed before the endothermic reactor.

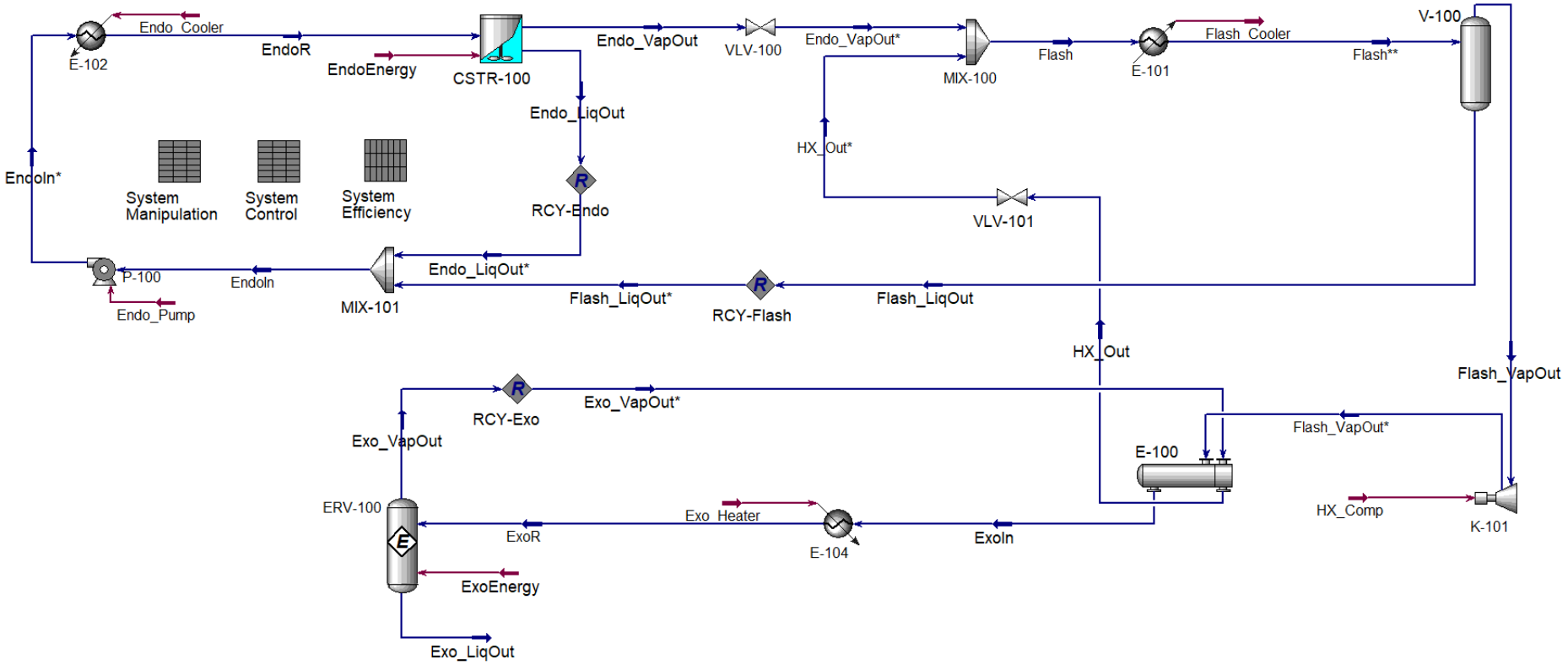

Figure 15 - Updated IAH system

After updating this system's schematics, it is finally time to begin its study. The first step is to identify the process variables which will be subjected to variation. These are presented in table 9.

Table 9 - Variables under study in the IAH system

Variable	Description	Variable's Units
T_{in} Endo	Endothermic reactor's inlet temperature	°C
T_r Endo	Endothermic reactor's operating temperature	°C
P Endo	Endothermic reactor's operating pressure	atm
T_{in} Flash	Flash separator's inlet temperature	°C
P Flash	Flash separator's operating pressure	atm
T_{in} Exo	Exothermic reactor's inlet temperature	°C
T_r Exo	Exothermic reactor's operating temperature	°C
P Exo	Exothermic reactor's operating pressure	atm

11.2.1. First experiment

Given the eight variables in study, 256 runs would be needed to study this system through a two-level full factorial design, which would mean an enormous waste of time, especially considering that one of DoE's big advantages is time-saving. Thus, a 2^{8-3} FFD was carried out. This design was chosen due to the relatively large number of variables in study, and its type IV resolution. Tables 10 and 11 present the information regarding this first experiment, such as factor levels, confounded variables, and generators used.

Table 10 - Designation and factor levels for the vaiables involved in the first experiment

Variable	Confounded?	Designation	Low-level (-)	High-level (+)
T_{in} Endo	Yes	G	45.00	55.00
T_r Endo	No	A	65.00	75.00
P Endo	No	B	1.00	2.00
T_{in} Flash	Yes	F	35.00	45.00
P Flash	No	D	1.00	2.00
T_{in} Exo	Yes	H	165.00	175.00
T_r Exo	No	C	190.00	210.00
P Exo	No	E	1.00	2.00

Table 11 - Generators used in the first experiment

Variable	Designation	Generator
T_{in} Flash	F	ABC
T_{in} Endo	G	ABD
T_{in} Exo	H	BCDE

This first experiment was carried out as presented in tables 12 and 13 where its results are also shown.

Table 12 - FFD's $2_{(IV)}^{8-3}$ matrix for the first experiment and results obtained from each run

		T_r Endo	P Endo	T_r Exo	P Flash	P Exo	Cost [M€/year]	Performance	
		A	B	C	D	E	Total	Effectiveness	Entransy
1	cd	-1	-1	1	1	-1	3.367	-2.5440	-8.2180
2	**e**	-1	-1	-1	-1	1	3.823	-0.7284	-2.1290
3	abc	1	1	1	-1	-1	5.169	-23.6060	-69.0030
4	ac	1	-1	1	-1	-1	3.994	-0.2455	-0.6873
5	ab	1	1	-1	-1	-1	2.948	0.0206	0.0522
6	c	-1	-1	1	-1	-1	5.169	-23.6060	-69.0030
7	abcde	1	1	1	1	1	1.643	-0.0688	-0.1928
8	**a**	1	-1	-1	-1	-1	2.869	-0.5435	-1.3770
9	acde	1	-1	1	1	1	2.416	-0.0723	-0.2024
10	bd	-1	1	-1	1	-1	1.526	-0.6303	-1.8430
11	**d**	-1	-1	-1	1	-1	3.236	-0.9687	-2.8320
12	**[1]**	-1	-1	-1	-1	-1	2.537	-1.0150	-2.9670
13	ad	1	-1	-1	1	-1	3.620	0.0028	0.0071
14	bde	-1	1	-1	1	1	1.544	-0.8308	-2.4280
15	de	-1	-1	-1	1	1	1.474	-0.5250	-1.5350
16	**b**	-1	1	-1	-1	-1	2.883	-21.4600	-62.7300

Table 13 - FFD's $2_{(IV)}^{8-3}$ matrix for the first experiment and results obtained from each run (continued)

		T_r Endo	P Endo	T_r Exo	P Flash	P Exo	Cost [€/year]	Performance	
		A	B	C	D	E	Total	Effectiveness	Entransy
17	bcd	-1	1	1	1	-1	1.927	-11.0900	-35.8400
18	ae	1	-1	-1	-1	1	4.598	-0.1541	-0.3903
19	abcd	1	1	1	1	-1	3.249	-0.3244	-0.9082
20	abd	1	1	-1	1	-1	2.595	0.1787	0.4527
21	abde	1	1	-1	1	1	1.567	0.0847	0.2145
22	bce	-1	1	1	-1	1	3.792	-5.3130	-17.1700
23	cde	-1	-1	1	1	1	1.668	-2.6340	-8.5080
24	bcde	-1	1	1	1	1	1.494	-0.9007	-2.9100
25	abce	1	1	1	-1	1	5.169	-23.6060	-69.0030
26	ade	1	-1	-1	1	1	2.378	0.0656	0.1662
27	bc	-1	1	1	-1	-1	2.891	-18.1700	-58.7000
28	ace	1	-1	1	-1	1	4.699	-0.0673	-0.1885
29	acd	1	-1	1	1	-1	4.109	-0.0343	-0.0959
30	be	-1	1	-1	-1	1	4.119	-3.3350	-9.7490
31	ce	-1	-1	1	-1	1	5.169	-23.6060	-69.0030
32	abe	1	1	-1	-1	1	3.836	0.1602	0.4058

Before moving on, it is important to highlight two aspects regarding the results obtained in this first experiment:

- Convergence was not attainable in assays 3, 6, 25, and 31 (highlighted). Given this situation, information regarding the system's cost and performance were not obtained, however, some data must be used when processing is carried out. Thus, a 10% penalty, with respect to the worst case, was applied (*e.g.* assay 28 represents the worst case regarding price, therefore, the assays' cost will be $\{4.699 \times 1.1 = 5.169\, M€\}$). This method was applied to each output metric (assay 16 represents the worst case regarding both performance metrics).
- The performance values obtained are in fraction form, not percentage, which means these should vary between 0 and 1. Any values outside of this range indicate that a given assay had this system's set of variables at such levels that its operation was severely compromised.

After applying the methodology presented above to all three outputs in consideration, a normal probability plot of the effects' estimates was built to judge the magnitude and the possible significance of the experiment's factors. If none of the effects is significant, then the estimates will behave like a normal distribution's random sample and the plotted effects would lie approximately along a straight line. The effects that depart from that straight line represent the possible significant factors/interactions. The normal probability plot of the effects for the response variables cost, effectiveness and entransy efficiency are represented in figures 16, 17, and 18.

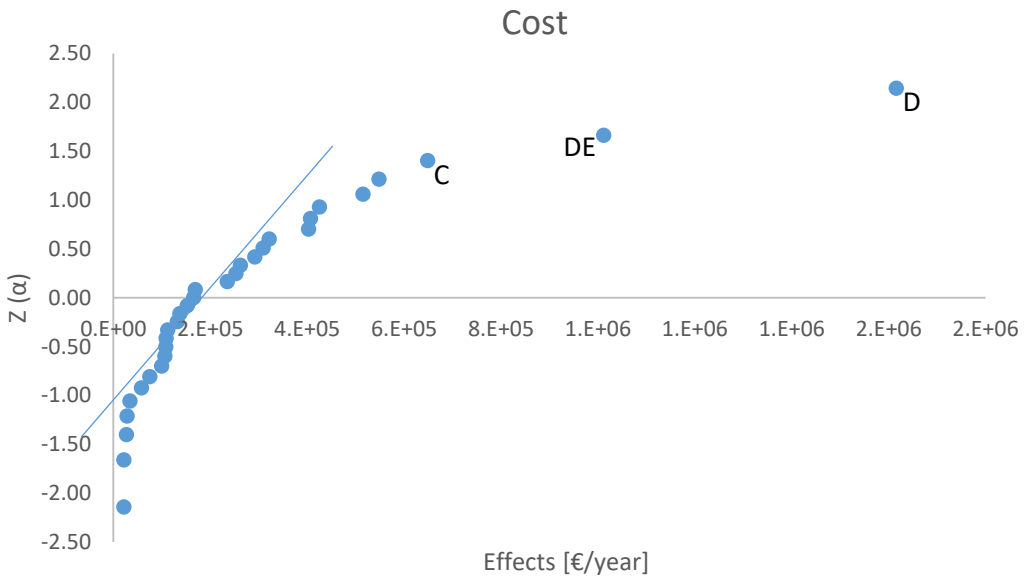

Figure 16 - Normal probability plot of the effects regarding cost

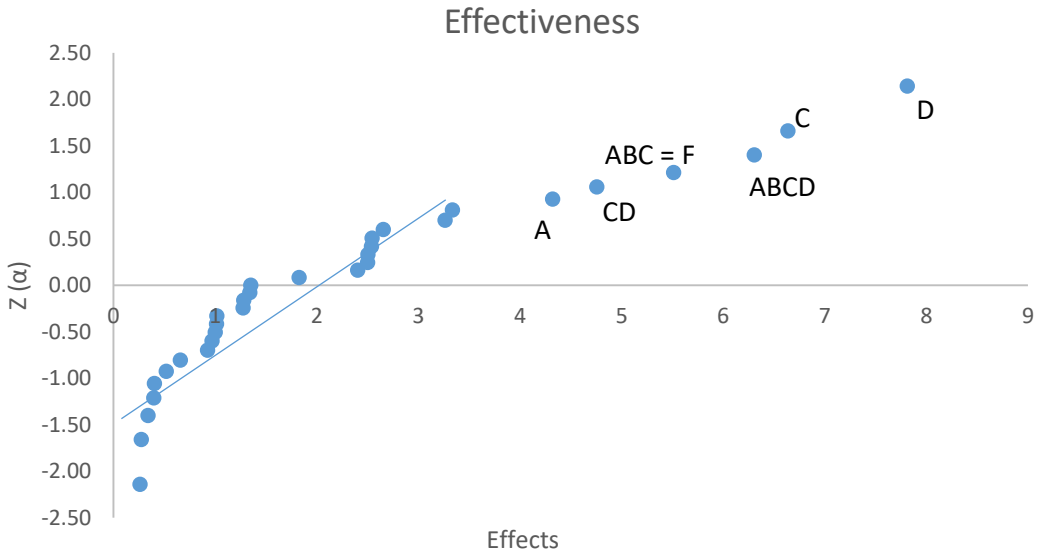

Figure 17 - Normal probability plot of the effects regarding effectiveness

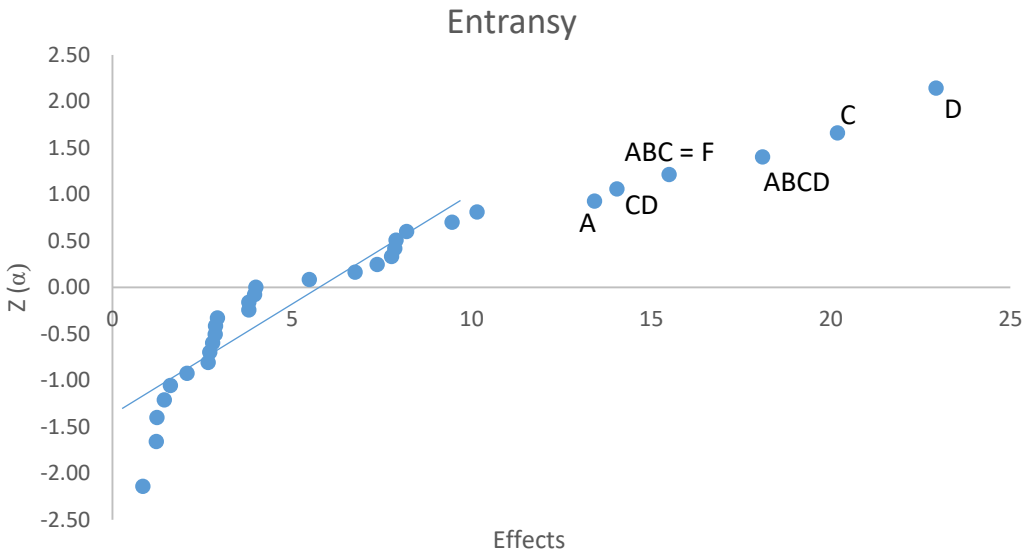

Figure 18 - Normal probability plot of the effects regarding entransy efficiency

Following this, an ANOVA was conducted in order to understand which factors/interactions affect each of the three response variables significantly, for a confidence level of 95% (tables 14, 15, and 16).

Table 14 - ANOVA results regarding cost

	SS	DF	MS	F_0	
C	3.363E+12	1	3.363E+12	5.470	
DE	8.191E+12	1	8.191E+12	13.321	
D	2.089E+13	1	2.089E+13	33.969	F. INV
Error	1.722E+13	28	6.149E+11		4.196

Table 15 - ANOVA results regarding effectiveness

	SS	DF	MS	F_0	
A	149.417	1	149.417	6.864	
CD	181.067	1	181.067	8.318	
ABC	243.071	1	243.071	11.166	
ABCD	318.288	1	318.288	14.622	
C	352.518	1	352.518	16.194	
D	488.152	1	488.152	22.425	F. INV
Error	522.432	25	21.768		4.242

Table 16 - ANOVA results regarding entransy efficiency

	SS	DF	MS	F_0	
A	1442.047	1	1442.047	7.317	
CD	1579.159	1	1579.159	8.013	
ABC	1922.792	1	1922.792	9.756	
ABCD	2622.652	1	2622.652	13.307	
C	3259.298	1	3259.298	16.538	
D	4208.327	1	4208.327	21.353	F. INV
Error	4729.958	25	197.082		4.242

After determining the significant factors/interactions, for each output, an RA was conducted to verify the model's validity. No significant deviations are noted in figures 78, 79, and 80 (Appendix C), which confirms the models' adequacy.

Before moving on to the results' analysis and discussion, it is paramount that we keep this experiment's defining relation (equation 23) and aliasing structure (table 92, appendix C) in mind as these will surely help in understanding if certain effects originate from the factors/interactions yielded directly from the ANOVA or if they may be a consequence of some alias.

$$I = ABCF = ABDG = CDFG = BCDEH = ADEFH = ACEGH = BEFGH \quad (23)$$

Now, bearing this information in mind, we can interpret the results obtained for each response.

It is possible to affirm confidently that the flash separator's operating pressure, as well as its interaction with the exothermic reactor's operating pressures influence are significant towards the system's total cost, particularly due to the fact that these two factors influence the number of compressors utilized. Factor C (exothermic reactor's operating temperature) also affects the system's cost significantly due to its influence on the cold utility needed to cool the stream entering the flash separator.

Regarding the system's performance responses (effectiveness and entransy efficiency), it is much more likely that the interaction ABCD is in fact the interaction between the flash separator's inlet temperature (F = ABC) and its operating pressure (D), especially as the former is the second most significant factor. The CD apparently stems from the exothermic reactor's operating temperature and the flash separator's operating pressure, however, this does not seem very intuitive. A much more plausible source of this result is the aliased interaction FG (endothermic reactor and flash separator's inlet temperatures), which means this uncertainty must be resolved in following experiments. The endothermic reactor's operating temperature (A) is likely to be in and of itself significant towards the system's performance, particularly considering this factor appears in both equations.

Overall, the results presented indicate that the flash separator's operating pressure and inlet temperature (D and F, respectively), as well as both endo and exothermic reactor's operating temperatures (A and C, respectively), influence the system's operation considerably. This could have lead us to disregard all other variables and focus only on these four, however, it must be noted that the factors' interactions also play an important role in the overall system. Thus, a reverse approach was taken, instead of focusing on the most influential factors, the least influential were set at the values indicated as best by their respective effects.

Table 17 presents a summary of each factor's improvement direction for all three outputs.

Table 17 - First experiment's faxtors' improvement direction summary

		Cost		Effectiveness		Entransy	
		S?	D?	S?	D?	S?	D?
T_{in} Endo	G	No	+	No	+	No	+
T_r Endo	A	No	-	Yes	+	Yes	+
P Endo	B	No	+	No	-	No	-
T_{in} Flash	F	No	-	Yes	-	Yes	-
P Flash	D	Yes	+	Yes	+	Yes	+
T_{in} Exo	H	No	+	No	+	No	+
T_r Exo	C	Yes	-	Yes	-	Yes	-
P Exo	E	No	+	No	+	No	+

Given the existence of multiple outputs, it may be difficult to choose a direction of study for the different variables in consideration, however, as stated earlier, the system's performance (effectiveness and entransy efficiency) will be our major focus for the time being. Thus, the following observations can be made by considering the information presented in table 17:

- Both reactors' inlet temperatures, as well as the exothermic reactor's operating pressure, will be set to their best levels performance-wise;
    - Both reactor's inlet temperatures will be set at this study's high level in both situations;
    - The exothermic reactor's operating pressure will also be set this study's high-level;
- The remaining variables will vary around this study's best level for each;
    - The endothermic reactor's operating temperature and the flash separator's operating pressure will revolve around their respective high level values;
    - The endothermic reactor's operating pressure, the flash separator's inlet temperature, and the exothermic reactor's operating temperature will revolve around their respective low level values.

In accordance with these observations, a 2^5 complete factorial design experiment will be carried out using the variables stated above (T_r Endo, P Endo, T_{in} Flash, P Flash, and T_r Exo)

11.2.2. Second experiment

Given the first experiment's findings, the system was updated as presented in table 18. The values chosen for the variables which will be studied were determined by taking their best level from the previous experiment and applying a somewhat similar amplitude. This selection is particularly important when pressure manipulation is involved due to the high costs typically involved, thus, special care was taken to avoid the need for duplicate equipment (*i.e.*, an attempt was made to employ the minimum amount possible of pressure increasing equipment).

Table 18 - Designation and factor levels for the vaiables involved in the second experiment

Variable	Designation	Low-level (-)	High-level (+)
T_{in} Endo			55.00
T_r Endo	A	70.00	78.00
P Endo	B	2.30	2.70
T_{in} Flash	F	30.00	40.00
P Flash	D	1.80	2.20
T_{in} Exo			175.00
T_r Exo	C	185.00	195.00
P Exo			2.10

This second experiment was carried out as presented in table 91 (Appendix B).

This study yielded the results presented in table 19.

Table 19 - Resuts obtained from the second experiment

		Cost [M€/year]	Performance	
		Total	Effectiveness	Entransy
1	**[1]**	1.441	-0.1934	-0.5111
2	**a**	1.635	0.2765	0.6558
3	**b**	1.441	-0.2659	-0.7027
4	ab	1.587	0.3004	0.7126
5	**c**	1.511	-0.7839	-2.1840
6	ac	1.574	0.2199	0.5496
7	bc	1.510	-1.0190	-2.8400
8	abc	1.525	0.2279	0.5697
9	**d**	1.633	-0.1807	-0.4475
10	ad	1.880	0.2673	0.6339
11	bd	1.613	-1.1930	-3.1520
12	abd	1.815	0.3115	0.7388
13	cd	1.619	-0.4548	-1.2670
14	acd	1.824	0.2034	0.5085
15	bcd	1.618	-0.5666	-1.5780
16	abcd	1.752	0.2271	0.5678
17	**f**	1.523	-0.4295	-1.1350
18	af	1.757	0.2985	0.7079
19	bf	1.540	-0.3554	-0.9392
20	abf	1.585	0.3165	0.7506
21	cf	1.494	-0.6692	-1.8640
22	acf	1.672	0.2345	0.5864
23	bcf	1.493	-0.8310	-2.3150
24	abcf	1.436	0.2375	0.5937
25	df	1.625	-0.2353	-0.6220
26	adf	1.716	0.2876	0.6821
27	bdf	1.624	-0.3161	-0.8354
28	abdf	1.734	0.3068	0.7277
29	cdf	1.580	-0.5906	-1.6450
30	acdf	1.710	0.2265	0.5663
31	bcdf	1.733	-1.2820	-3.5710
32	abcdf	1 601	0.2313	0.5782

Even before moving on to this data's ANOVA, it is possible to confidently declare that this new experiment was a step in the right direction as, compared to the first experiment, this new study does not present any situation in which convergence was not attained, and the number of situations in which the system was inoperable (*i.e.*, negative performance values) has also

decreased. However, despite these improvements, 50% of this experiments' assays resulted in inoperable solutions, meaning there is still ample room for enhancement.

After applying the methodology described above to all three outputs in consideration, the following graphs were obtained (figures 19, 20, and 21).

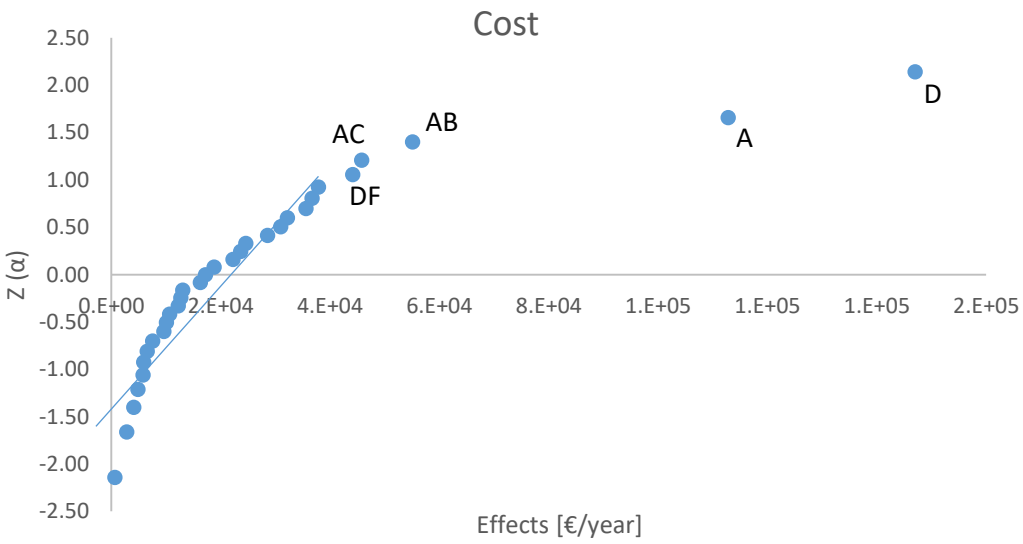

Figure 19 - Normal probability plot of effects regarding cost

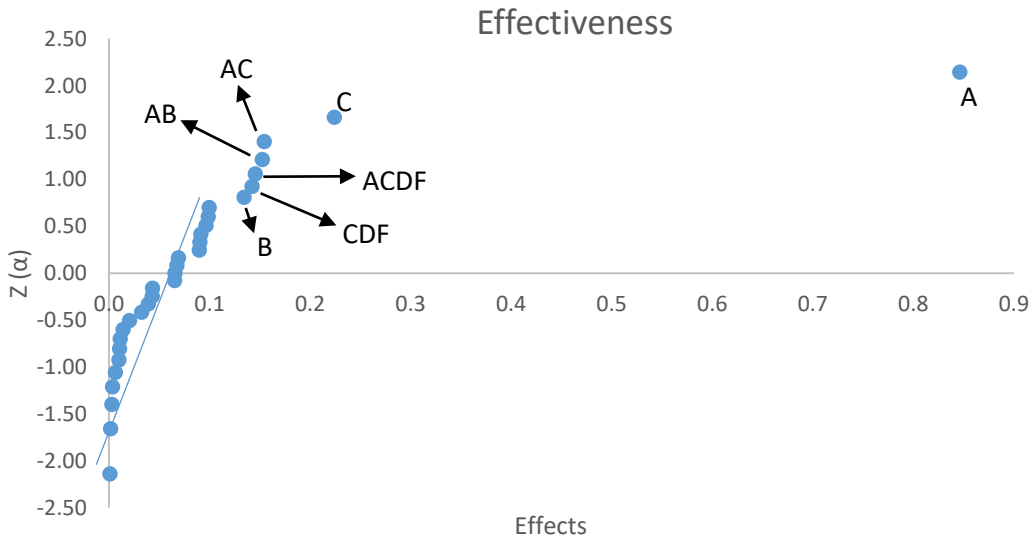

Figure 20 - Normal probability plot of effects regarding effectiveness

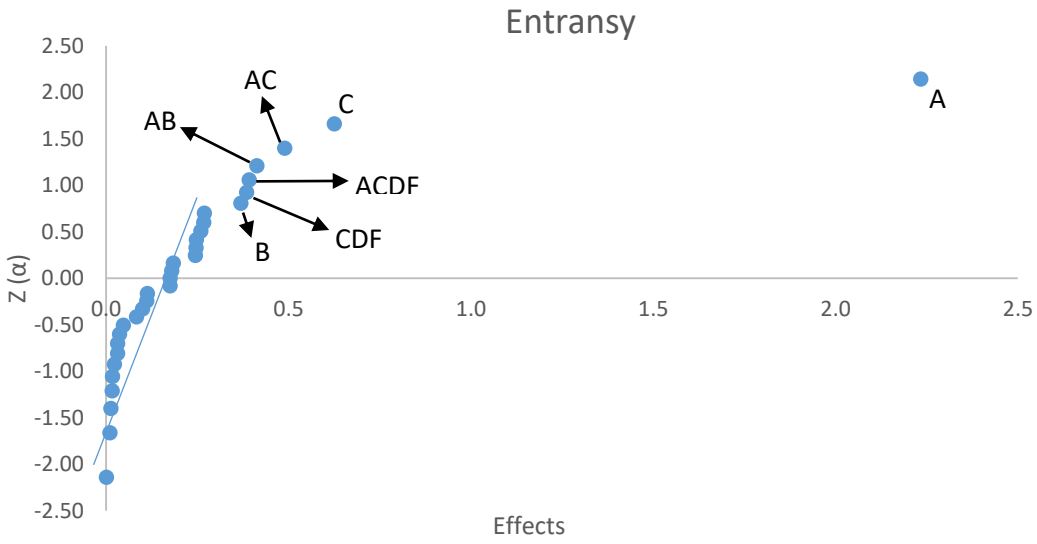

Figure 21 - Normal probability plot of effects regarding entransy efficiency

After this, an ANOVA was conducted in order to understand which factors/interactions significantly affect each output, for a confidence level of 95% (tables 20, 21, and 22).

Table 20 - ANOVA results regarding cost

	SS	DF	MS	F_0	
DF	1.557E+10	1	1.557E+10	5.410	
AC	1.676E+10	1	1.676E+10	5.824	
AC	2.426E+10	1	2.426E+10	8.429	
A	1.018E+11	1	1.018E+11	35.359	
D	1.729E+11	1	1.729E+11	60.093	F. INV
Error	7.195E+10	25	2.878E+09		4.242

Table 21 - ANOVA results regarding effectiveness

	SS	DF	MS	F_0	
B	0.144	1	0.144	6.039	
CDF	0.162	1	0.162	6.789	
ACDF	0.169	1	0.169	7.098	
AB	0.186	1	0.186	7.779	
AC	0.191	1	0.191	8.000	
C	0.402	1	0.402	16.840	
A	5.729	1	5.729	240.231	F. INV
Error	0.548	24	0.024		4.260

Table 22 - ANOVA results regarding entransy efficiency

	SS	DF	MS	F_0	
B	1.091	1	1.091	6.315	
CDF	1.185	1	1.185	6.859	
ACDF	1.232	1	1.232	7.131	
AB	1.364	1	1.364	7.894	
AC	1.916	1	1.916	11.088	
C	3.130	1	3.130	18.117	
A	39.914	1	39.914	231.010	F. INV
Error	3.974	24	0.173		4.260

After determining the significant factors/interactions, for each output, an RA was conducted to verify the model's validity. No significant deviations are noted in figures 81, 82, and 83 (Appendix C), which confirms the models' adequacy.

The results obtained from this second experiment indicate that the endothermic reactor's operating temperature (A) and the flash separator's operating pressure influence the system's cost significantly. This is due to their influence on the heat-exchanger set after the reactor, and the utility it needs to operate, which will be more expensive as their respective values increase. The system's performance is mostly affected by both reactors' operating temperatures, which does not come as a surprise as these values are directly present in both equations. Aside from these, the endothermic reactor's operating pressure (B) also influences the system's performance as it impacts the heat receiving capacity of the endothermic reaction, and the flash separator's operating conditions also influence the system due to their role in separating the components sent to each reactor. Given these findings, the flash separator's inlet temperature will be set at its best level and the remaining variables will serve as the next study's focus. The new values are determined by using the information presented in table 23 which presents a summary of each factor's improvement direction for all three outputs.

Table 23 - Second experiment's faxtors' improvement direction summary

		Cost		Effectiveness		Entransy	
		S?	D?	S?	D?	S?	D?
T_r Endo	A	Yes	-	Yes	+	Yes	+
P Endo	B	No	+	Yes	-	Yes	-
T_{in} Flash	F	No	+	No	+	No	+
P Flash	D	Yes	-	No	-	No	-
T_r Exo	C	No	+	Yes	-	Yes	-

Considering the information presented above, the following decisions can be made:

- The flash separator's inlet temperature should be set to this study's high-level (40 °C);
- The remaining variables should vary thusly:
    - The endothermic reactor's operating temperature should vary around this study's high-level;
    - All other variables should vary around their respective low-level in this study.

Accordingly, a 2^4 complete factorial design experiment will be carried out using the variables stated above (T_r Endo, P Endo, P Flash, and T_r Exo).

11.2.3. Third experiment

This being said, table 24 presents the system's updated operation parameters.

Table 24 - Designation and factor levels for the vaiables involved in the third experiment

Variable	Designation	Low-level (-)	High-level (+)
T_{in} Endo			55.00
T_r Endo	A	75.00	78.00
P Endo	B	1.80	2.20
T_{in} Flash			40.00
P Flash	D	1.50	2.00
T_{in} Exo			175.00
T_r Exo	C	180.00	185.00
P Exo			2.10

This third experiment was carried out as presented in table 90 (Appendix B).

This study yielded the results presented in table 25.

Table 25 - Results obtained from the third experiment

		Cost [M€/year]	Performance	
		Total	Effectiveness	Entransy
1	**[1]**	2.068	0.2699	0.6477
2	**a**	2.444	0.2744	0.6331
3	**b**	2.004	0.3109	0.7463
4	ab	2.277	0.3319	0.7659
5	**c**	2.123	0.2331	0.5749
6	ac	2.334	0.2506	0.5944
7	bc	2.113	0.2174	0.5361
8	abc	2.206	0.2981	0.7071
9	**d**	2.037	0.2621	0.6290
10	ad	2.526	0.2468	0.5695
11	bd	1.797	0.2668	0.6402
12	abd	1.983	0.3103	0.7161
13	cd	1.942	0.2235	0.5512
14	acd	2.465	0.2176	0.5162
15	bcd	1.721	0.2342	0.5776
16	abcd	1.911	0.2837	0.6729

Even before any data processing, it is once again possible to affirm confidently that this new study was a step in the right direction since all 16 assays in the present experiment yielded viable solutions (i.e., positive performance values).

After applying the same methodology as earlier to all responses considered, the graphs in figures 22, 23, and 24 were obtained.

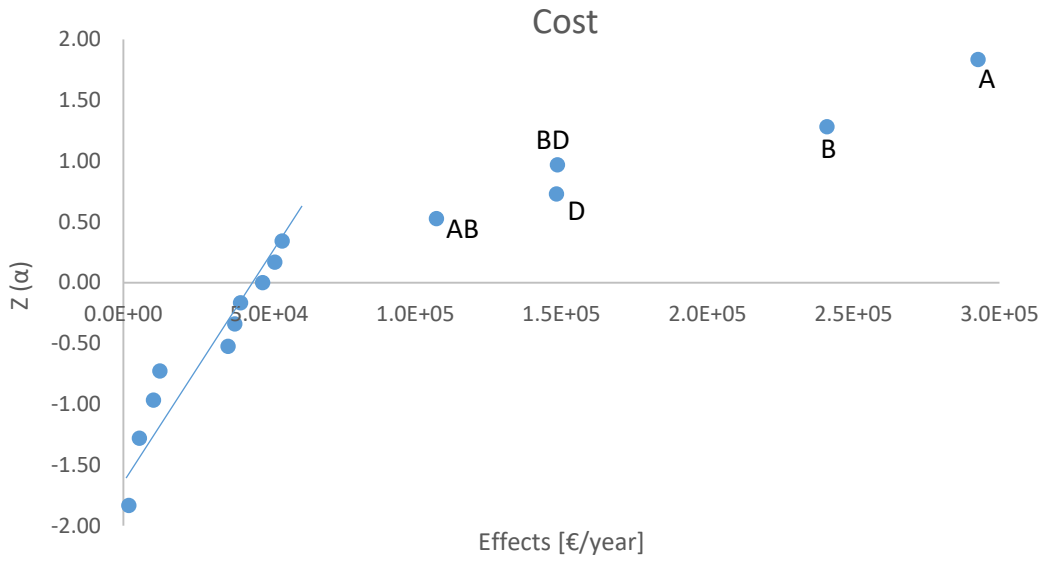

Figure 22 - Normal probability plot of effects regarding cost

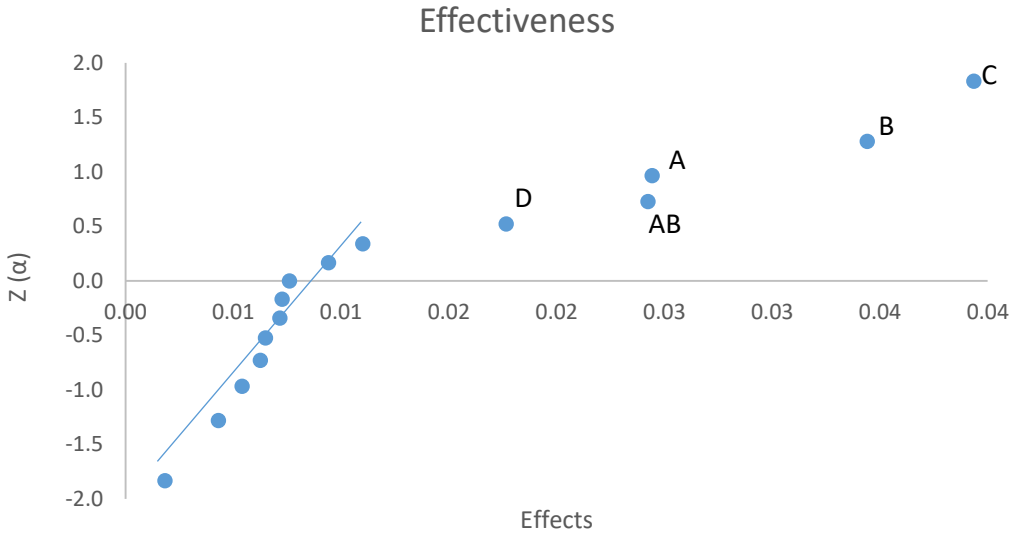

Figure 23 - Normal probability plot of effects regarding effectiveness

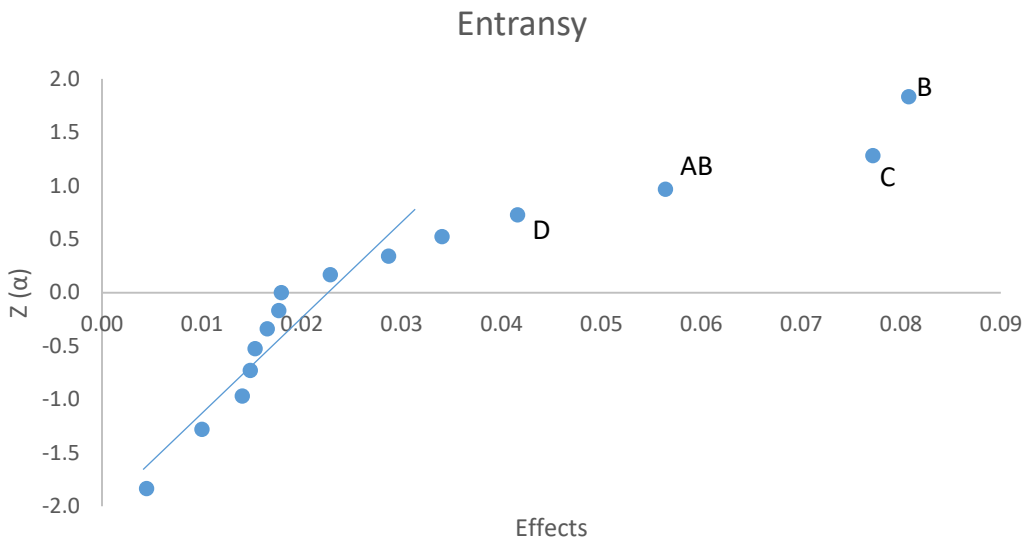

Figure 24 - Normal probability plot of effects regarding entransy efficiency

As per the explanation above, this study's ANOVA and RA are available in appendix C (tables 93, 94, and 95, and figures 84, 85, and 86, respectively). There are no significant deviations in the figures mentioned, which validates the model in use.

Similarly to the previous experiments, the endothermic reactor's operating conditions and the flash separator's operating pressure are the most impactful factors regarding the system's cost. Regarding the system's performance, there are some minor differences between the two responses considered here. Whereas the system's effectiveness, which translates its enthalpy efficiency, is most significantly influenced by the exothermic reactor's operating temperature, which correlates to its heat-promotion capacity, the entransy efficiency, which translates the system's entropy efficiency, is most significantly influenced by the endothermic reactor's operating pressure, which correlates to its heat-receiving capacity.

The results obtained from this experiment indicate that all considered variables are significant in one way or another. This means a following study would involve the same variables studied here with slightly different variation ranges around each's best value, however, it is important to understand how these variables behave, and interact with one another, in smaller, more contained, scenarios. As such, it was decided that the next study will involve the endothermic reactor's operating pressure and the flash separator's inlet temperature.

Table 26 presents a summary of each factor's improvement direction for all three outputs. This information will be used to determine each variables' new range/value for the following study.

Table 26 - Third experiment's faxtors' improvement direction summary

		Cost		Effectiveness		Entransy	
		S?	D?	S?	D?	S?	D?
T_r Endo	A	Yes	-	Yes	+	No	+
P Endo	B	No	+	Yes	+	Yes	+
P Flash	D	Yes	+	Yes	-	Yes	-
T_r Exo	C	No	+	Yes	-	Yes	-

According to the information presented:

- The endothermic reactor's operating temperature should be set to this study's high-level (78 °C);
- The flash separator's operating pressure should be set to this study's low-level (1.50 atm);
- The exothermic reactor's operating temperature should be set to this study's low-level (180 °C);
- The endothermic reactor's operating pressure should vary around this study's high-level (2.20 atm), however, a decision was made to use a similar variation range so as to evaluate this variable's behavior in a situation where no other equipment's operating pressure is under study.
- Given the flash separator's inlet temperature's evolution throughout the studies presented above, its value should fluctuate around 40 °C.

Accordingly, a 2^2 complete factorial design experiment will be carried out using the variables stated above (P Endo and T_{in} Flash).

11.2.4. Fourth experiment

Given the previous experiment's findings, the system was updated as presented in table 27. The values chosen for the variables which will be studied were determined by taking their best level from the previous experiment and applying a somewhat similar amplitude.

Table 27 - Designation and factor levels for the vaiables involved in the fourth experiment

Variable	Designation	Low-level (-)	High-level (+)
T_{in} Endo			55.00
T_r Endo			78.00
P Endo	B	1.70	2.20
T_{in} Flash	F	35.00	40.00
P Flash		1.50	
T_{in} Exo			175.00
T_r Exo		180.00	
P Exo			2.10

This fourth experiment was carried out as presented in table 88 (Appendix B).

This study yielded the results presented in table 28.

Table 28 - Results obtained from the fourth experiment

		Cost [M€/year]	Performance	
		Total	Effectiveness	Entransy
1	**[1]**	2.556	0.2456	0.5668
2	**b**	2.276	0.3164	0.7302
3	**f**	2.751	0.2535	0.5850
4	bf	2.277	0.3319	0.7659

Due to the low number of variables in study, it is possible to observe that the best results occur when B (P Endo) is at its high-level. Another important aspect is that these results indicate that a higher system performance is accompanied by a lower cost, which is extremely desirable from a system optimization standpoint.

Figures 25, 26, and 27, show that the present study only yielded the endothermic reactor's operating pressure as a significant factor, which means this variable's influence on the system is much greater than the flash separator's inlet temperature's.

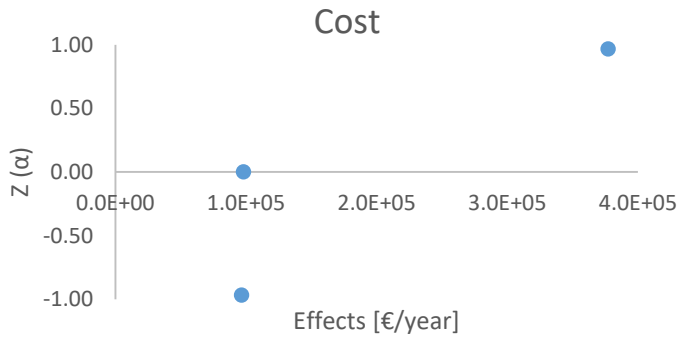

Figure 25 - Normal probability plot of effects regarding cost

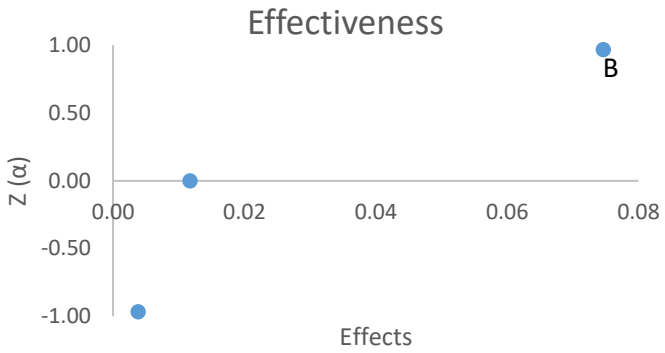

Figure 26 - Normal probability plot of effects regarding effectiveness

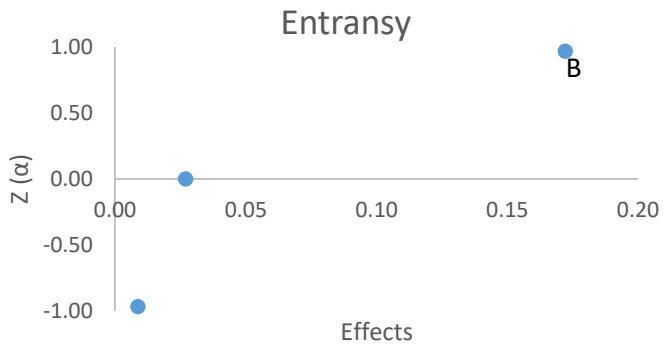

Figure 27 - Normal probability plot of effects regarding entransy efficiency

Figures 87 and 88, in Appendix C, attest to the model's adequacy.

Table 29 presents a summary of each factor's improvement direction for all three outputs. This information will be used to determine each variables' new range/value for the following study.

Table 29 - Fourth experiment's factors' improvement direction summary

		Cost		Effectiveness		Entransy	
		S?	D?	S?	D?	S?	D?
P Endo	B	No	+	Yes	+	Yes	+
T_{in} Flash	F	No	-	No	+	No	+

Given these findings, the endothermic reactor's operating pressure should vary close to its high-level (2.2 atm), and the flash separator's inlet temperature should be set to its high-level (40 °C).

11.2.5. Fifth experiment

Given the studies performed and the results obtained thus far, a new experiment in which the endothermic reactor's inlet temperature and operating pressure, as well as the exothermic reactor's operating pressure, will be studied was developed. Table 30 presents the values/ranges used in this experiment.

Table 30 - Designation and factor levels for the vaiables involved in the fifth experiment

Variable	Designation	Low-level (-)	High-level (+)
T_{in} Endo	G	55.00	65.00
T_r Endo			78.00
P Endo	B	2.00	2.20
T_{in} Flash			40.00
P Flash		1.50	
T_{in} Exo			175.00
T_r Exo		180.00	
P Exo	E	2.00	2.50

This fifth experiment was carried out as presented in table 89 (Appendix B).

This study yielded the results presented in table 31.

Table 31 - Results obtained from the fifth experiment

		Cost [M€/year]	Performance	
		Total	Effectiveness	Entransy
1	**[1]**	2.313	0.3096	0.7145
2	**g**	2.410	0.3158	0.7288
3	**b**	2.240	0.3263	0.7529
4	bg	2.332	0.3420	0.7893
5	**e**	2.905	0.3058	0.7056
6	eg	3.022	0.3192	0.7367
7	be	2.842	0.3304	0.7624
8	beg	2.939	0.3464	0.7995

Figures 28, 29, and 30, show that all three factors in study are significant regarding the system's cost, but a clear detachment can be observed regarding the exothermic reactor's operating pressure, which is to be expected given its direct influence on the system's main cost source, the energy needed for the compressor's operation. The system's performance is most significantly influenced by the endothermic reactor's operating pressure, which is the only factor in this study that exerts any influence on the system's heat receiving, or promotion, capabilities.

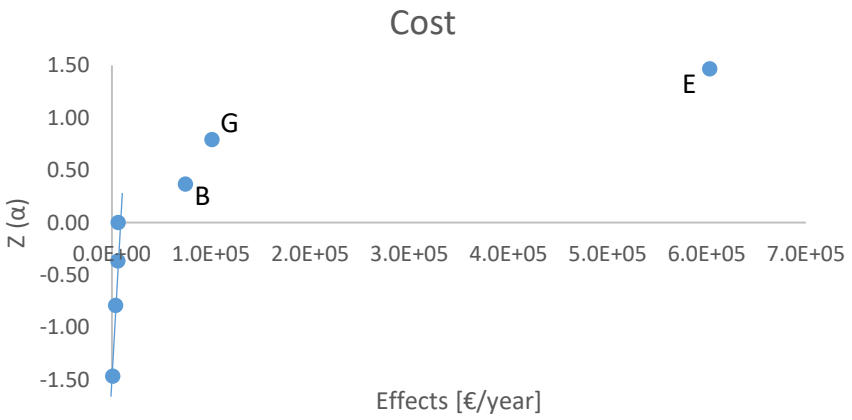

Figure 28 - Normal probability plot of effects regarding cost

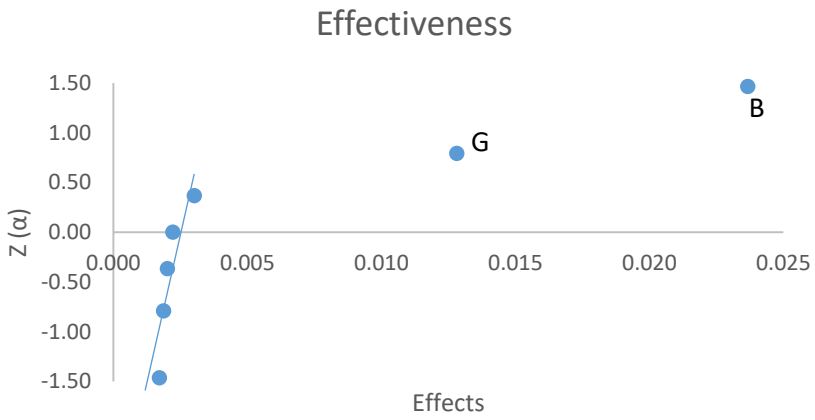

Figure 29 - Normal probability plot of effects regarding effectiveness

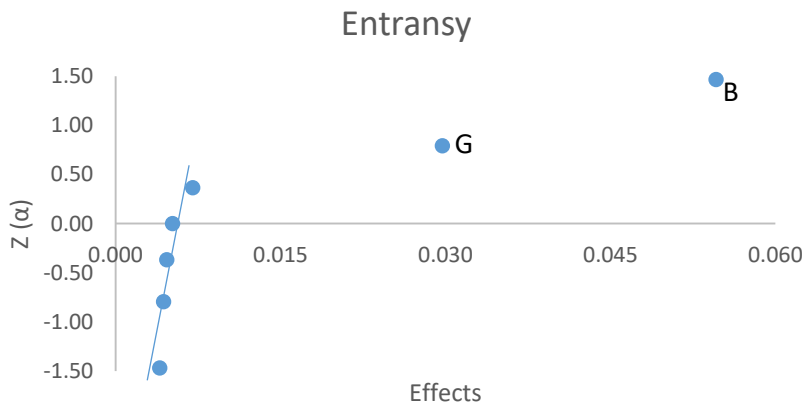

Figure 30 - Normal probability plot of efects regarding entransy efficiency

Figures 89, 90, and 91, in Appendix C, do not show significant any deviations, therefore attesting to the model's adequacy

Table 32 presents a summary of each factor's improvement direction for all three outputs. This information will be used to determine each variables' new range/value for the following study.

Table 32 - Fifth experiment's factors' improvement direction summary

		Cost		Effectiveness		Entransy	
		S?	D?	S?	D?	S?	D?
T_{in} Endo	G	Yes	-	Yes	+	Yes	+
P Endo	B	Yes	-	Yes	-	Yes	+
P Exo	E	Yes	-	No	+	No	+

Given the information presented and the focus given to the endothermic reactor's operating pressure, a decision was made to shift our focus to the other variables going forward. Thus:

- The endothermic reactor's operating pressure shall be set to its high-level (2.20 atm);
- The endothermic reactor's inlet temperature shall vary around this study's high-level (65 °C);
- Seeing as it is only significant regarding the system's cost, the exothermic reactor's operating pressure shall vary around this study's low-level (2.00 atm).

11.2.6. Sixth experiment

Given the previous experiment's findings, the system was updated as presented in table 33. The values chosen for the variables which will be studied were determined by taking their best level from the previous experiment and applying a somewhat similar amplitude.

Table 33 - Designation and factor levels for the vaiables involved in the sixth experiment

Variable	Designation	Low-level (-)	High-level (+)
T_{in} Endo	G	65.00	75.00
T_r Endo			78.00
P Endo			2.20
T_{in} Flash			40.00
P Flash		1.50	
T_{in} Exo			175.00
T_r Exo		180.00	
P Exo	E	1.80	2.10

This sixth experiment was carried out as presented in table 88 (Appendix B).

This study yielded the results presented in table 34.

Table 34 - Results obtained from the sixth experiment

		Cost [M€/year]	Performance	
		Total	Effectiveness	Entransy
1	**[1]**	2.069	0.3398	0.7841
2	**g**	2.131	0.3606	0.8322
3	**e**	2.191	0.3486	0.8045
4	eg	2.448	0.3597	0.8301

Due to the low number of variables in study, it is possible to observe that the best cost-wise results occur when both factors are at their low-level. Performance-wise, the best results occur when G (T_{in} Endo) is at its high-level and E (P Exo) is at its low-level.

Figures 92, 93, and 94, show that the present study did not yield any of the two factors, nor their interaction, as significant, which means these two variables will surely have very little influence on the system's overall operation. Given that there are no significant factors/interactions, it is not possible to perform this experiment's ANOVA for any of the responses.

Table 35 presents a summary of each factor's improvement direction for all three outputs. This information will be used to determine each variables' new range/value for the following study.

Table 35 - Sixth experiment's factors' improvement direction summary

		Cost		Effectiveness		Entransy	
		S?	D?	S?	D?	S?	D?
T_{in} Endo	G	No	-	No	+	No	+
P Exo	E	No	-	No	+	No	+

Given these findings, especially the fact that neither variables are significant toward any of the outputs considered, the least expensive line of progress is considered the most attractive, therefore both variables should fluctuate towards each of their low-level values (65 °C and 1.80 atm).

11.2.7. Seventh experiment

Given the studies performed thus far, and their results, a new experiment in which the endo and exothermic reactors' and the flash separator's inlet temperatures will be studied was developed. This experiment aims to understand if the reactors offer better results when operating in isothermal mode, *i.e.*, equal inlet and operating temperatures. Table 36 presents the values/ranges used.

Table 36 - Designation and factor levels for the vaiables involved in the seventh experiment

Variable	Designation	Low-level (-)	High-level (+)
T_{in} Endo	G	75.00	78.00
T_r Endo			78.00
P Endo			2.20
T_{in} Flash	F	40.00	50.00
P Flash		1.50	
T_{in} Exo	H	175.00	180.00
T_r Exo		180.00	
P Exo		1.80	

This seventh experiment was carried out as presented in table 89 (Appendix B).

This study yielded the results presented in table 37.

Table 37 - Results obtained from the seventh experiment

		Cost [M€/year]	Performance	
		Total	Effectiveness	Entransy
1	**[1]**	2.155	0.3595	0.8296
2	**g**	2.209	0.3628	0.8372
3	**f**	2.305	0.3589	0.8282
4	fg	2.321	0.3626	0.8368
5	**h**	2.256	0.3858	0.8903
6	gh	2.289	0.3919	0.9044
7	fh	2.221	0.4097	0.9454
8	fgh	2.417	0.4096	0.9452

Figures 31, 32, and 33, show that none of the factors considered here are significant towards the system's cost and that the exothermic reactor and the flash separator's inlet temperatures are significant towards the system's performance. Additionally, the former is considerably more impactful than the latter, as can also be seen in table 37.

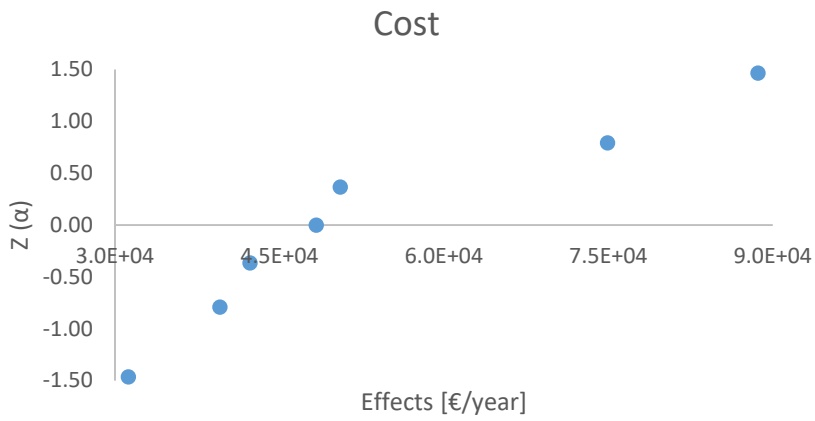

Figure 31 - Normal probability plot of effects regarding cost

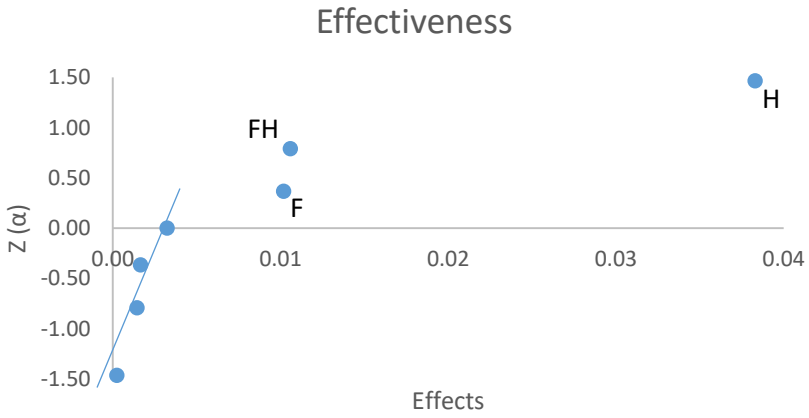

Figure 32 - Normal probability plot of effects regarding effectiveness

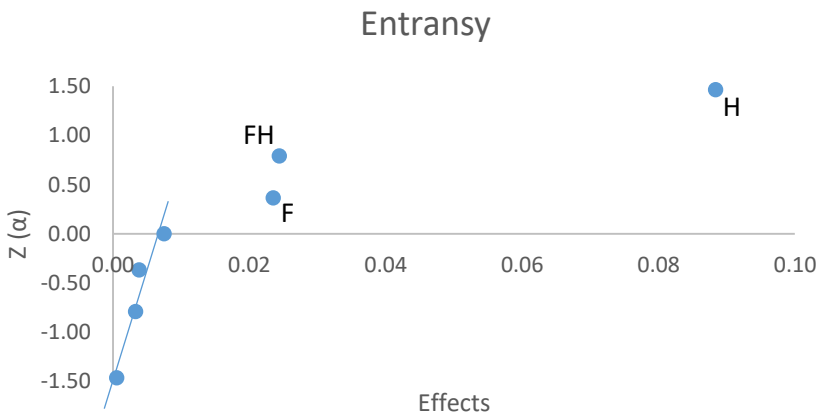

Figure 33 - Normal probability plot of effects regarding entransy efficiency

Figures 95 and 96, in Appendix C, do not show significant any deviations, therefore attesting to the model's adequacy.

Table 38 presents a summary of each factor's improvement direction for all three outputs.

Table 38 - Seventh experiment's factors' improvement direction summary

		Cost		Effectiveness		Entransy	
		S?	D?	S?	D?	S?	D?
T_{in} Endo	G	No	-	No	+	No	+
T_{in} Flash	F	No	-	Yes	+	Yes	+
T_{in} Exo	H	No	-	Yes	+	Yes	+

These results indicate that the endothermic reactor does not offer better results in isothermal mode, however, the contrary is verified for the exothermic reactor, which should not come as a surprise since this means that all the heat produced by the exothermic reaction will be available for release. The flash separator's inlet temperature yields better results at this study's high-level although, as with both other variables, this influence must be weighed against the associated increased costs.

Given this information and the number of experiments carried out, we believe it is time to expand this system's study into other territories such as testing its EComp and the viability of other structural designs.

11.2.8. Summary of the Designed Experiments study

Given the large amount of information presented thus far, it is important to condense and summarize some of the DoE studies' major findings.

As can be seen by the figures presented, the system's cost (figure 34) tends to increase alongside the performance (figure 35), which seems to indicate that this performance increase comes at the expense of the increased cost, however, noting that experiment 6 sees an increase in performance and a decrease in cost, means this correlation can be rejected. Another important consideration regarding the system's cost comes from the use, or not, of duplicate equipment, especially those responsible for pressure increasing. Experiments 2 and 3 are good examples of this situation where an additional compressor was sometimes needed due to the operating pressure ranges chosen for the reactors and the flash separator.

Regarding the system's performance, we must keep in mind that these are a product of its heat capacity (figure 36), which means high performance values should always be considered next to their respective heat capacity values. This care is crucial in the sense that it prevents hasty conclusions and statements that solution X is better than Y or Z, which could be the case when comparing experiments 5, 6, and 7, for example. Looking at their performance values, one would immediately declare experiment 7 as the best, however, this experiment sees a decrease of around 450 kW in high-temperature heat capacity. This decrease may not seem significant, but the fact is that it might be the difference between a competitive and non-competitive solution. In addition, decreasing low-temperature heat capacity values may not always be desired, meaning these must also be considered in some manner when discussing a given solution's viability.

Overall, the system's performance and heat capacity improved as the experiments progressed. The endothermic reactor's operating temperature and pressure and the exothermic reactor's operating temperature were the most influential factors toward these two responses, meaning the former are the most impactful variables toward the system's low-temperature heat absorption capacity, and the latter is the most influential toward the system's high-temperature heat generation capability.

Regarding the system's cost, this response's behavior is not linear, mainly due to the exothermic reactor's operating pressure, which assumed lower values in experiments 6 and 7. Considering this factor's direct influence on the flowsheet's most expensive equipment, both from an acquisition and operating standpoint, we can affirm that the exothermic reactor's

operating pressure is the most influential factor regarding the system's total cost. Though much less influential *per se*, the flash separator's operating pressure can also affect the system's cost if the different pressure values used throughout the system result in the need for an additional compressor before this equipment, meaning close attention must also be payed to this factor.

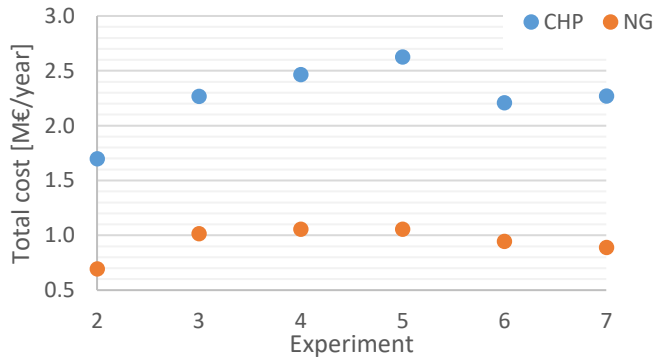

Figure 34 - Average CHP and NG costs for each experiment in the IAH system's DoE study

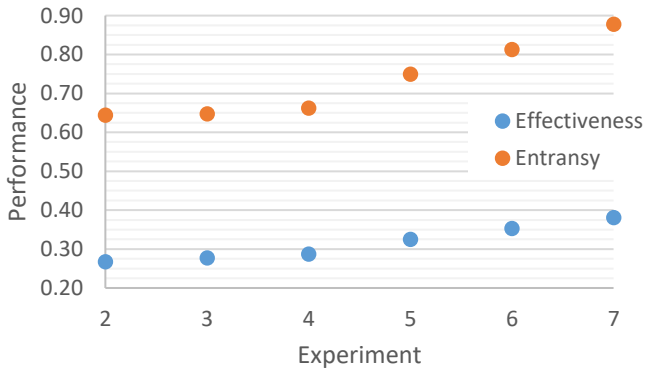

Figure 35 - Average performance for each experiment in the IAH system's DoE study

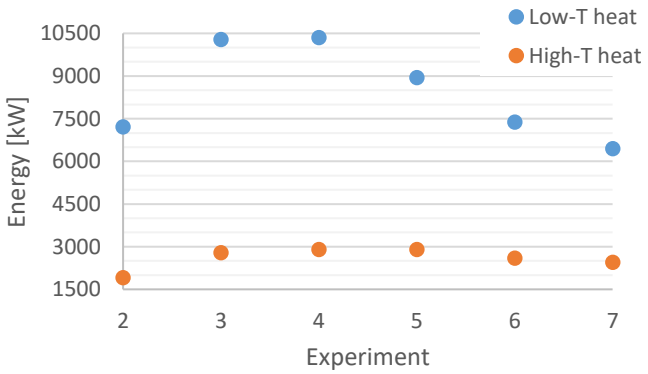

Figure 36 - Average low- and high-T heats for each experiment in the IAH system's DoE study

11.2.9. Competitive Assays

Given the large number of experiments carried out, table 39 presents the “best” operating conditions for the IAH system.

Table 39 - “Best” operating conditions for the IAH system

Variable	“Best” level	Variable	“Best” level
T_{in} Endo	78.00	P Flash	1.50
T_r Endo	78.00	T_{in} Exo	180.00
P Endo	2.20	T_r Exo	180.00
T_{in} Flash	50.00	P Exo	1.80

Although this set of conditions results in the best performance/cost scenario, it does not account for the issue of EComp. This may seem odd, however, it is important to keep in mind that higher performance values do not necessarily translate to higher heat promotion values. More often than naught, higher performance is accompanied by lower heat values, which is explicable by the fact that lower heat values result in lower heat losses and entropy generation throughout the system, thus resulting in higher performance.

As mentioned above, this system’s EComp will only be assessed against the use of natural gas (NG), however, it must be noted that, in a real-world implementation scenario, all solutions capable of reaching the same outcome must be compared against one another.

To make this comparison, it is necessary to determine the cost of producing the same amount of heat as that recovered in the exothermic reactor. Aiming to simplify the problem at hand, and given that our goal is to determine this system’s viability, only the raw-material cost[145,146] (table 40) and carbon tax (CT)[147–149] (table 41) will be taken into account.

Table 40 - Natural gas price used in this work[h]

Source	Price	Units
Eurostat	0.030	€/kW

[h] Considering the systems’ continuously working nature, an operation of 8000 h/year was employed.

Table 41 - Carbon tax values used in this work

Rate used in	Value	Units
(European average)	35.85	€/ton CO_2
Finland	62.18	
Sweden	108.81	

In view of the fact that the CHP solutions found thus far are more expensive than the use of natural gas, equation 24 will be used to translate just how much more expensive the former are relative to the latter, *i.e.*, the CHP solutions will be more competitive the closer equation 24's results approach zero, and will be "better" than using natural gas if negative excess cost (ECst)[i] values are obtained.

$$ECst\ (\%) = \frac{CHP_{Tcost} - NG_{cost}}{CHP_{Tcost}} \times 100 \quad (24)$$

where,

CHP_{Tcost} – CHP system's total cost

NG_{cost} – Natural gas' acquisition cost

Before moving on, it is important to clarify that the natural gas costs used to determine the system's ECst utilize the European average's CT value.

The three CT values used in this work are employed in a sensitivity analysis (SA; figure 97, appendix D) where the NG's cost variation with these different values will be represented along with the best solution produced by each of the studies conducted on the IAH system. This representation enables a simple visual observation of the improvement achieved through each study, and also facilitates the understanding of the EComp associated with each solution, which is paramount since it may be very different depending on the CT value practiced by the country where it will be implemented.

Now that we have all the necessary information, the 15 most competitive assays, *i.e.*, those with lower ECst values, were identified (tables 42 and 43).

[i] EComp and ECst are, in this work, different forms of perceiving the same notion (*e.g.* an ECst decrease of X% is the same as stating that a system's EComp increased by the same amount).

Table 42 - Operating conditions of the 15 most competitive assays

		Endo			Flash		Exo		
Experiment	*Assay*	T_{in}	T_r	P	T_{in}	P	T_{in}	T_r	P
3	***12***	**55.00**	**78.00**	**2.20**	**40.00**	**2.00**	**175.00**	**180.00**	**2.10**
2	***18***	**55.00**	**78.00**	**2.30**	**40.00**	**1.80**	**175.00**	**185.00**	**2.10**
2	*2*	55.00	78.00	2.30	30.00	1.80	175.00	185.00	2.10
2	*26*	55.00	78.00	2.30	40.00	2.20	175.00	185.00	2.10
6	***1***	**65.00**	**78.00**	**2.20**	**40.00**	**1.50**	**175.00**	**180.00**	**1.80**
7	***5***	**75.00**	**78.00**	**2.20**	**40.00**	**1.50**	**180.00**	**180.00**	**1.80**
3	*16*	55.00	78.00	2.20	40.00	2.00	175.00	185.00	2.10
7	*6*	78.00	78.00	2.20	40.00	1.50	180.00	180.00	1.80
5	***3***	**55.00**	**78.00**	**2.20**	**40.00**	**1.50**	**175.00**	**180.00**	**2.00**
4	*2*	55.00	78.00	2.20	35.00	1.50	175.00	180.00	2.10
7	*2*	78.00	78.00	2.20	40.00	1.50	175.00	180.00	1.80
3	*2*	55.00	78.00	1.80	40.00	1.50	175.00	180.00	2.10
3	*10*	55.00	78.00	1.80	40.00	2.00	175.00	180.00	2.10
3	*14*	55.00	78.00	1.80	40.00	2.00	175.00	185.00	2.10
5	*2*	65.00	78.00	2.00	40.00	1.50	175.00	180.00	2.00

It is clear, from table 42, that the best value regarding the endothermic reactor's operating temperature is indeed 78 °C, whereas all other variables assume different values. This might indicate that using an additional, comparative, metric, which sets the system(s) under study against relevant competing technologies, such as this work's ECst, could bring forth some interesting findings regarding the issue of EComp. Of course, in such a scenario, clear minimum thresholds regarding performance and upgraded heat would need to be defined before the study is carried out, or used simultaneously as optimization targets/study responses.

The use of a comparative metric during an optimization study brings a new dimension of complexity to the problem since it would be necessary to determine the optimal solutions for each competing technology, for each set of operating conditions of the system(s) under study. Although this added complication of the base problem is categorically undesirable, its benefits might be worth it, especially considering the vast amount of information available regarding heat pumps, and competing technologies.

Table 43 - Cost, performance, heat supplied and recovered, and excess costs of the 15 most competitive assays

		CHP's cost	**Performance**		**Heat [kW]**		**NG's cost**	**ECst**
Experiment	*Assay*	[M€/year]	Effectiveness	Entransy	Q_L	Q_H	[M€/year]	-
3	*12*	1.983	0.3103	0.7161	8891	2759	1.004	49.37%
2	*18*	1.757	0.2985	0.7079	8052	2403	0.877	50.12%
2	*2*	1.635	0.2765	0.6558	8056	2227	0.811	50.37%
2	*26*	1.716	0.2876	0.6821	8067	2320	0.844	50.82%
6	*1*	2.069	0.3398	0.7841	8059	2738	0.997	51.83%
7	*5*	2.256	0.3858	0.8903	7666	2958	1.077	52.28%
3	*16*	1.911	0.2837	0.6729	8732	2477	0.902	52.80%
7	*6*	2.289	0.3919	0.9044	7547	2958	1.077	52.96%
5	*3*	2.240	0.3263	0.7529	8552	2790	1.015	54.69%
4	*2*	2.276	0.3164	0.7302	8915	2821	1.029	54.76%
7	*2*	2.209	0.3628	0.8372	7547	2738	0.997	54.89%
3	*2*	2.444	0.2744	0.6331	11040	3029	1.102	54.90%
3	*10*	2.526	0.2468	0.5695	12580	3104	1.131	55.22%
3	*14*	2.465	0.2176	0.5162	13860	3017	1.099	55.44%
5	*2*	2.410	0.3158	0.7288	9317	2942	1.073	55.48%

11.2.10. Excess Hydrogen

Despite representing the 15 most competitive assays, the savings obtained from using natural gas instead of this CHP solution, which are around 50%, render this system unattractive. Bearing this in mind, we sought to further improve the system.

Given that the system's operation parameters have already been "optimized", the only variable left which can be manipulated is the excess hydrogen (H_2) in the exothermic reactor. It is possible to determine the hydrogen percentage (H_2%) in the exothermic reactor from the stream immediately before the equipment. This being said, the information in table 7 (reproduced here for easier access) was used to determine this value and create three other scenarios with lower H_2% (table 44) since a lower hydrogen excess in this section will lead to lower total matter volumes in circulation, thus decreasing the system's overall costs.

Table 44 - Updated excess hydrogen scenarios

		RCY Exo			
	Scenario	**1**	**2**	**3**	**4**
Molar flow (kgmole/h)	Isopropanol	514.2183	514.2183	514.2183	514.2183
	Acetone	287.8274	287.8274	287.8274	287.8274
	Hydrogen	2647.3402	1871.4400	1203.0686	802.0457
	H_2%	76.75%	70.00%	60.00%	50.00%

Now, before proceeding, it is imperative to determine the best scenario, *i.e.*, which scenario yields the most attractive solutions through the smallest performance/heat upgrade loss.

The 15 assays presented in table 42 were repeated under each new scenario and their cost, performance, upgraded heat, and ECst information were averaged so that the best scenario going forward may be determined.

Figures 37, 38, and 39, present the system's cost, performance, and ECst variations for the different excess hydrogen scenarios. table 45 presents the various scenarios' heat upgrade capacities. This table also presents each scenario's variation relative to the original case, and to the immediately preceding scenario.

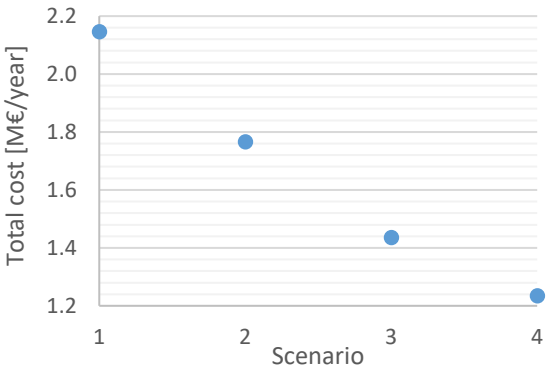

Figure 37 - System's cost variation with excess hydrogen

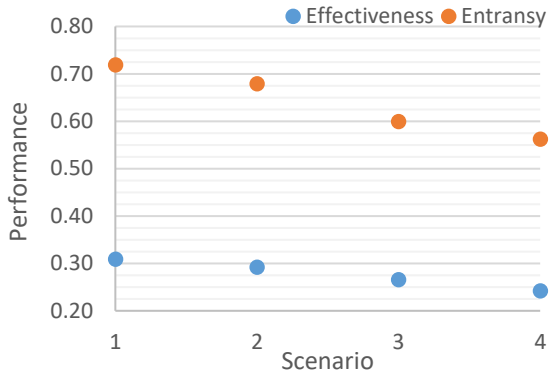

Figure 38 - System's performance variation with excess hydrogen

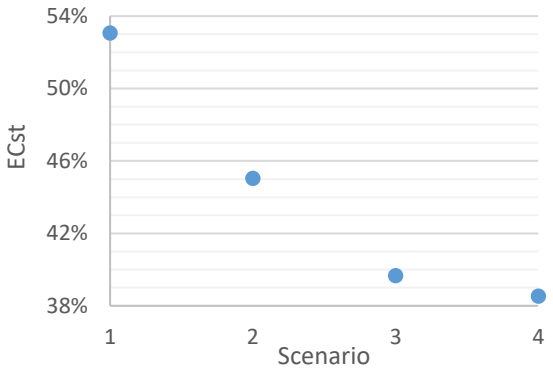

Figure 39 – Excess cost variation with excess hydrogen

Table 45 - System's upgraded heat variation with excess hydrogen

		Variation (relative to)	
Scenario	Q_H	Original	Previous
1	2752.07		
2	2654.27	3.55%	-
3	2353.33	14.49%	11.34%
4	2054.00	25.37%	12.72%

The most immediate conclusion from the data presented above is that scenarios 3 and 4 have almost identical ECst, meaning that scenario 4 can be promptly discarded as is offers no benefits in relation to scenario 3. Consequently, only scenarios 2 and 3 remain. Despite scenario 2's advantages (retains performance values close to 70% and 30% and is able to upgrade 300 more kW than scenario 3), the ECst under each scenario is the deciding factor, which ultimately means scenario 3 is the one chosen going forward, although a strong case could be made for scenario 2.

In a real-world implementation situation, this type of study is conducted several times throughout development until the final equipment sizing is carried out.

Bearing in mind that the assays presented in table 42 have several different operating conditions among them, it is important to mention that the hydrogen manipulation being discussed will not have the same effect on all of them, meaning that whereas some may improve (better performance, for example), others may present worse results under the new scenario. This being said, table 46 presents the 5 most competitive assays under the scenario chosen going forward (scenario 3). Their operating conditions are highlighted in table 42.

Table 46 - Cost, performance, heat supplied and recovered, and excess cost of the 5 most competitive assays under scenario 3

		Cost [M€/year]	**Performance**		**Heat [kW]**		**ECst**
Experiment	*Assay*	Total	Effectiveness	Entransy	Q_L	Q_H	-
2	*18*	1.045	0.2557	0.6065	7821	2000	30.38%
6	*1*	1.306	0.3057	0.7055	8090	2473	30.91%
5	*3*	1.393	0.2915	0.6726	8660	2524	33.92%
3	*12*	1.273	0.2631	0.6071	8547	2248	35.69%
7	*5*	1.488	0.3422	0.7896	7601	2601	36.18%

Figure 97 shows that a significant improvement was attained and that the current best solution is almost competitive for CT values of around 110 €/ton CO_2. This representation also shows how simply manipulating the system's volume can result in substantial decreases in its cost, although special attention must be given to the resultant heat capacity decrease.

11.2.11. Exothermic reactors in series

Xu *et al.* designed an IAH CHP with exothermic reactors in series and found that this new design's performance was greater than when using one reactor.[139] Here, we aim to determine if this increase in performance is accompanied by an enhancement from an economic standpoint or if the increase in cost renders this line of solutions unappealing.

Two different solutions were studied, one incorporating two exothermic reactors (figure 98, appendix E), and another with three exothermic reactors (figure 99, appendix E). Due to their implementation in series, there are several operation details that must be accounted for:

- Bearing in mind that the system's HX's purpose is to pre-heat the exothermic reactor's feed, the stream coming from the process ("Flash_VapOut*") is set in counter-current with respect to the reactors, *i.e.*, it will pass through the HXs in descending order ($3 \rightarrow 2 \rightarrow 1$), before passing through each reactor and its respective HX. This arrangement will maximize each HX's driving-force, *i.e.*, the ΔT between the HX's hot and cold streams, thus maximizing the pre-heating mentioned above;
    - Given the arrangement described above, it is imperative that each reactor's operating temperature be lower than that of the one directly after. This ensures that each HX's ΔT_{min} is guaranteed;
- Lastly, since special attention was given to avoid the need for duplicated pressure increasing equipment, only one compressor was used in this study, which means each reactor will operate at a lower pressure than the previous.

Given this description, this experiment was designed as follows:

- The lowest operating temperature in each scenario is 180 °C, and the lowest temperature difference between consecutive reactors' operating temperature is 10 °C;
- The lowest operating pressure in each scenario is 2.0 atm, and the lowest pressure difference between consecutive reactors' operating pressure is 0.5 atm.

Table 47 presents a summary of the various operating conditions employed in this study.

Table 47 - Operating conditions used for each reactor and corresponding scenarios

	Reactor 1	Reactor 2	Scenario
Operating temperature [°C]	180.00	190.00	A1
	180.00	200.00	A2
	190.00	200.00	A3
Operating pressure [atm]	2.00	2.50	B1
	2.00	3.00	B2
	2.50	3.00	B3

The experiment/assay sets used in this experiment are those presented in table 46 (each pair's operating conditions are presented/highlighted in table 42). Given that each set presents a different ΔT between the reactor's inlet and operating temperatures, this ΔT was maintained in this study (*e.g.*, the set "experiment 2/assay 18" has a ΔT of 10 °C, which means the inlet temperature for each reactor in that set's study was 10 °C lower than its respective operating temperature).

All 9 scenario combinations were run (table 48 gives an example for all assays which fall under scenarios A1 and B2) and the simulation results were averaged for each scenario (A1, A2, etc.) for easier analysis.

Table 48 - Scenario combination examples for scenarios A1 and B2

Reactor	**A1**	**B1**	**B2**	**B3**	**A1**	**A2**	**A3**	**B2**
1	180.0	2.00	2.00	2.50	180.0	180.0	190.0	2.00
2	190.0	2.50	3.00	3.00	190.0	200.0	200.0	3.00

Table 103 (Appendix C) presents the cost, performance, heat, and ECsts obtained from these experiments.

Although it is confirmed that the system's performance improves through the use of two exothermic reactors in series, reaching increases of 13/14%, the heat upgraded is lower in this situation than when only one reactor is used. This decrease, allied with the increase in price from the greater compression work involved and the addition of two new pieces of equipment

results in a decline in the system's overall EComp, meaning this solution is found to be uninviting.

Bearing in mind that some results seemed promising from a performance and upgraded heat standpoint, an experiment employing three exothermic reactors in series was carried out to determine if this solution would be capable of achieving a desirable outcome, however, all results yielded impracticable solutions where the third reactor needed to be supplied with external high-grade heat to operate, which directly contradicts this system's purpose.

11.2.12. Parametric Evaluation

After determining this system's variables' "best" values through the DoE study, it is important to conduct a more rigid parametric analysis in order to determine the most impactful variables, the endothermic and exothermic reactors' operating pressures, actual best values. Table 49 presents the operating conditions for the remaining variables. These values were chosen based on the results obtained from the DoE studies presented above.

Table 49 - Operating conditions for the variables not under investigation (note that T is in °C and P is in atm)

Endo		**Flash**		**Exo**	
T_{in}	T_r	T_{in}	P	T_{in}	T_r
55.00	78.00	40.00	1.80	180.00	180.00

Table 50 shows the ranges in which the reactors' operating pressures were varied.

Table 50 - Reactors' operating pressure ranges for the parametric evaluation

Reactor	**Operating Pressure**						
Endothermic	1.90	2.00	2.10	2.20	2.30	2.40	2.50
Exothermic	-	-	2.10	2.20	2.30	2.40	2.50

As occurred earlier, special care was taken so as to not duplicate any pressure increasing equipment, which is why the exothermic reactor's operating was not lowered beyond 2.10 atm.

Figures 40 to 43 present the results obtained from this parametric analysis.

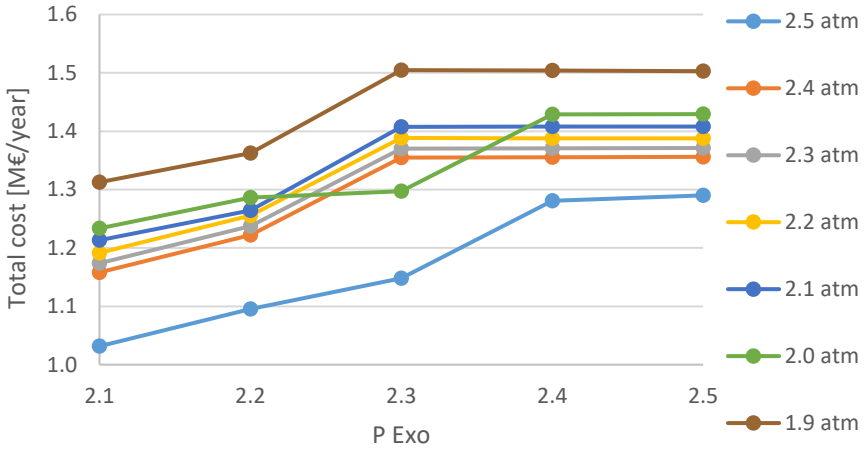

Figure 40 - System's cost variation with reactors' pressures

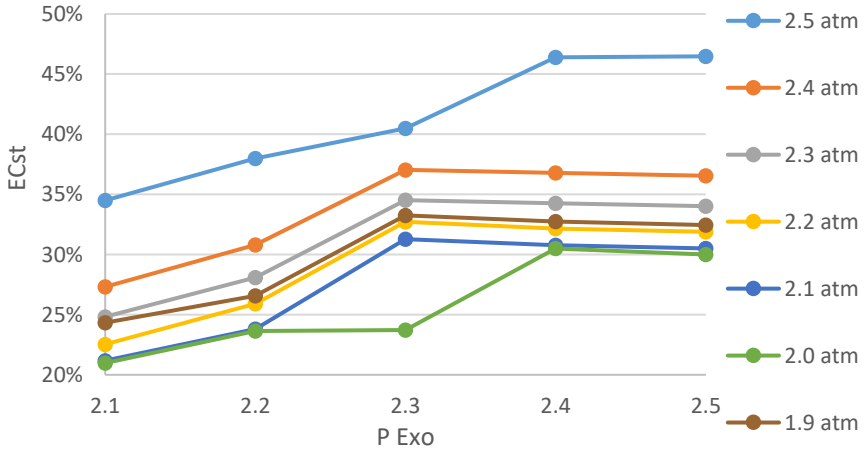

Figure 41 – Excess cost variation with reactors' pressures

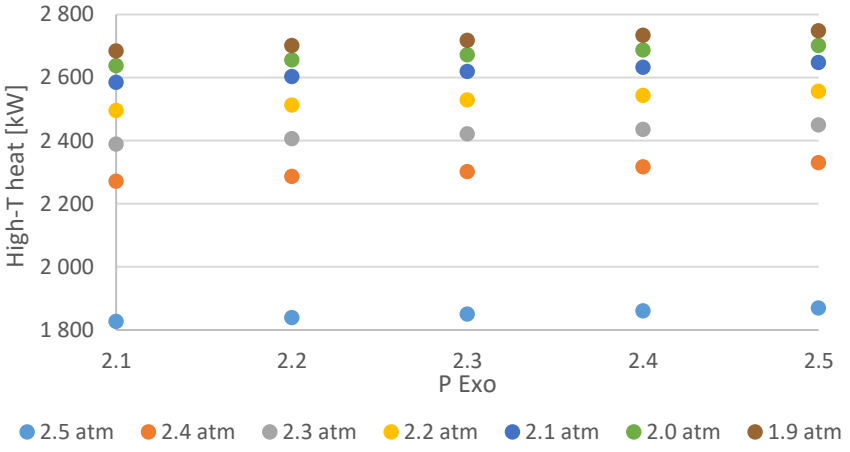

Figure 42 - System's upgraded heat variation with reactors' pressures

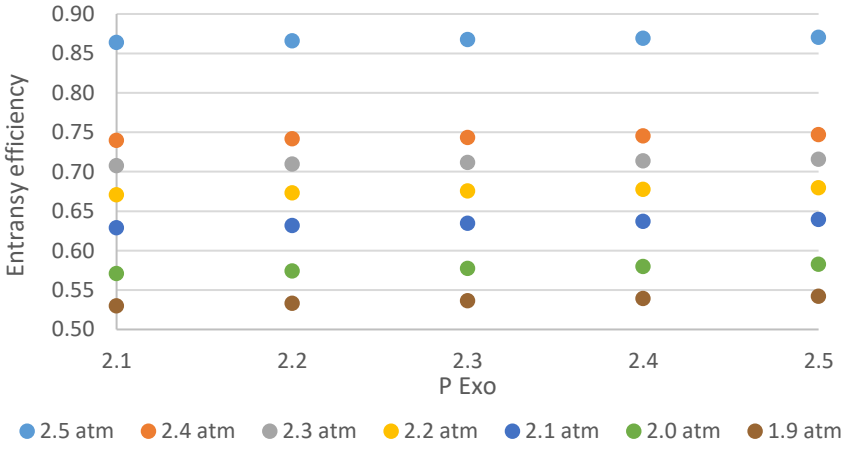

Figure 43 - System's performance variation with reactors' pressures

The first thing to notice is that a higher P Exo results in a higher system cost, which is no surprise as this is due to the greater compression work needed, which directly translates to a higher energy consumption by that equipment and, consequently, higher operating costs. This higher system cost also translates into higher ECsts, or, in other words, a less competitive CHP solution.

Though a slight, but clear, improvement towards higher values is unquestionable, the exothermic reactor's operating pressure does not appear to be very influential regarding the upgraded heat and the system's performance.

These results show that the endothermic reactor's operating pressure is clearly one, if not the, most influential process variable with regard to the IAH CHP system.

Despite a clear decrease in total system cost with increased pressure, the opposite is true for the system's ECst, meaning this variable's optimal value will result from a balance between the system's cost and the upgraded heat attained.

Pressures of 2.2 and 2.3 atm offer high performance and upgrade heat values, however, these also present ECst values of approximately 25%, meaning they are at least 25% more expensive than using natural gas to produce the same amount of heat. In contrast, pressures of 2.0 and 2.1 atm offer the best ECsts, which means these are the most competitive solutions, and also yield the 2nd and 3rd highest upgrade heat values, respectively. Despite this, these present low system performances.

Overall:

- Higher P Endo yields better cost and performance, but worse ECst and upgraded heat;
- Higher P Exo yields better performance and upgraded heat, but worse cost and ECst.

It is also very significant to mention that this study results in what can be referred to as the first competitive solution, even if this is only true when considering the highest CT value used in this work (figure 97).

11.2.13. Flash separator vs Distillation column

Earlier, we stated that although the CHP structure most often presented by the literature involves a distillation column, this system only required a simple flash separator due to the large temperature difference between isopropanol and acetone's boiling points. Now, while this is fundamentally true, as evidenced by the fact that the system works and achieves fairly attention-grabbing solutions (sadly, the best solutions are still about 20% more expensive than the alternative considered), it is certainly interesting to understand how implementing a distillation column will affect the system's outputs.

The leading motive behind this line of study is the predicted decrease in compression costs, which will stem from the increased separation efficiency provided by the use of a distillation column instead of a flash separator, however, this solution will only be viable if the cost reduction is greater than the added investment and operating costs.

The utilization of a distillation column will also result in an increase in the amount of upgraded heat since the reboiler will, akin to the endothermic reactor, operate through the input of excess-heat. This increased heat promotion is certainly an advantage compared to the previous scenario, and more, it might help counteract the increased costs mentioned above since the alternative's cost will also increase.

Table 51 shows the system's reactors' operating conditions.

Table 51 - Operating conditions for the variables not in study (note that T is in °C and P is in atm)

Endothermic Reactor			**Exothermic Reactor**		
T_{in}	T_r	P	T_{in}	T_r	P
55.0	78.0	2.30	180.0	180.0	2.10

Table 104 (Appendix C) presents the results of a small study carried out to ascertain the distillation column's best operating conditions. Although this study followed an OFAT method, the low number of variables involved (total number of trays, feed tray, inlet temperature and operating pressure) allows for this line of investigation to be followed without fear of any significant errors as far as this work's goals are concerned.

At first, this study's most striking finding appears to be the operating pressure's influence on the system's overall EComp, however, as explained above, this influence does not stem from

the distillation column *per se*, but due to the fact that a lower pressure before the compressor, *i.e.*, lower DC operating pressure, will result in a greater compression work needed in said compressor, which leads to higher system costs, consequence of the higher energy consumption. This being said, it is interesting to note that this equipment influences the effectiveness and entransy inversely, meaning any effort to maximize one will degrade the other. Expectedly, a higher operating pressure leads to lower 2nd law efficiencies since the entropy generated under these conditions is greater than at lower pressures.

Regarding the column's inlet temperature, the best value was found to be 80 °C, regardless of the output metric considered. This is a fairly simple phenomenon in which lower inlet temperatures make it necessary to supply the reboiler with a larger amount of heat, thus decreasing the system's overall performance.

This system delivers the best results when using a DC with 14 trays. Regarding the feed tray's optimal position, this was found to be slightly below the middle of the column. In addition to yielding the most competitive solution, this positioning also yields the highest performance, although the differences to choosing the middle of the column are minimal.

Figures 44 to 47 present the comparison between the solution using an FS and the solution using a DC.

The first thing to notice is that, as expected, the system with a DC is more expensive than the system with a FS. Also, the earlier observations that higher P Exo, and lower P Endo, yield more costly solutions are corroborated.

Figure 46 shows that the system is capable of releasing a higher amount of upgraded heat when utilizing a DC. Also noteworthy is that the exothermic reactor's pressure seems to have even less influence on the total upgraded heat when using a DC.

As transpired earlier, the exothermic reactor's operating pressure does not appear to be very influential regarding the system's overall performance, however, it is notable how these fundamentally equivalent pieces of equipment lead to different efficiency behaviors. Whereas the flash separator originates higher entransy efficiency values due to its lower entropy generation, the distillation column allows for higher effectiveness values due to its higher heat efficiency. Thus, this opposite behavior will make it very difficult to choose one of these solutions solely based off their system's overall performance due to the existing tradeoff.

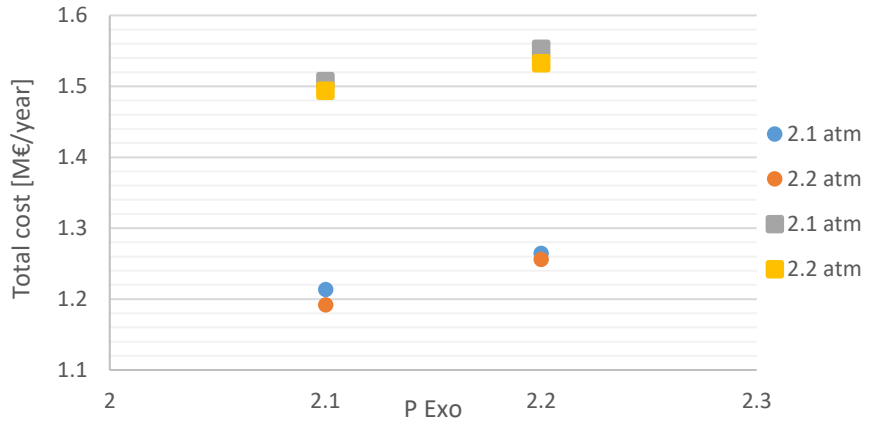

Figure 44 - System's cost with FS (circles) and DC (squares)

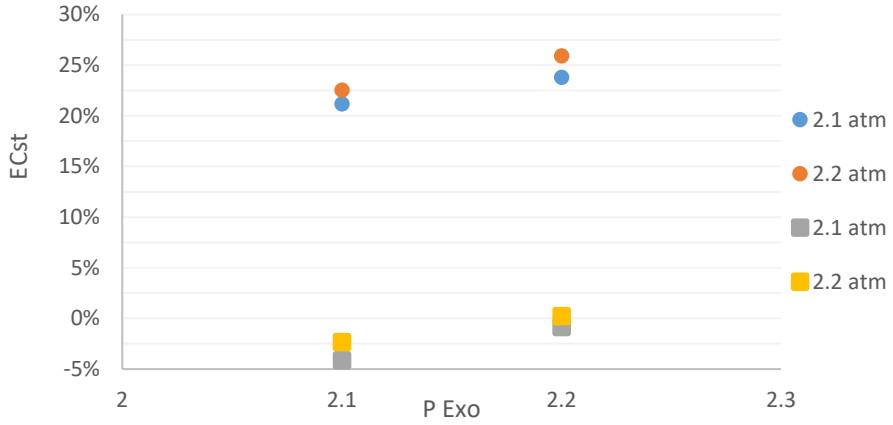

Figure 45 - Excess cost with FS (circles) and DC (squares)

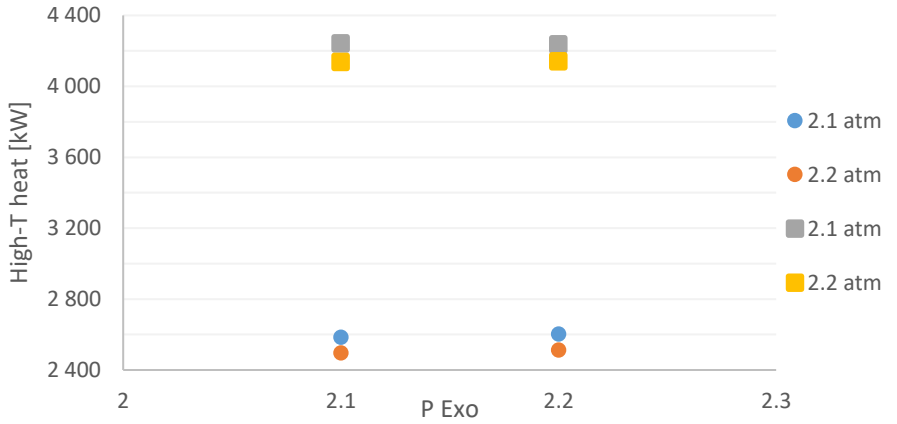

Figure 46 - System's upgraded heat with FS (circles) and DC (squares)

Figure 47 - System's performance (effectiveness [filled] and entransy efficiency [no fill]) with FS (circles) and DC (squares))

Lastly, but undoubtedly more importantly, the system incorporating a DC offers lower ECst solutions than the system incorporating a FS, which means the former is more competitive than the latter. Furthermore, two of these present negative ECst values, meaning they are less expensive than the use of natural gas, even if only by a small margin.

Figure 97 shows that, although the solution using a DC is just barely competitive when considering the lowest CT value, this difference is much larger when considering the other tax values (around -40% and -16% for the highest and second highest CTs, respectively).

The existence of solutions with negative ECst values makes it possible to estimate their payback time, which effectively reflects their economic attractiveness. This is done by determining the point in time when the accumulated cash flow (ACF; equation 25) starts presenting positive values, or, in other words, when the project reaches its break-even point.[150,151]

$$Accumulated\ cash\ flow\ =\ Updated\ cash\ flow_y + \ Updated\ cash\ flow_{y-1} \tag{25}$$

The updated cash flow (UCF) is given by equation 26 and is responsible for updating the annual cash flow from year *y* to the present.[150,151]

$$Updated\ cash\ flow = \frac{YCF + \ Amortization_y - MC}{(1 + IRR)^y} \tag{26}$$

where,

YCF – Yearly cash flow,

IRR – Internal rate of return,

MC – Maintenance costs (equal to 1% of the system's capital costs).

The yearly cash flow (YCF), given by equation 27, is the savings obtained when using a given CHP solution instead of natural gas.

$$Yearly\ cash\ flow\ =\ NG\ solution's\ cost - CHP\ solution's\ cost \tag{27}$$

The internal rate of return (IRR) is a metric used in financial analysis to estimate the profitability of potential investments. It translates the annual growth rate a given investment is expected to create, therefore, the higher an IRR, the more desirable an investment is to undertake.[150–152]

In this situation, several IRR values will be chosen and each translate the stress under which the project's accounts are placed, *i.e.*, higher IRR values will require the solution to be more economically robust, whereas lower IRR values mean the solution will be weaker.[150,151]

Figure 48 presents the accumulated cash flows for the best solution, under different IRR values. This representation is very elucidative of the poor economic performance that still plagues these systems. With payback periods of 14 and 16 years when considering extremely low IRRs of 3% and 5%, respectively, it becomes incredibly arduous to argue in favor of these solutions, and even more so when realizing that this solution's shortest, or best, payback period, achieved when considering the highest tax value presented in table 41, is still 8 years, for an IRR of only 3%.

Nonetheless, a strong case can be made, and special attention should be paid, to the CO_2 emissions that could be prevented if this system were implemented, which can reach over 7500 ton CO_2/year. This "green potential", and this technology's relatively low level of development, should be more than enough motivation to pursue new and innovative R&D efforts aiming towards its improvement.

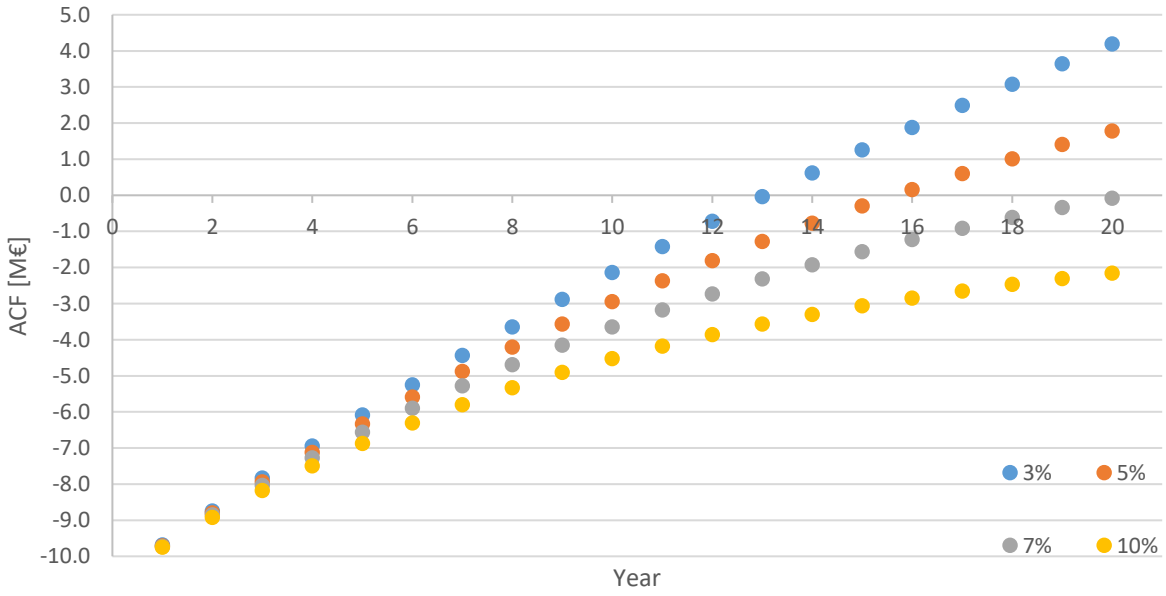

Figure 48 - Accumulated cash flows for the best CHP solution, under different IRR values

12. *tert*-Butanol/Isobutene/Water System

Seeing as this system is fairly similar to the IAH system, the general considerations presented above still hold for this case. The flowsheet constructed for this system and its intricacies and operating details are presented next.

12.1. Implementation

This system's endothermic reaction is responsible for the conversion of *tert*-butanol into isobutene and water, and the exothermic reaction is responsible for the conversion of isobutene and water back into tert-butanol. As was the case for the first system, a bibliographic research was conducted and the following kinetics for endo (table 52) and exothermic (table 53) reactions were discovered:

Table 52 - Endothermic reaction's kinetic equation and parameters[78]

$\boldsymbol{r_{dW} = \frac{k\, C_{tB}}{1 + (K_W C_W)^2 + K_{iB}\, C_{iB}}}$	$[\boldsymbol{kmol\ kg^{-1}\ s^{-1}}]$
$k = e^{(-3.385 - 2863/T)}$	$[m^3\ kg^{-1}\ s^{-1}]$
$K_W = e^{(-20.99 + 7051/T)}$	$[m^6\ kmol^{-2}]$
$K_{iB} = e^{(-30.03 + 10245/T)}$	$[m^3\ kmol^{-1}]$

Table 53 - Exothermic reaction's kinetic equation and parameters[78,80,153,154]

$\boldsymbol{r_{hW} = \frac{k\,(C_{iB}\, C_W - C_{tB}/K_c)}{1 + K_W\, C_W}}$	$[\boldsymbol{kmol\ kg^{-1}\ s^{-1}}]$
$k = e^{(-27.56 + 6074/T)}$	$[kmol\ kg^{-1}\ s^{-1}]$
$K_c = e^{(-6.78 + 3160/T)}$	$[m^3\ kmol^{-1}]$
$K_W = e^{(-23.41 + 8881/T)}$	$[m^6\ kmol^{-2}]$

where:

r – Reaction rate (dW – dehydration, and hW – hydration);

k – Rate constant;

K – Adsorption equilibrium constant (iB – isobutene and W – water);

K_c – Chemical equilibrium constant;

C – Concentration [kg m^{-3}].

Although both equations, and respective parameters, were found, neither could be implemented due to limitations regarding the software. Thus, both were implemented as conversion reactions with a 60% approach.[108,155,156]

Two very important system details, which make it much more troublesome, and problematic, than the first, were identified before moving to the simulator, *tert*-butanol's boiling point (83 °C) is located between isobutene and water's (-6.9 °C and 100 °C, respectively), which means these three components cannot be separated as desired in a single distillation step. In addition to this, water and *tert*-butanol form a minimum boiling point azeotrope (79.9 °C), characterized by 11.7% H_2O and 88.3% *t*B (wt %), which means these two components cannot be separated through simple distillation.[111,112] Thus, the concrete system was built on the basis of needing two reactors, some separation equipment, capable of breaking azeotropic mixtures, and a heat exchanger. However, there are a set of important details which cannot be overlooked before this assembly can be put in place in the software. What type of azeotropic separation will be employed? Will it require the addition of any new components? If so, which one(s)?

After consulting the literature, we identified the heterogeneous azeotropic distillation as the most suitable process to break the azeotrope mentioned above. This method involves the addition of an entrainer which is much more miscible with one of the components that form the binary azeotrope and very immiscible with the other, thus originating two liquid phases upon condensing, which can be separated by density.[157–159] Given that we wish to separate water and an alcohol, organic species, such as pentane, hexane, and benzene, are all strong candidates. After referring to the literature once again, benzene and cyclohexane were identified as the top contenders to be used in the present system, even though they give rise to three other azeotropes.[111,112] Benzene was ultimately chosen due to an easier simulation convergence. The resulting azeotrope's characteristics are presented in table 54.

Table 54 - Boiling points and compositions of the azeotropic mixtures[112]

Azeotrope	**Boiling point [°C]**	**Composition [wt %]**		
		Water	Alcohol	Other
1	79.90	11.70	88.30	-
2	69.25	8.83	-	91.17
3	79.30	-	7.40	92.60
4	67.30	8.10	21.40	70.50

Now that this system's main intricacies have been sorted out, it can be assembled within the simulation software (figure 49). First, the endothermic reactor was defined as a Conversion Reactor (CRV) with a volume of 10 m^3. After this, a separation equipment was needed, which could either be a flash or a three-phase separator, or both. After some study, a solution containing both equipment was found to be acceptable. This arrangement effectively operates as a pre-concentrator. Afterwards comes the azeotropic distillation column (ADC), which consists of an absorber with a reboiler, a condenser, and a three-phase separator. This assembly mimics the working principle of a three-phase distillation column. Lastly, the exothermic reactor was also defined as a Conversion Reactor, with a volume of 10 m^3. As with the first system, a heat exchanger was added, in this case between the azeotropic distillation column and the exothermic reactor in order to pre-heat the exothermic reactor's feed through the reuse of some excess-heat that the vapor stream leaving said reactor may still retain, which would, otherwise, be integrated into another section of the process, or, in a worst-case scenario, wasted. Other equipment was used when/where necessary.

This system's main separation equipment, the ADC, is highly sensitive, which is no surprise given the complexity of the mixture within it. This means a careful selection of its operating specification must be made, especially considering this column only possesses one degree of freedom. This being said, we attempted to utilize specifications guided towards obtaining a bottom stream of "pure" (>99% molar composition) *tert*-butanol, which is this equipment's goal. Even though these resulted in successful simulation convergence, the column would have to be reset and rerun whenever any variable's operating point was changed, meaning a system-wide analysis could not be carried out. This led us to test different specifications, mainly following a reverse train of thought, *i.e.*, specifications guided towards obtaining the water-benzene binary azeotrope in the distillate stream. This course of action ultimately resulted in implementing a benzene recovery specification (99% molar) towards the distillate stream.

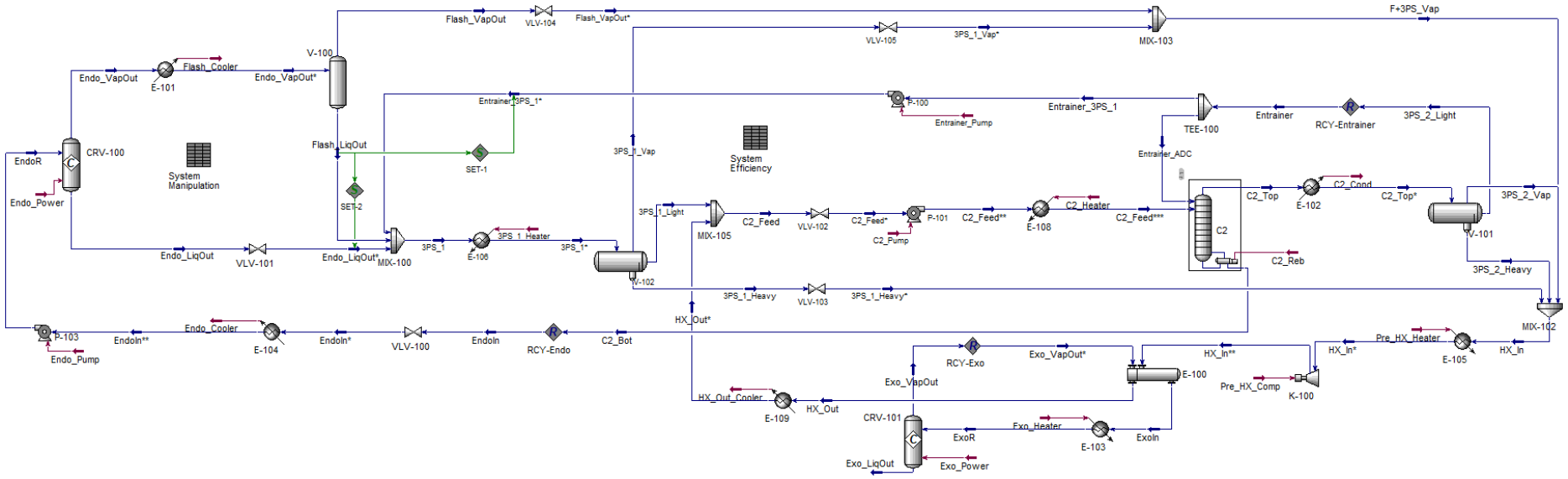

Figure 49 - *t*B/iB system's first design

Table 55 presents the initial convergence conditions (inlet and reaction temperatures, pressures, and total number and feed tray). Additionally, the ADC has 20 trays with the feed entering at the 10th tray, and the splitter was specified with a 70% recovery towards the column.

Table 55 - Initial convergence conditions for the *t*B/iB system

	Endothermic reactor	**Flash separator**	**1st Three-phase separator**	**Azeotropic distillation column**	**2nd Three-phase separator**	**Exothermic reactor**
Inlet Temperature [°C]	55	45	62	55	55	160
Reaction Temperature [°C]	65	-	-	-	-	180
Vessel Pressure [atm]	1.55	1.50	1.35	1.204	1.00	1.65

Table 56 presents the base molar flows of the different species in the system. The quantities shown relate to the recycled streams attached to the logical operations of the same name as the table's columns, and were used as the starting point for all studies carried out on this system.

Table 56 - Molar flows for the *t*B/iB system (in kgmole/h)

	RCY Endo	**RCY Entrainer**	**RCY Exo**
tert-Butanol	275.8910	63.7642	208.1323
Isobutene	0.0000	36.6973	110.3429
Water	3.9364	17.2294	28.6680
Benzene	3.1307	203.9848	116.2445

Table 8 presents the pressure drops used throughout the system's heat exchangers. In addition to these, a pressure drop of 0.1 psi/tray was used for the ADC.[143,144]

As was the case with the first system, the recycle streams' process re-entry points were determined based on each component's molar flow, however, the ADC's working principle must also be accounted for. Thus, the bottoms stream from the ADC, which is mostly *tert*-butanol (approximately 97% molar), is recycled to the endothermic reactor, whereas the gaseous stream from the exothermic reactor is recycled to the ADC due to its high isobutene and benzene contents. Lastly, the entrainer-rich stream from the second tri-phase separator is recycled to the top of the column (due to the fact that the water-benzene azeotrope has a lower boiling point than *tert*-butanol, making it a minimum azeotrope), and to the first three-phase separator, where it will play a fundamental role in helping to pre-concentrate the mixture entering the ADC by originating a water-rich stream which can be sent to the exothermic reactor, bypassing the distillation column.

12.2. Optimization

Before moving on to the system's optimization, it is important to remember, and keep the considerations prefaced in section 11.2 in mind.

Since this system is already equipment-efficient, its flowsheet (figure 49) does not require further changes before the study begins.

As occurred with the previous system's analysis, this study's first step requires the identification of all process variables that can be optimized (table 57).

Table 57 - Variables under study in the *t*B/iB system († - this variable is represened as spacing from the top of the column; ‡ - this variable fluctuates between 0 and 1, and represents the fraction sent towards the first three-phase separaotr)

Variable	Description	Variable's Units
T_{in} Endo	Endothermic reactor's inlet temperature	°C
T_r Endo	Endothermic reactor's operating temperature	°C
P Endo	Endothermic reactor's operating pressure	atm
T_{in} Flash	Flash separator's inlet temperature	°C
P Flash	Flash separator's operating pressure	atm
T_{in} 3PS_1	First three-phase separator's inlet temperature	°C
P 3PS_1	First three-phase separator's operating pressure	atm
T_{in} ADC	Azeotropic distillation column's inlet temperature	°C
Trays ADC	Azeotropic distillation column's total number of trays	-
Feed ADC†	Azeotropic distillation column's feed tray	%
Splitter‡	Stream splitter's division towards the 3PS_1	-
T_{in} 3PS_2	Second three-phase separator's inlet temperature	°C
T_{in} Exo	Endothermic reactor's inlet temperature	°C
T_r Exo	Endothermic reactor's operating temperature	°C
P Exo	Endothermic reactor's operating pressure	atm

12.2.1. First experiment

Given the fifteen variables in study, a full, two-level, experiment is simply not viable. As such, a $2_{(III)}^{15-11}$ FFD was utilized (this is the only design available for such a large number of factors). Tables 58 and 59 present the information regarding this first experiment, such as factor levels, confounded variables, and generators used.

Table 58 - Designation and factor levels for the variables in the first experiment

Variable	Confounded?	Designation	Low-level (-)	High-level (+)
T_{in} Endo	Yes	K	45.00	55.00
T_r Endo	No	A	65.00	75.00
P Endo	No	B	1.00	2.00
T_{in} Flash	Yes	H	40.00	45.00
P Flash	Yes	J	1.00	2.00
T_{in} 3PS_1	Yes	O	60.00	65.00
P 3PS_1	Yes	L	1.00	1.50
T_{in} ADC	Yes	G	50.00	60.00
Trays ADC	Yes	M	20	30
Feed ADC	Yes	F	35%	65%
Splitter	Yes	P	0.20	0.30
T_{in} 3PS_2	Yes	N	50.00	55.00
T_{in} Exo	Yes	E	160.00	180.00
T_r Exo	No	C	180.00	200.00
P Exo	No	D	1.50	2.00

Table 59 - Generators used in the first experiment

Variable	T_{in} Endo	T_{in} Flash	P Flash	T_{in} 3PS_1	P 3PS_1
Designation	K	H	J	O	L
Generator	AB	BCD	ABCD	BD	AC

Variable	T_{in} ADC	Trays ADC	Feed ADC	Splitter	T_{in} 3PS_2	T_{in} Exo
Designation	G	M	F	P	N	E
Generator	ACD	AD	ABD	CD	BC	ABC

This first experiment was carried out as presented in Table 60 and the results obtained are also shown.

Table 60 - FFD´s $2_{(III)}^{15-11}$ matrix for the first experiment and its results

		T_r Endo	P Endo	T_r Exo	P Exo	Cost [M€/year]	Performance	
		A	B	C	D	Total	Effectiveness	Entransy
1	**d**	-1	-1	-1	1	3.929	0.8984	0.4603
2	**c**	-1	-1	1	-1	3.353	0.4164	0.3186
3	abc	1	1	1	-1	3.820	0.5388	0.4782
4	**a**	1	-1	-1	-1	4.251	0.5155	0.4389
5	cd	-1	-1	1	1	3.961	0.5939	0.4666
6	bd	-1	1	-1	1	2.521	0.2754	0.1889
7	acd	1	-1	1	1	2.855	0.2379	0.2559
8	**[1]**	-1	-1	-1	-1	3.423	0.5980	0.2968
9	abcd	1	1	1	1	3.087	0.3839	0.3367
10	ab	1	1	-1	-1	3.718	0.4478	0.4473
11	bc	-1	1	1	-1	3.929	0.9272	0.4880
12	bcd	-1	1	1	1	3.428	0.5564	0.2871
13	ad	1	-1	-1	1	4.977	0.5087	0.4349
14	**b**	-1	1	-1	-1	4.217	0.9592	0.6886
15	ac	1	-1	1	-1	4.588	0.3357	0.3703
16	abd	1	1	-1	1	3.486	0.5474	0.5550

Contrarily to what happened with the first system, all assays from this experiment yielded operable solutions, which is a good start in and of itself.

After applying the methodology presented above to all three outputs in consideration, a normal probability plot of the effects' estimates was built to judge the magnitude and the possible significance of the experiment's factors. As explained above, if none of the effects is significant, then the estimates will behave like a normal distribution's random sample and the plotted effects would lie approximately along a straight line. The effects that depart from that straight line represent the possibly significant factors/interactions. The normal probability plot of the effects for the response variables cost, effectiveness and entransy efficiency are represented in figures 50, 51, and 52.

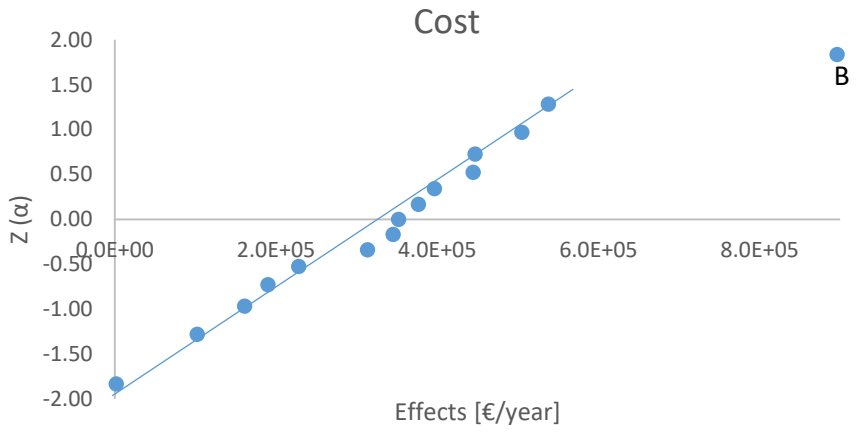

Figure 50 - Normal probability plot of effects regarding cost

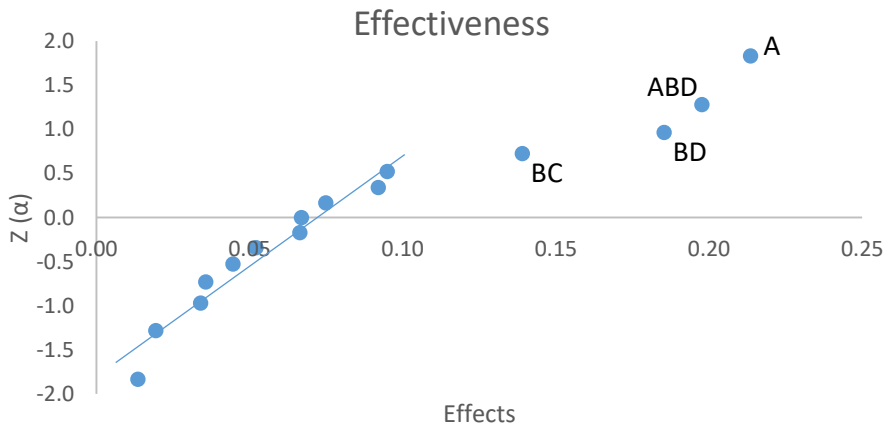

Figure 51 - Normal probability plot of effects regarding effectiveness

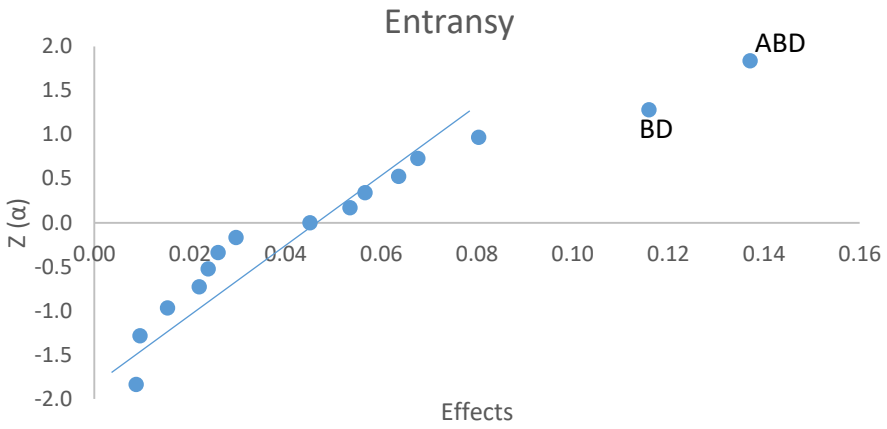

Figure 52 - Normal probability plot of effects regarding entransy efficiency

After this, an ANOVA was conducted in order to understand which factors/interactions affect each response significantly, for a confidence level of 95% (tables 61, 62, and 63).

Table 61 - ANOVA results regarding cost

	SS	DF	MS	F_0	
B	3.21E+12	1	3.21E+12	7.35	F. INV
Error	5.68E+12	14	4.37E+11		4.600

Table 62 - ANOVA results regarding effectiveness

	SS	DF	MS	F_0	
BC	0.0775	1	0.07745	6.31	
BD	0.1375	1	0.13749	11.20	
ABD	0.1564	1	0.15638	12.74	
A	0.1826	1	0.18259	14.87	F. INV
Error	0.1228	11	0.01228		4.844

Table 63 - ANOVA results regarding entransy efficiency

	SS	DF	MS	F_0	
BD	0.0538	1	0.05377	8.18	
ABD	0.0752	1	0.07517	11.43	F. INV
Error	0.0789	13	0.00657		4.667

After determining the significant factors/interactions for each output, an RA was conducted to verify the model's validity. No significant deviations are noted in figures 100, 101, and 102 (Appendix F), which confirms the model's adequacy.

Before examining the results obtained from this experiment, it is crucial to keep in mind that this experiment followed a resolution III design, meaning all main factors are confounded with 2-factor interactions. As such, special care is required to understand if these results stem from the confounded factors/interactions.

The ANOVA indicates that factor B (P Endo) is the only significant variable towards the system's cost, however, this factor is confounded with interaction FM which seems much more likely to be this result's source as the balance between the ADC's feed tray (F) and its total number of trays (M) affects the column's cost and the hot utility supplied to the reboiler, two of the system's largest cost-related parameters. Aside from this, factor B is confounded with many more 2-factor interactions, indicating that further experimentation is required.

The system's performance is shown to be affected by the ADC's feed tray (ABD = F), the endothermic reactor's operating temperature (A), and both three-phase separators' inlet temperature temperatures (first, O, and second, N), however, factor A is confounded with a 2-factor interaction between factors B and K which correspond to the flash separator's inlet temperature and operating pressure, respectively, factor O is confounded with interaction BD, which represents the endo and exothermic reactors' operating pressures respectively, and with interaction JL (flash separator and first three-phase separator's respective operating pressures), and factor N is confounded with interaction FG (ADC's feed tray and inlet temperature, respectively).

As can be understood just from these few examples, the extensions to which these factors are confounded makes it extremely difficult to identify a certain result's origin confidently. Moreover, given the large number of variables under consideration, it is impractical to study all of them simultaneously, making it necessary to select a few that will be set at their best levels so that the rest can be studied in greater detail.

Keeping the system's performance as our major focus, we decided to adopt a reversed approach in which the least influential factors are set at their best values, as given by table 64. Thusly, the endo and exothermic reactors' and the flash separator's inlet temperatures will be fixated at each factor's high-level, and the first three-phase separator's operating pressure and the splitter at their respective low-level. The ADC's feed enters the column at the center tray. The remaining variables' new values will oscillate around this study's best values:

- Low-level – Endo and exothermic reactors' operating temperatures, flash separator and exothermic reactor's operating pressure, the first three-phase separator's inlet temperature, and the ADC's total number of trays;
- High-level – Endothermic reactor's operating pressure, and the ADC and the second three-phase separator's inlet temperatures.

In accordance with these observations, a $2_{(IV)}^{9-4}$ FFD experiment will be carried out next.

Table 64 presents a summary of each factor's improvement direction for all three outputs.

Table 64 - First experiment's factors' improvement direction summary

		Cost		Effectiveness		Entransy	
		S?	D?	S?	D?	S?	D?
T_{in} Endo	K	No	+	No	+	No	+
T_r Endo	A	No	-	Yes	-	No	+
P Endo	B	Yes	+	No	+	No	+
T_{in} Flash	H	No	-	No	+	No	+
P Flash	J	No	-	No	-	No	-
T_{in} 3PS_1	O	No	+	Yes	-	Yes	-
P 3PS_1	L	No	+	No	-	No	-
T_{in} ADC	G	No	+	No	-	No	-
Trays ADC	M	No	+	No	+	No	+
Feed ADC	F	No	-	Yes	+	Yes	+
Splitter	P	No	+	No	-	No	-
T_{in} 3PS_2	N	No	-	Yes	+	No	-
T_{in} Exo	E	No	+	Yes	-	No	+
T_r Exo	C	No	+	No	-	No	-
P Exo	D	No	+	No	-	No	-

12.2.2. Second experiment

Given the first experiment's findings, the system's operating conditions were updated and the values chosen for the variables which will be studied were determined by taking their best level from the previous experiment and applying a somewhat similar amplitude. This selection is particularly important when pressure manipulation is involved due to the high costs typically involved. Thus, special precaution was taken to avoid the need for duplicate equipment (*i.e.*, an attempt was made to employ the minimum amount possible of pressure increasing equipment). Tables 65 and 66 present the information regarding this second experiment, such as factor levels, confounded variables, and generators used.

Table 65 - Designation and factor levels for the variables in the second experiment

Variable	Confounded?	Designation	Low-level (-)	High-level (+)
T_{in} Endo				55.00
T_r Endo	No	A	60.00	70.00
P Endo	Yes	B	1.60	2.40
T_{in} Flash				45.00
P Flash	Yes	J	1.20	1.50
T_{in} 3PS_1	No	O	55.00	60.00
P 3PS_1			1.10	
T_{in} ADC	No	G	55.00	65.00
Trays ADC	No	M	18	22
Feed ADC			50%	
Splitter			0.20	
T_{in} 3PS_2	No	N	53.00	57.00
T_{in} Exo				175.00
T_r Exo	Yes	C	180.00	190.00
P Exo	Yes	D	1.30	1.70

Table 66 - Generators used in the second experiment

Variable	Designation	Generator
P Endo	B	OGMN
P Flash	J	AGMN
T_r Exo	C	AOMN
P Exo	D	AOGN

This second experiment was carried out as presented in tables 67 and 68, where its results are also shown.

Table 67 - FFD's $2_{(IV)}^{9-4}$ matrix for the second experiment and its results

		T_r Endo	**T_{in} 3PS_1**	**T_{in} ADC**	**Trays ADC**	**T_{in} 3PS_2**	**Cost [M€/year]**	**Performance**	
		A	O	G	M	N	Total	Effectiveness	Entransy
1	agmn	1	-1	1	1	1	2.921	0.7641	0.4576
2	agn	1	-1	1	-1	1	2.515	0.9391	0.5762
3	omn	-1	1	-1	1	1	4.127	3.4110	0.5607
4	aog	1	1	1	-1	-1	3.822	1.0080	0.8109
5	**[1]**	-1	-1	-1	-1	-1	3.137	1.0980	0.4073
6	agm	1	-1	1	1	-1	2.900	0.6367	0.4923
7	**n**	-1	-1	-1	-1	1	4.115	3.4080	0.5632
8	ao	1	1	-1	-1	-1	3.694	0.6767	0.5349
9	gn	-1	-1	1	-1	1	3.289	3.6230	0.5854
10	**o**	-1	1	-1	-1	-1	3.882	1.6330	0.6168
11	gm	-1	-1	1	1	-1	3.104	1.4930	0.5424
12	on	-1	1	-1	-1	1	3.606	2.7340	0.4496
13	amn	1	-1	-1	1	1	3.160	0.6423	0.3757
14	aogn	1	1	1	-1	1	3.900	1.0360	0.6336
15	**a**	1	-1	-1	-1	-1	2.873	0.5366	0.3980
16	aon	1	1	-1	-1	1	4.082	0.9185	0.5448

Table 68 - FFD's $2_{(IV)}^{9-4}$ matrix for the second experiment (continued)

		T_r Endo	T_{in} 3PS_1	T_{in} ADC	Trays ADC	T_{in} 3PS_2	Cost [M€/year]	Performance	
		A	O	G	M	N	Total	Effectiveness	Entransy
17	gmn	-1	-1	1	1	1	4.047	4.2890	0.7592
18	ogn	-1	1	1	-1	1	3.907	4.1470	0.7266
19	mn	-1	-1	-1	1	1	2.557	1.3930	0.2255
20	**g**	-1	-1	1	-1	-1	4.060	2.0350	0.8259
21	aogmn	1	1	1	1	1	4.070	1.1080	0.6928
22	ag	1	-1	1	-1	-1	2.827	0.6024	0.4565
23	**m**	-1	-1	-1	1	-1	3.905	1.6540	0.6282
24	ogm	-1	1	1	1	-1	4.114	2.1910	0.8950
25	og	-1	1	1	-1	-1	1.754	0.2221	0.0795
26	an	1	-1	-1	-1	1	2.987	0.5360	0.3263
27	am	1	-1	-1	1	-1	3.490	0.6329	0.4968
28	ogmn	-1	1	1	1	1	3.266	3.2200	0.5170
29	om	-1	1	-1	1	-1	3.246	1.0580	0.3920
30	aomn	1	1	-1	1	1	3.249	0.7756	0.4789
31	aogm	1	1	1	1	-1	3.957	0.8119	0.6297
32	aom	1	1	-1	1	-1	4.179	0.7582	0.5731

In light of these results, it is impossible to proceed without addressing some of the effectiveness values obtained. Although some assays yield values greater than 1, this may be due to the equations in use. We must not forget that many of these were developed for mechanical heat pump systems, which operate under a scenario of generating more heat than the electrical energy fed to the system ($Q_H > Q_L$), which is impossible for the chemical heat pump systems. This conveys the need for an updated effectiveness equation which accounts for the distillation column's contribution towards the system's end-goal. Nonetheless, even if this is true, the remainder of this work will be carried out using the equation presented in the literature for consistency's sake.

Moving on, the graphs presented in figures 53, 54, and 55, were obtained after applying the methodology described above.

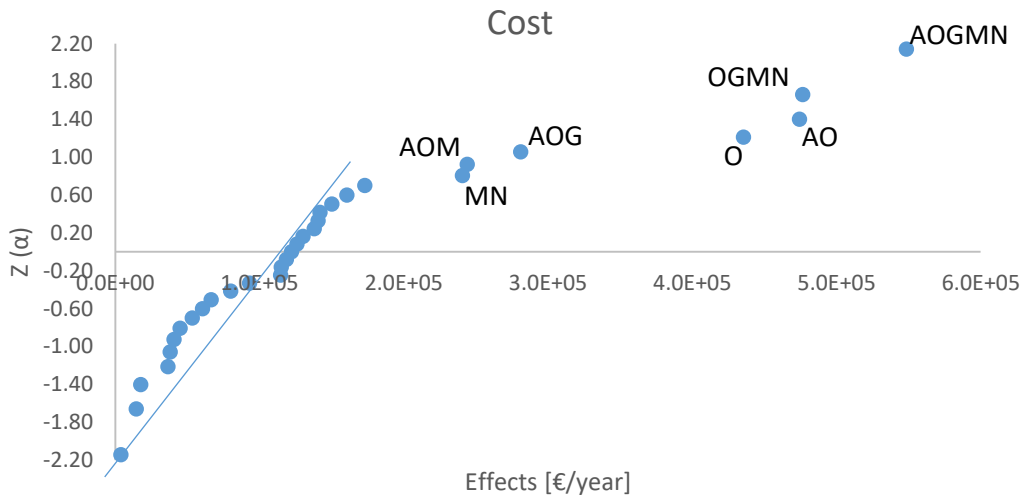

Figure 53 - Normal probability plot of effects regarding cost

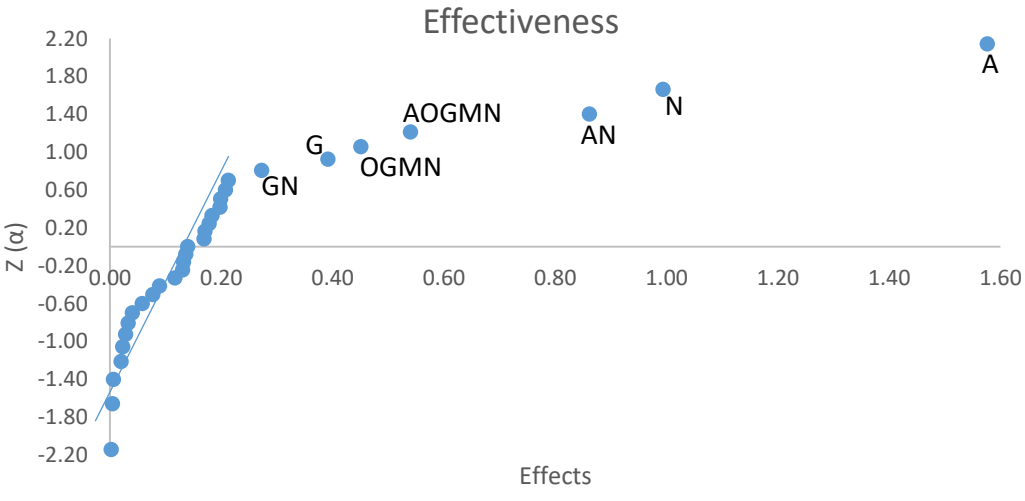

Figure 54 - Normal probability plot of effects regarding effectiveness

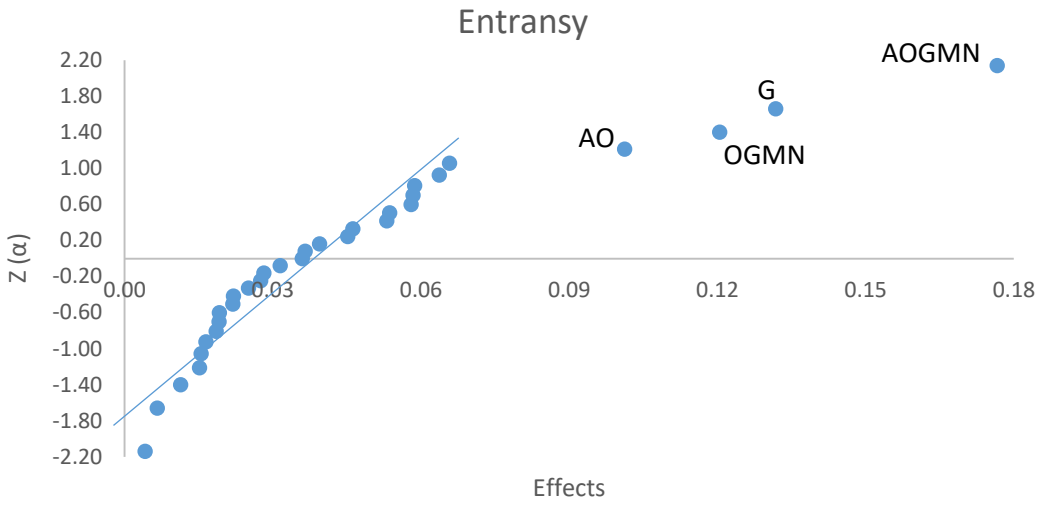

Figure 55 - Normal probability plot of effects regarding entransy efficiency

After this, an ANOVA was conducted to understand which factors/interactions influence each response significantly, for a confidence level of 95% (tables 69, 70, and 71).

Table 69 - ANOVA results regarding cost

	SS	DF	MS	F_0	
MN	4.64E+11	1	4.64E+11	5.840	
AOM	4.76E+11	1	4.76E+11	5.999	
AOG	6.32E+11	1	6.32E+11	7.964	
O	1.52E+12	1	1.52E+12	19.120	
AO	1.80E+12	1	1.80E+12	22.681	
OGMN	1.82E+12	1	1.82E+12	22.880	
AOGMN	2.41E+12	1	2.41E+12	30.311	F. INV
Error	1.83E+12	24	7.94E+10		4.260

Table 70 - ANOVA results regarding effectiveness

	SS	DF	MS	F_0	
GN	0.593	1	0.593	4.841	
G	1.225	1	1.225	10.003	
OGMN	1.627	1	1.627	13.286	
AOGME	2.332	1	2.332	19.046	
AN	5.938	1	5.938	48.495	
N	7.897	1	7.897	64.496	
A	19.886	1	19.886	162.405	F. INV
Error	2.816	24	0.122		4.260

Table 71 - ANOVA results regarding entransy efficiency

	SS	DF	MS	F_0	
AO	0.082	1	0.082	7.725	
OGMN	0.116	1	0.116	10.946	
G	0.139	1	0.139	13.103	
AOGMN	0.250	1	0.250	23.538	F. INV
Error	0.276	27	0.011		4.210

After determining the significant factors/interactions for each output, an RA was conducted to verify the model's validity. No significant deviations are noted in figures 103, 104, and 105 (Appendix F), which confirms the model's adequacy.

During the results' analysis, it is essential that this design's defining relation (equation 28), as well as its resulting aliasing structure (table 105, appendix F) be present as these will be crucial in understanding the factors/interactions that contributed to certain system's behavioral aspects.

$$I = OGMNB = AGMNJ = AOBJ = AOMNC = AGBC = OGJC = MNBJC = AOGND = AMBD = OMJD = GNBJD = GMCD = ONBCD = ANJCD = AOGMBJCD \quad (28)$$

The results indicate that the system's cost is significantly affected by the high-order interaction ABCDE, however, the sparsity of effects principle states that most systems are dominated by their main factors and low-order interactions, which fits nicely in this situation since the generator OGMN = B turns this into a 2-factor interaction AB. Although this seems more likely than crediting the original interaction, this design's aliasing structure tells us that AB is confounded with interaction MD (ADC's total trays and exothermic reactor's operating pressure, respectively), which encompasses two of the largest cost sources in the present system, leading us to believe this relation is the effect's source. Similarly, OGMN is confounded with interaction AMD through the generator mentioned above, which adds the endothermic reactor's operating temperature (A) to factors M and D.

Despite the possibilities that arise from the design's aliasing structure, the endothermic reactor's operating temperature (A) and the second three-phase separator's inlet temperature (N), which is effectively the column's condenser's temperature, influence the system's effectiveness directly (they are explicitly present in this metric's equation), meaning these are very likely to be the results' actual source. Likewise, the system's entransy efficiency results

are likely to stem from interaction AB and factor B, however, factor G's (T_{in} ADC) ABC alias, which encompasses both reactors' operating temperatures (A and C), as well as the endothermic reactor's operating pressure (B) is more likely to be the true source of influence upon this response.

Given the results presented, a clear investigation path needed to be outlined. As such, we chose to study the system's temperature factors (T_r Endo, T_{in} 3PS_1, T_{in} ADC, T_{in} 3PS_2, and T_r Exo) first. These will be shifted towards their high-level, except for the endothermic reactor's operating temperature, which will be shifted towards its low-level. The remaining variables will be set to their respective best levels in the current study. Also, now that the amount of variables has been decreased considerably, it will be possible to devise a complete factorial design experiment, so a 2^5 experiment will be carried out next.

Table 72 presents a summary of each factor's improvement direction for all three outputs.

Table 72 - Second experiment's factors' improvement direction summary

		Cost		Effectiveness		Entransy	
		S?	D?	S?	D?	S?	D?
T_r Endo	A	No	+	Yes	-	No	-
P Endo	B	Yes	+	Yes	-	Yes	-
P Flash	J	No	-	No	+	No	+
T_{in} 3PS_1	O	Yes	-	No	+	No	+
T_{in} ADC	G	No	+	Yes	+	Yes	+
Trays ADC	M	No	-	No	-	No	+
T_{in} 3PS_2	N	No	-	Yes	+	No	-
T_r Exo	C	No	-	No	+	No	+
P Exo	D	No	-	No	+	No	-

12.2.3. Third experiment

Table 73 presents the system's updated parameters. Due to the previous experiment's ambiguous results regarding the ADC's total number of trays and the exothermic reactor's operating pressure, a choice was made to set these values at that experiment's average.

Table 73 - Designation and factor levels for the variables in the third experiment

Variable	Designation	Low-level (-)	High-level (+)
T_{in} Endo			55.00
T_r Endo	A	60.00	65.00
P Endo		1.60	
T_{in} Flash			45.00
P Flash			1.50
T_{in} 3PS_1	O	58.00	62.00
P 3PS_1		1.10	
T_{in} ADC	G	60.00	70.00
Trays ADC		*20*	
Feed ADC		50%	
Splitter		0.20	
T_{in} 3PS_2	N	55.00	60.00
T_{in} Exo			175.00
T_r Exo	C	185.00	195.00
P Exo		*1.50*	

This third experiment was carried out as presented in table 91 (appendix B), and produced the results presented in table 74.

Table 74 - Results obtained from the third experiment

		Cost [M€/year]	Performance	
		Total	Effectiveness	Entransy
1	**[1]**	3.749	2.3490	0.6533
2	**a**	3.042	0.7841	0.3875
3	**o**	3.897	2.2850	0.6334
4	ao	3.934	1.2270	0.6261
5	**g**	3.889	3.5050	1.0350
6	ag	2.803	1.0820	0.5473
7	og	4.063	3.5580	1.0530
8	aog	3.555	1.3420	0.6886
9	**n**	3.876	0.7580	0.2108
10	an	4.811	1.6160	0.4174
11	on	4.224	2.5190	0.6864
12	aon	4.447	1.6190	0.4180
13	gn	3.292	2.2740	0.6258
14	agn	3.846	2.5140	0.6714
15	ogn	4.084	2.8730	0.7883
16	aogn	3.480	2.8620	0.7749
17	**c**	3.814	2.2410	0.6458
18	ac	3.703	0.9813	0.5080
19	oc	3.868	2.1440	0.6135
20	aoc	3.792	1.1190	0.5857
21	gc	3.507	2.9660	0.8893
22	agc	3.910	1.5940	0.8757
23	ogc	3.544	2.9140	0.8699
24	aogc	3.486	1.4810	0.8028
25	nc	4.234	1.0150	0.4933
26	anc	3.559	1.4390	0.3824
27	onc	4.075	1.0600	0.4721
28	aonc	3.984	1.4440	0.3830
29	gnc	3.640	1.6120	0.4126
30	agnc	3.800	2.2660	0.6223
31	ognc	2.814	0.7057	-0.0379
32	aognc	3.470	1.5730	0.4243

The first thing to note regarding the data shown is that assay 31 yielded a negative entransy efficiency, which indicates the set of operating conditions under which that assay was run severely impairs the system's working.

Figures 56, 57, and 58, were obtained after applying the methodology described earlier to all three outputs.

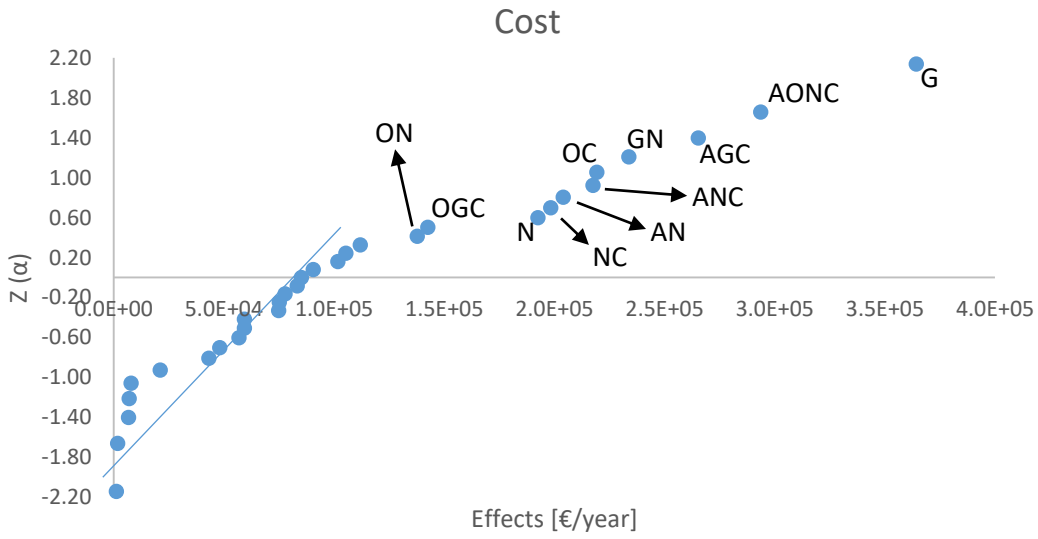

Figure 56 - Normal probability plot of effects regarding cost

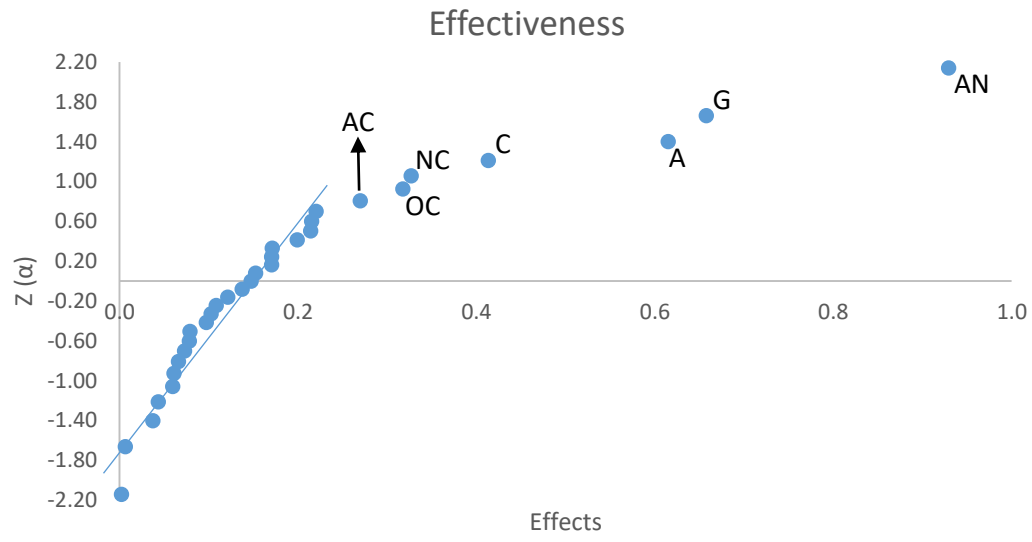

Figure 57 - Normal probability plot of effects regarding effectiveness

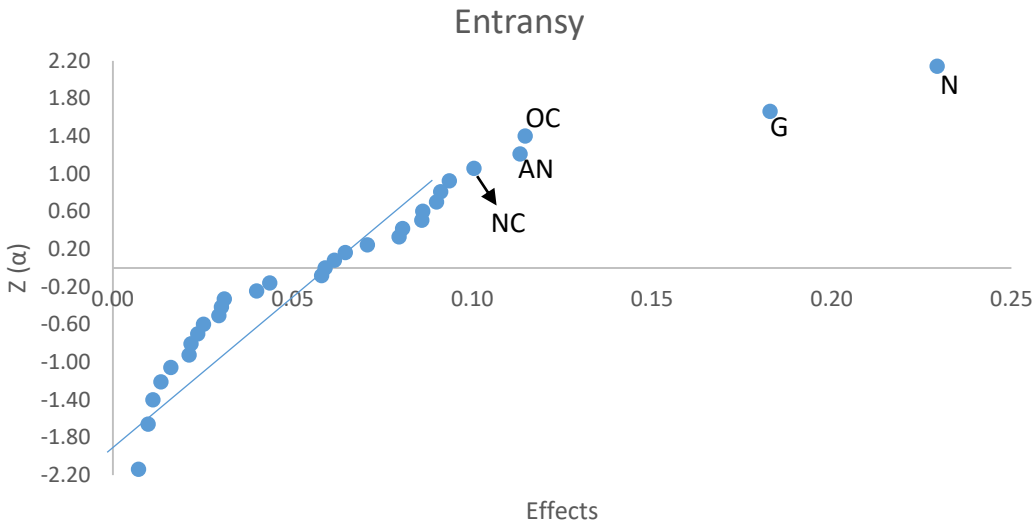

Figure 58 - Normal probability plot of effects regarding entransy efficiency

This experiment's ANOVA and its RA are available in appendix F (tables 106, 107, and 108, and figures 106, 107, and 108, respectively). The model used is considered valid as the figures mentioned do not present any significant deviations, however, it is important to mention that the point that appears quite distant from the others in the entransy efficiency's graph was caused by assay 31.

Moving to the result's analysis, these clearly indicate that all factors influence the system's cost substantially, especially the ADC's inlet temperature, which is understandable since this is connected to the heat, *i.e.*, hot utility, needed by the column's reboiler.

Regarding the system's performance, the effectiveness is more influenced by the reactors' operating and the ADC's inlet temperatures, which translates into the reactors' and the reboiler's heat-receiving and releasing capacities, whereas the entransy efficiency is more influenced by the ADC and the second three-phase separator's inlet temperatures. The system's entransy efficiency, though related to its heat-absorption and promotion capacities, is more intimately related to the entropy lost during the process, which supports the ADC's parameter's influence on this response since it is the largest source of entropy generation, and loss, in the entire system.

Table 75 presents a summary of each factor's improvement direction for all three outputs.

Table 75 - Third experiment's factors' improvement direction summary

		Cost		Effectiveness		Entransy	
		S?	D?	S?	D?	S?	D?
T_r Endo	A	No	+	Yes	-	No	-
T_{in} 3PS_1	O	No	-	No	+	No	+
T_{in} ADC	G	Yes	+	Yes	+	Yes	+
T_{in} 3PS_2	N	Yes	-	No	-	Yes	-
T_r Exo	C	No	+	Yes	-	No	-

According to this data:

- Although through an increase in cost, both reactor's operating temperatures give better results when set to their low-level;
- Both three-phase separator's inlet temperatures give better results, cots and performance-wise, when set to their low-level;
- The distillation column's inlet temperature offers better solutions at its high-level.

Going forward, both reactor's operating temperatures and both three-phase separator's inlet temperatures will be set to their best overall levels between this and the previous experiment. The next experiment will encompass both reactors', the flash separator's, and the ADC's inlet temperatures (T_{in} Endo, T_{in} Exo, T_{in} Flash, and T_{in} ADC), meaning a 2^4 complete factorial design experiment will be carried out.

12.2.4. Fourth experiment

Given the cumulative findings of the last two experiments, the system was updated as shown in table 76.

Table 76 - Designation and factor levels for the variables in the second experiment

Variable	Designation	Low-level (-)	High-level (+)
T_{in} Endo	K	55.00	60.00
T_r Endo		60.00	
P Endo		1.60	
T_{in} Flash	H	45.00	50.00
P Flash			1.50
T_{in} 3PS_1		55.00	
P 3PS_1		1.10	
T_{in} ADC	G	65.00	75.00
Trays ADC			*20*
Feed ADC		50%	
Splitter		0.20	
T_{in} 3PS_2		55.00	
T_{in} Exo	E	175.00	185.00
T_r Exo		185.00	
P Exo			*1.50*

This fourth experiment was carried out as presented in table 90 (appendix B) and yielded the results presented in table 77.

Table 77 - Results obtained from the fourth experiment

		Cost [M€/year]	Performance	
		Total	Effectiveness	Entransy
1	**[1]**	4.500	2.6980	0.7688
2	**k**	6.596	2.9610	0.8407
3	**h**	3.585	2.9260	0.8512
4	kh	3.929	2.9380	0.8482
5	**g**	3.632	3.7840	1.1280
6	kg	2.449	2.0500	0.5676
7	hg	2.928	2.8540	0.8163
8	khg	2.033	0.5180	0.1378
9	**e**	4.041	3.1640	0.9181
10	ke	6.395	3.1390	0.8868
11	he	2.986	1.9400	0.5296
12	khe	3.639	2.0460	0.5576
13	ge	2.562	2.5040	0.6988
14	kge	1.909	2.5030	0.6965
15	hge	2.998	3.1930	0.9131
16	khge	2.997	3.2340	0.9222

Unlike the previous experiment's results, all assays yielded practicable solutions, a good indicator that the operating values for the fixed factors were properly chosen.

Figures 59, 60, and 61, were obtained after applying the methodology described earlier to all three outputs.

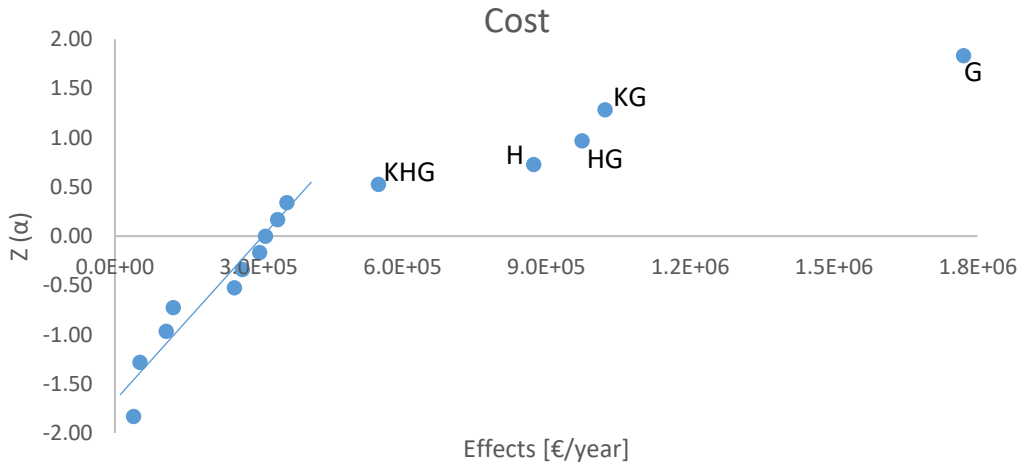

Figure 59 - Normal probability plot of effects regarding cost

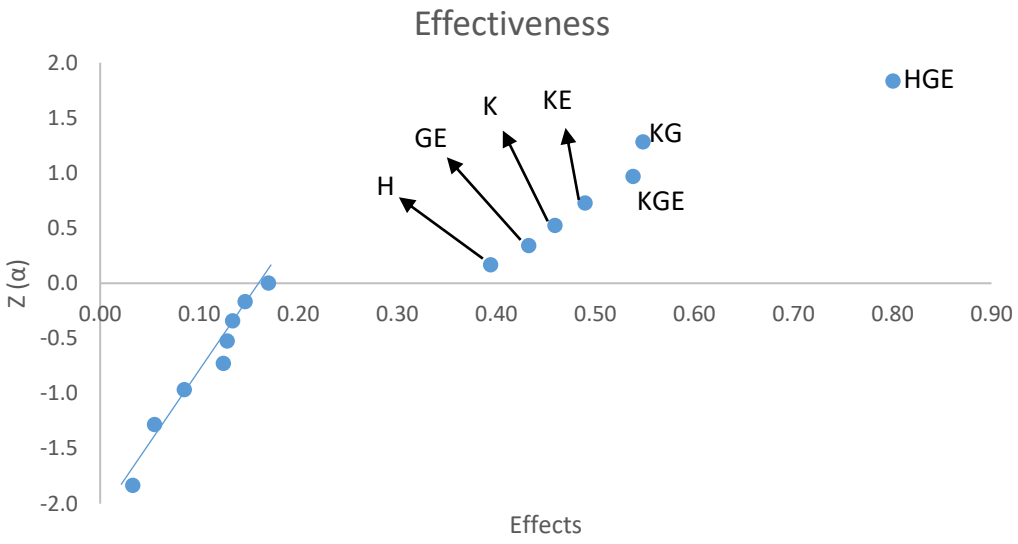

Figure 60 - Normal probability plot of effects regarding effectiveness

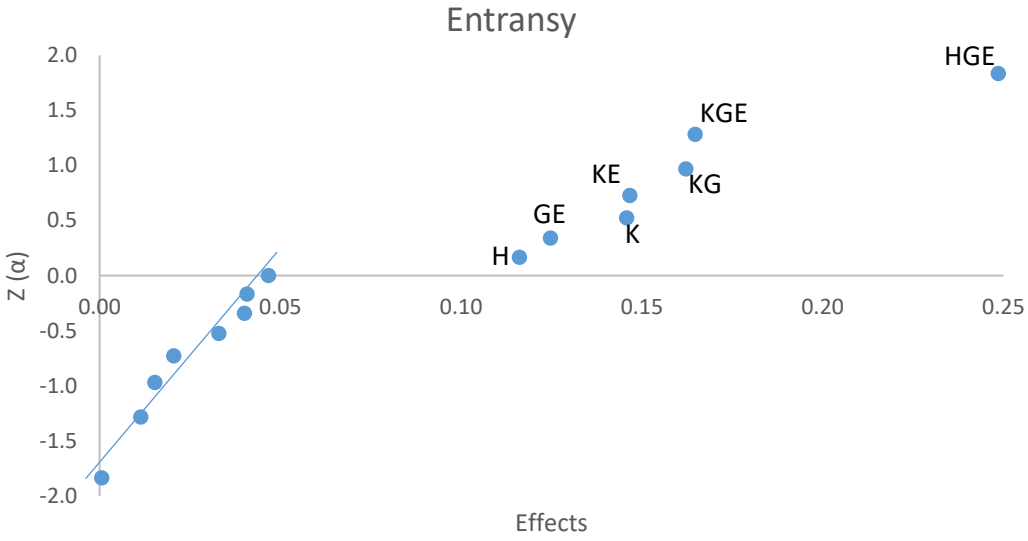

Figure 61 - Normal probability plot of effects regarding entransy efficiency

This experiment's ANOVA and its RA are available in appendix F (tables 109, 110, and 111, and figures 109, 110, and 111, respectively). The model used is considered valid as the figures mentioned do not present any significant deviations.

Regarding this experiment's results, we can see that:

- The system's cost is, once again, largely influenced by the ADC's inlet temperature. It is also somewhat influenced by this factor's interactions with the endothermic reactor and flash separator's inlet temperatures;
- Both this system's effectiveness and its entransy efficiency are largely influenced by the ADC's and the exothermic reactor's inlet temperatures, reinforcing their crucial roles in the system's ability to absorb excess-heat and promote it to higher temperatures.

Table 78 presents a summary of each factor's improvement direction for all three outputs.

Table 78 - Fourth experiment's factors' improvement direction summary

		Cost		Effectiveness		Entransy	
		S?	D?	S?	D?	S?	D?
T_{in} Endo	K	No	-	Yes	-	Yes	-
T_{in} Flash	H	Yes	+	Yes	-	Yes	-
T_{in} ADC	G	No	+	No	-	Yes	-
T_{in} Exo	E	No	+	No	+	No	+

Given this information, the endothermic reactor, the flash separator and the ADC's inlet temperatures offer better results when set to their respective low-level values, although this comes at a greater cost regarding the flash separator and the ADC. The exothermic reactor's inlet temperature offers better results, both cost and performance-wise, when set to its high-level.

Considering the several experiments carried out so far, the next experiment will further the investigation efforts surrounding the flash separator and the ADC's inlet temperatures (T_{in} Flash and T_{in} ADC), as well as the former's operating pressure (P Flash) and the latter's number of trays (Trays ADC), which means a 2^4 complete factorial design experiment will be carried out.

12.2.5. Fifth experiment

Given last experiment's findings, the system was updated as shown in table 79.

Table 79 - Designation and factor levels for the variables in the second experiment

Variable	Designation	Low-level (-)	High-level (+)
T_{in} Endo		55.00	
T_r Endo		60.00	
P Endo		1.60	
T_{in} Flash	H	40.00	45.00
P Flash	J	1.20	1.50
T_{in} 3PS_1		55.00	
P 3PS_1		1.10	
T_{in} ADC	G	65.00	70.00
Trays ADC	M	18	20
Feed ADC		50%	
Splitter		0.20	
T_{in} 3PS_2		55.00	
T_{in} Exo			185.00
T_r Exo		185.00	
P Exo		*1.50*	

This experiment was carried out as presented in table 90 (appendix B) and yielded the results presented in table 80.

Table 80 - Results obtained from the fifth experiment

		Cost [M€/year]	Performance	
		Total	Effectiveness	Entransy
1	**[1]**	3.851	3.0540	0.8761
2	**h**	4.938	2.9070	0.8177
3	**j**	4.541	2.8490	0.7996
4	hj	4.045	3.1950	0.9283
5	**g**	3.718	4.0900	1.2270
6	hg	3.538	3.4300	0.9936
7	jg	2.852	2.4280	0.6758
8	hjg	3.534	3.4170	0.9892
9	**m**	3.681	2.7790	0.7808
10	hm	3.836	3.0210	0.8646
11	jm	5.306	3.2810	0.9392
12	hjm	5.246	3.0070	0.8491
13	gm	3.549	3.4570	1.0030
14	hgm	3.527	3.4200	0.9901
15	jgm	3.849	4.1790	1.2570
16	hjgm	3.548	3.4540	1.0020

Figures 62, 63, and 64, were obtained after applying the methodology described earlier to all three outputs.

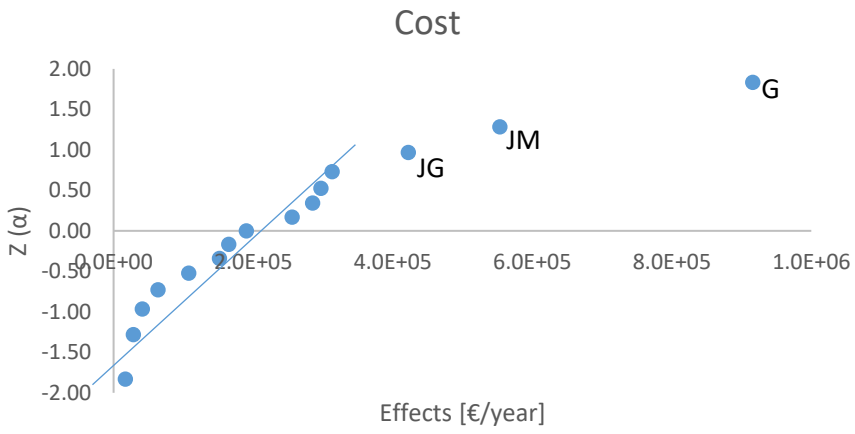

Figure 62 - Normal probability plot of effects regarding cost

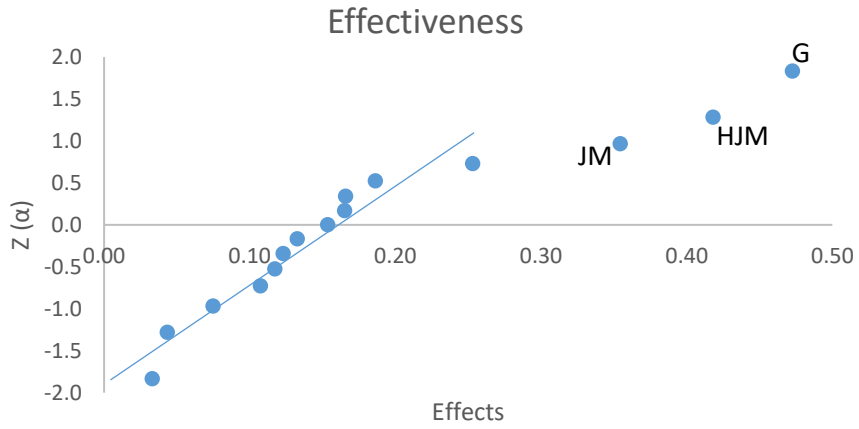

Figure 63 - Normal probability plot of effects regarding effectiveness

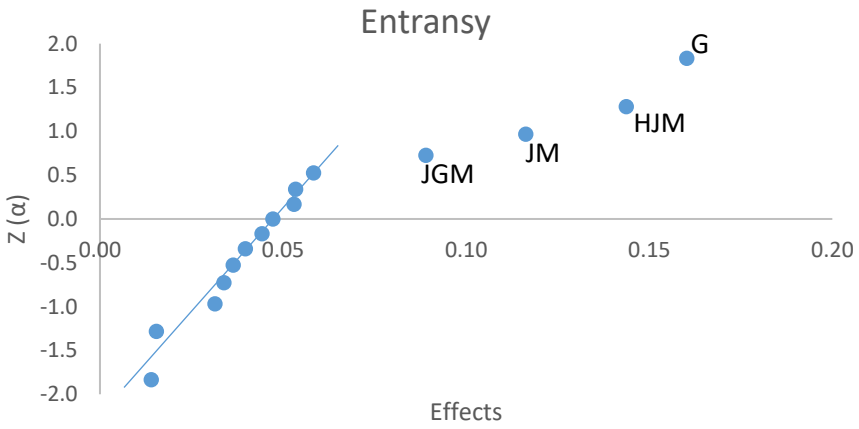

Figure 64 - Normal probability plot of effects regarding entransy efficiency

This experiment's ANOVA and its RA are available in appendix F (tables 112, 113, and, 114, and figures 112, 113, and 114, respectively). The model used is considered valid as there are no significant deviations.

Regarding the data shown above, we can see that:

- The ADC's inlet temperature is the most significant factor for all three outputs;
- The remaining factors are not significant on their own, but several of their interactions are.

Table 81 presents a summary of each factor's improvement direction for all three outputs.

Table 81 - Fifth experiment's factors' improvement direction summary

		Cost		Effectiveness		Entransy	
		S?	D?	S?	D?	S?	D?
T_{in} Flash	H	No	-	No	-	No	-
P Flash	J	Yes	-	No	-	No	-
T_{in} ADC	G	Yes	+	Yes	+	Yes	+
Trays ADC	M	No	-	No	+	No	+

Given this data, we can affirm that both the flash separator's inlet temperature and its operating pressure produce better solutions when set to their respective low-level (40 °C and 1.20 atm), while the ADC's inlet temperature and number of trays produce better performance solutions when set to their respective high-level (70 °C and 20 trays), although the larger number of trays translates into an increase in the equipment's cost.

12.2.6. Summary of the Designed Experiments study

As earlier, the large amount of information presented regarding the *t*B/iB system, it is important to condense and summarize some of the DoE studies' major findings.

Figures 65 and 66, which respectively present the cost and performance variation throughout the several experiments conducted, seem to indicate that the system's increase in performance comes at the expense of the increased cost, however, experiment 5's simultaneous decrease in cost and increase in performance allows us to reject this direct correlation.

This system's cost is strongly affected by the exothermic reactor's operating pressure due to this factor's influence on the compressor. Furthermore, the additional equipment that this system requires increases the utility costs related to temperature corrections.

The system's performance and heat capacity (figures 66 and 67) improved as the experiments progressed and both reactors, as well as the ADC, played an important role regarding these responses. The column's operation, *i.e.*, its separation efficiency, in particular, determines the quantities sent to each reactor, which in turn affects their performance, and this becomes even

more important when considering the presence of benzene, which will act as an inert, hindering each reactor's capability to absorb and release heat.

Still regarding the system's heat capacity, it is crucial to highlight the impact of utilizing low-temperature excess heat in the ADC's reboiler, particularly in view of the large matter volumes in circulation, which mean the reboiler will require huge amounts of energy to operate. To put it simply, using excess-heat instead of some hot utility saved, in this case, from around 150 €/hr to 235 €/hr, which would otherwise increase the system's TAC about 1.5 M€/year. To give an idea of the order of magnitude surrounding these savings, the system's costs would register an increase of about 65% if the column's reboiler could not be operated through the input of low-temperature excess heat.

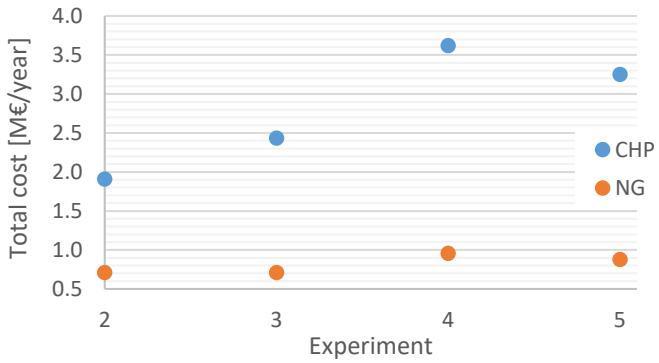

Figure 65 - Average CHP and NG costs for each experiment in the *t*B/iB system's DoE study

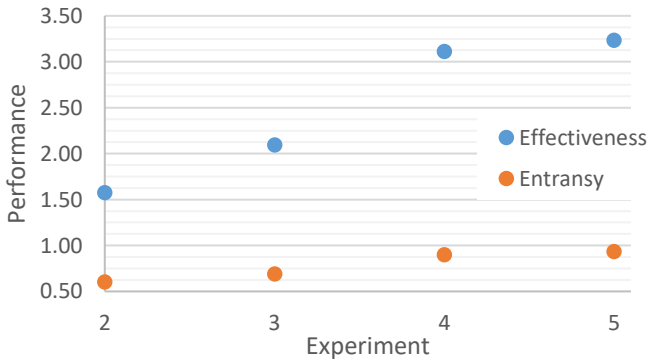

Figure 66 - Average performance for each experiment in the *t*B/iB system's DoE study

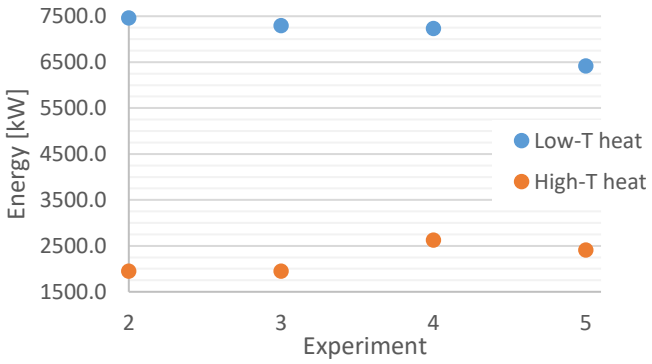

Figure 67 - Average low- and high-T heats for each experiment in the *t*B/iB system's DoE study

12.2.7. Competitive Assays

Given the number of experiments carried out and the large number of variables involved in the current system, table 82 presents a summary of the “best” operating conditions for the *t*B/iB system.

Table 82 - "Best" operating conditions for the *t*B/iB system

Variable	“Best” level	Variable	“Best” level	Variable	“Best” level
T_{in} Endo	55.00	T_{in} 3PS_1	55.00	Splitter	0.20
T_r Endo	60.00	P 3PS_1	1.10	T_{in} 3PS_2	55.00
P Endo	1.60	T_{in} ADC	70.00	T_{in} Exo	185.00
T_{in} Flash	40.00	Trays ADC	20	T_r Exo	185.00
P Flash	1.20	Feed ADC	50%	P Exo	1.50

As occurred with the IAH system, even though this set of conditions results in the best performance/cost scenario, it does not account for the issue of EComp.

As explained earlier, this system’s EComp will only be assessed against the use of natural gas and only the raw-material cost, and CT, will be taken into account (tables 40 and 41, respectively). The system’s ECst is given by equation 18.

Now that we have all the necessary information, the 15 most competitive assays (*i.e.*, those with lower ECst values) were identified (tables 83 and 84).

Table 83 - Operating conditions of the 15 most competitive assays

		Endo			Flash		3PS_1		ADC		Splitter	3PS_2	Exo		
Experiment	*Assay*	T_{in}	T_r	P	T_{in}	P	T_{in}	P	T_{in}	Trays	-	T_{in}	T_{in}	T_r	P
2	*17*	55.00	60.00	1.60	45.00	1.20	55.00	1.10	55.00	18	0.20	57.00	175.00	180.00	1.30
2	*20*	55.00	70.00	2.40	45.00	1.50	60.00	1.10	55.00	18	0.20	57.00	175.00	180.00	1.30
2	*27*	55.00	60.00	1.60	45.00	1.50	60.00	1.10	55.00	22	0.20	57.00	175.00	180.00	1.70
2	*9*	55.00	60.00	1.60	45.00	1.20	55.00	1.10	55.00	22	0.20	53.00	175.00	180.00	1.70
2	*4*	55.00	70.00	1.60	45.00	1.20	60.00	1.10	55.00	18	0.20	53.00	175.00	190.00	1.70
2	*3*	55.00	60.00	1.60	45.00	1.50	60.00	1.10	55.00	18	0.20	53.00	175.00	180.00	1.30
3	*1*	55.00	60.00	1.60	45.00	1.50	58.00	1.10	60.00	20	0.20	55.00	175.00	185.00	1.50
3	*4*	55.00	65.00	1.60	45.00	1.50	62.00	1.10	60.00	20	0.20	55.00	175.00	185.00	1.50
3	*11*	55.00	60.00	1.60	45.00	1.50	62.00	1.10	60.00	20	0.20	60.00	175.00	185.00	1.50
3	*17*	55.00	60.00	1.60	45.00	1.50	58.00	1.10	60.00	20	0.20	55.00	175.00	195.00	1.50
3	*25*	55.00	60.00	1.60	45.00	1.50	58.00	1.10	60.00	20	0.20	60.00	175.00	195.00	1.50
3	*3*	55.00	60.00	1.60	45.00	1.50	62.00	1.10	60.00	20	0.20	55.00	175.00	185.00	1.50
3	*20*	55.00	65.00	1.60	45.00	1.50	62.00	1.10	60.00	20	0.20	55.00	175.00	195.00	1.50
2	*12*	55.00	70.00	2.40	45.00	1.50	60.00	1.10	55.00	22	0.20	53.00	175.00	180.00	1.70
2	*24*	55.00	70.00	1.60	45.00	1.20	60.00	1.10	65.00	18	0.20	57.00	175.00	180.00	1.70

From table 83, it appears that the best values regarding the endothermic reactor and the flash separator's inlet temperatures, and the splitter's division, are indeed 55 °C and 45 °C, and 0.20, respectively, whereas all other variables assume different values, except for the first three-phase

separator's operating pressure, however, as explained above, this value stemmed more from a need to ensure the simulation's convergence and guarantee the operating conditions necessary towards this equipment's proper functioning.

Table 84 - Cost, performance, heat supplied and recovered, and excess costs of the 15 most competitive assays

		CHP's cost	**Performance**		**Heat**	**[kW]**		**NG's cost**	**ECst**
Experiment	*Assay*	[M€/year]	Effectiveness	Entransy	Q_L	Q_r	Q_H	[M€/year]	-
2	*17*	2.060	3.4080	0.5632	2453	7512	2485	0.906	56.03%
2	*20*	2.119	0.9185	0.5448	2314	7170	2367	0.862	59.31%
2	*27*	2.172	3.4110	0.5607	2357	7138	2370	0.862	60.32%
2	*9*	2.226	1.6540	0.6282	2309	6454	2397	0.873	60.78%
2	*4*	2.046	0.6767	0.5349	3019	6036	2064	0.753	63.20%
2	*3*	2.309	1.6330	0.6168	2228	6238	2286	0.833	63.92%
3	*1*	2.213	2.3490	0.6533	2242	5609	2186	0.797	64.00%
3	*4*	2.380	1.2270	0.6261	2709	5751	2273	0.829	65.15%
3	*11*	2.225	2.5190	0.6864	2241	5025	2119	0.771	65.33%
3	*17*	2.278	2.2410	0.6458	2328	5794	2113	0.771	66.15%
3	*25*	2.167	1.0150	0.4933	2320	7541	2006	0.731	66.27%
3	*3*	2.335	2.2850	0.6334	2206	5706	2144	0.782	66.50%
3	*20*	2.238	1.1190	0.5857	2570	5675	1978	0.720	67.82%
2	*12*	2.691	0.7582	0.5731	2269	6735	2350	0.855	68.23%
2	*24*	2.575	1.0360	0.6336	3026	4836	2214	0.808	68.65%

From table 84, we can immediately see that, sadly, this CHP system does not even come close to being a competitive solution since its best scenarios are still around two times more expensive than acquiring natural gas to produce the same amount of heat. This low EComp is a direct consequence of the system's cost/upgraded heat balance, which is itself certainly a consequence of its low reaction heat (table 3), translated here into a relatively low ability to absorb heat in the endothermic reactor.

12.2.8. Parametric Evaluation

After determining this system's variables' "best" values through DoE, it is important to conduct a more rigid parametric analysis in order to determine the most impactful variables', the endothermic and exothermic reactors' operating pressures, actual best values. Table 85 presents the operating conditions for the remaining variables.

Table 85 - Operating conditions for the variables not contemplated in the parametric analysis (note that T is in °C and P is in atm)

Endo		**Flash**		**3PS_1**		**ADC**		**Splitter**	**3PS_2**	**Exo**	
T_{in}	T_r	T_{in}	P	T_{in}	P	T_{in}	Trays	-	T_{in}	T_{in}	T_r
60.0	60.0	45.0	1.20	55.0	1.10	55.0	18	0.20	57.0	180.0	180.0

These values correspond to the findings from a small investigation carried out upon this system's best solution (experiment 2, assay 17 (above)), with the aim of determining if the reactors gave better solutions when working in isothermal mode, which they do.

Table 86 shows the ranges in which the reactor's operating pressures were varied.

Table 86 - Reactors' operating pressure ranges for the parametric evaluation

Reactor	**Operating Pressure**				
Endothermic	1.40	1.60	1.80	2.00	2.20
Exothermic	1.30	1.50	1.70	1.90	2.10

As mentioned several times throughout this work, special care was taken to avoid duplicating any pressure increasing equipment. Figures 68 to 70 present the results obtained from this parametric analysis.

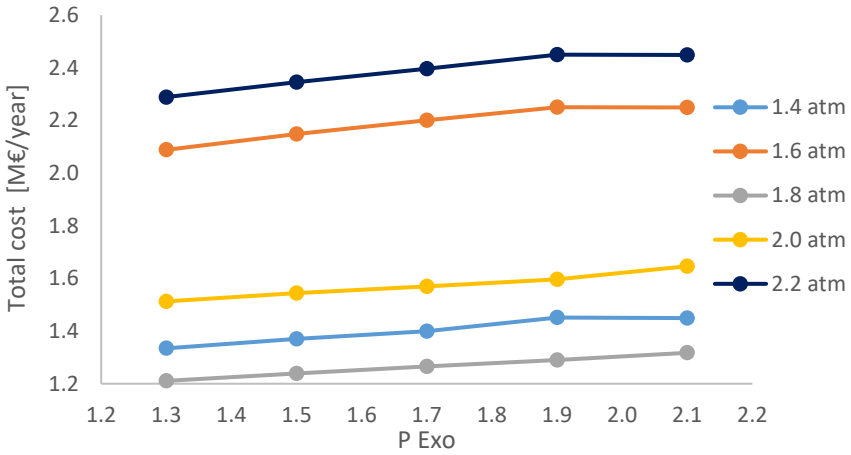

Figure 68 - System's cost variation with the reactors' pressures

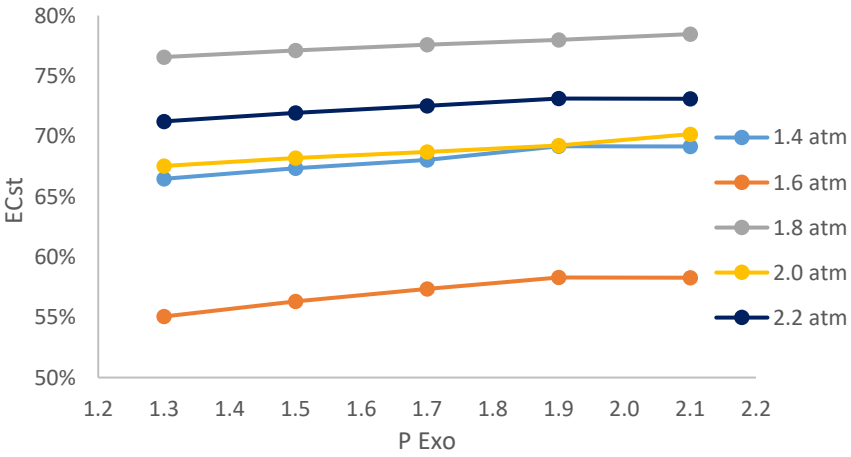

Figure 69 - System's excess cost variation with the reactors' pressures

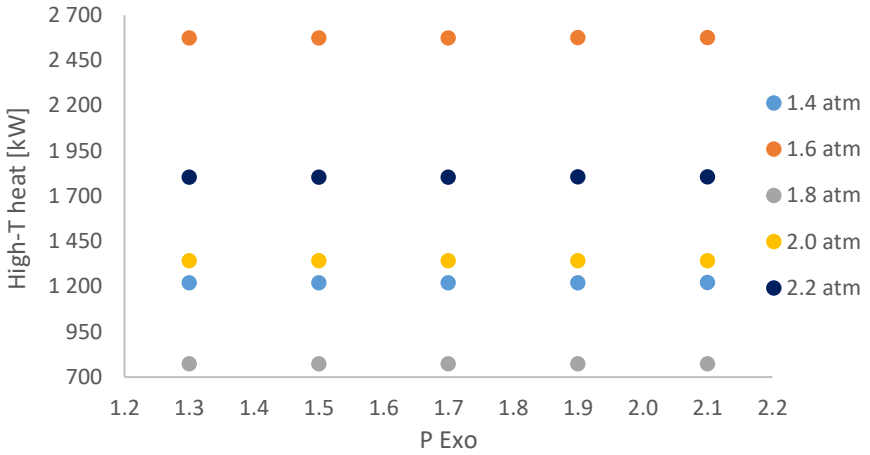

Figure 70 - System's upgraded heat variation with the reactors' pressures

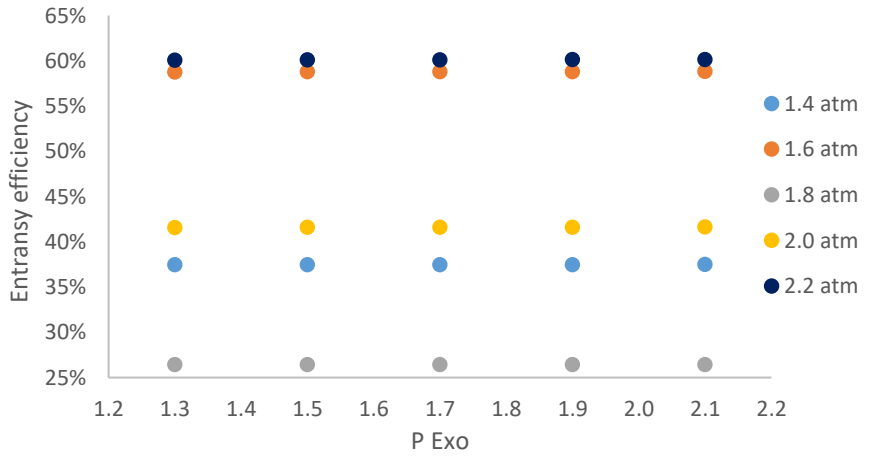

Figure 71 - System's performance variation with the reactors' pressures

The first thing to notice is that, unlike what was expected, a higher P Exo does not necessarily translate to higher total cost. Given the system's size and, therefore, high number of heat-exchangers necessary, this non-linear behavior may be due to the utilities needed in each situation.

Regarding the ECst attained, it is possible to see that the best case scenario (P Endo = 1.60 atm and P Exo = 1.30 atm) is still two times more expensive than the alternative, and more, the remaining solutions are three to five times more expensive.

Although it presents acceptable upgraded heat and performance values, this system's extremely low EComp means it is not a viable solution in a real-world implementation scenario.

While a large difference is not expected, a condensed study was carried out to establish if there are any operating conditions capable of delivering better results than those mentioned above. This study found that an operating pressure of 1.50 atm for the endothermic reactor yielded a slight improvement in the system's results (table 87), however, this difference is so insignificant that our observations thus far are not affected by it in any way.

Table 87 - *t*B/iB system's "best" solutions

		CHP's cost	**Performance**		**Heat [kW]**			**NG's cost**	**ECst**
P Endo	*P Exo*	[M€/year]	Effectiveness	Entransy	Q_L	Q_r	Q_H	[M€/year]	-
1.60	*1.30*	2.088	3.5650	0.5879	2361	7502	2573	0.938	55.06%
1.50	*1.30*	2.069	3.5230	0.5816	2465	7438	2553	0.931	55.00%

V – CONCLUSIONS AND FUTURE WORK

13. Conclusions

It is undeniable that heat recovery and promotion is absolutely paramount to achieve the much needed decarbonization of the global industrial machine and the technology studied in this work, especially the IAH system, presents strong arguments for its continuous growth, progress, and enhancement.

Even though this work found, without surprise, that a non-optimized chemical heat pump is not capable of competing with the use of natural gas to produce the same amount of high-temperature heat, being around 58% and 64% more expensive, for the IAH and *t*B/iB system, respectively, the finding that these systems were still 49% and 56% more costly, after their respective optimization studies, was not expected. This finding does, however, serve as an excellent indicator of the poor economic performance that plagues these systems.

The *t*B/iB system, in particular, is far too complex both from a design and an operation perspective to reach any degree of EComp. This was verified by the fact that its best solution is still, unfortunately, 55%, *i.e.*, more than two times, more expensive than using natural gas. Nonetheless, this system's study was fundamental in the realization that the performance equations related to the system's effectiveness, namely equation 4, which gives the system's theoretical maximum enthalpy efficiency, is not suitable for this type of system, and should be revised to account for the input of low-temperature excess heat in any type of distillation column, if applicable, of course.

The IAH system underwent several additional optimization studies which allowed it to achieve some degree of EComp. These studies focused on:

- The excess hydrogen in circulation, which saw an improvement of around 19%;
- The reactor's operating pressures, which resulted in an increase in the system's EComp by another 8%;
- And the use of a distillation column, which registered the largest improvement, reaching negative ECsts, *i.e.*, resulting in a solution less expensive than the alternative, natural gas.

Despite having registered several fluctuations regarding the system's performance metrics and heat capacities throughout the different studies, the IAH system's final study, which incorporated the use of a distillation column, ultimately culminated in a solution that presented satisfactory performance values (around 38% for the enthalpy efficiency and around 53% for the entropy efficiency) and a large high-temperature heat capacity (around 4.2 MW). Even though these results are fairly attractive, it is important to highlight that this solution is only able to promote approximately 25% of the low-temperature received, meaning there is still ample room for improvement, which is extremely encouraging, especially when considering that this investment's least ambitious economic scenario presents a payback period of 14 years.

A very important aspect of this work is that every study assumed all of the CHP systems' hot and cold energy needs, aside from the low-temperature excess heat, obviously, would come from utility plants, *i.e.*, they did not account for any heat integration with an existing industrial process, which is what should happen in a real-world implementation scenario, meaning there is still ample room for improvement of these solutions.

Another very important aspect concerning these systems is that they appear to become more competitive with increasing heat capacity (figure 97, appendix D), but not proportionately to their cost, meaning they have some interesting scale-up potential, which increases the range of possible implementation scenarios.

Regarding these systems' applications, the most interesting scenario, particularly due to their increasing EComp with increasing heat capacity, might be their implementation coupled with a distillation column where the column's condenser feeds the endothermic reactor and its reboiler is then fed by the CHP's exothermic reactor, thus possibly enabling the creation of a self-sustaining distillation system.

Overall, this work found that these chemical heat pump systems based on reversible organic endo-exothermic reactions are both technically and economically feasible, but not yet quite as competitive as desired.

14. Future work

Despite first being envisioned in 1824, these CHP systems have only recently started attracting significant attention from the scientific community, which effectively means they are still in a relatively infant stage of development, and implies there are a myriad of unexplored paths leading to their development and improvement.

Research concerning the catalysts involved in both the endo and exothermic reactions are one of the main investigation topics that could help improve these systems. Solutions for the inhibition and deactivation that affects the catalysts involved in these systems' endothermic reactions, whether through the modification of existing compounds, or the development of entirely new ones, may be a particularly promising area of research.

In addition to the focus on the reactions' catalysts, the use of reactive distillation setups, to circumvent said problems altogether, presents the extra benefit of condensing the system's endothermic reactor and distillation column into a single piece of equipment, possibly helping to lower the system's capital costs, and, consequently, its total costs.

Parallel to the topics mentioned above, the development of new reaction systems, preferably with large reaction enthalpies, capable of operating in wide temperature ranges, and that obey the criteria mentioned above for the selection of appropriate ORCHP solutions, should always be considered a crucial subject pertaining to the world of chemical heat pumps.

Leaving the laboratory, it is vital that actual implementation studies be carried out. Even if these ultimately find that this technology is not yet quite ready to be implemented, its many strengths must be highlighted so that more attention and interest is created around it, which in turn attracts more investigative efforts, thus creating a positive snowball/feedback effect surrounding these CHP systems.

REFERENCES

1. Benton, G. S. Carbon dioxide and its role in climate change. *Proc. Natl. Acad. Sci.* **67**, 898–899 (1970).

2. Wang, W., Wang, S., Ma, X. & Gong, J. Recent advances in catalytic hydrogenation of carbon dioxide. *Chem. Soc. Rev.* **40**, 3703–3727 (2011).

3. Doney, S. C., Fabry, V. J., Feely, R. A. & Kleypas, J. A. Ocean Acidification: The Other CO_2 Problem. *Ann. Rev. Mar. Sci.* **1**, 169–192 (2009).

4. Samanta, A., Zhao, A., Shimizu, G. K. H., Sarkar, P. & Gupta, R. Post-Combustion CO_2 Capture Using Solid Sorbents: A Review. *Ind. Eng. Chem. Res.* **51**, 1438–1463 (2012).

5. Song, C. Global challenges and strategies for control, conversion and utilization of CO_2 for sustainable development involving energy, catalysis, adsorption and chemical processing. *Catal. Today* **115**, 2–32 (2006).

6. Blunden, J. & Arndt, D. S. *State of the Climate in 2019*. *Bulletin of the American Meteorological Society* vol. 101 https://journals.ametsoc.org/doi/10.1175/2020BAMSStateoftheClimate.1 (2020).

7. NOAA. Trends in Atmospheric Carbon Dioxide. *Earth System Research Laboratory* https://gml.noaa.gov/ccgg/trends/global.html.

8. IPCC. *Climate Change 2014: Synthesis Report. Contribution of Working Groups I, II and III to the Fifth Assessment Report of the Intergovernmental Panel on Climate Change*. (2014).

9. Lewis, N. S. & Nocera, D. G. Powering the planet: Chemical challenges in solar energy utilization. *Proc. Natl. Acad. Sci.* **103**, 15729–15735 (2006).

10. Lüthi, D. *et al.* High-resolution carbon dioxide concentration record 650,000–800,000 years before present. *Nature* **453**, 379–382 (2008).

11. Dietz, T. & Rosa, E. A. Effects of population and affluence on CO2 emissions. *Proc. Natl. Acad. Sci.* **94**, 175–179 (1997).

12. Eurostat. *Share of renewable energy in the EU up to 18.0%*. *NewsRelease* https://ec.europa.eu/eurostat/documents/2995521/10335438/8-23012020-AP-EN.pdf/292cf2e5-8870-4525-7ad7-188864ba0c29 (2020).

13. Eurostat. *Share of renewable energy in the EU up to 19.7% in 2019*. https://ec.europa.eu/eurostat/en/web/products-eurostat-news/-/ddn-20201218-1 (2020).

14. IEA. *Energy and Climate Change*. *World Energy Outlook* https://www.iea.org/reports/energy-and-climate-change (2015).

15. Dincer, I. Renewable energy and sustainable development: A crucial review. *Renew. Sustain. Energy Rev.* **4**, 157–175 (2000).

16. Mekhilef, S., Saidur, R. & Safari, A. A review on solar energy use in industries. *Renew. Sustain. Energy Rev.* **15**, 1777–1790 (2011).

17. Panwar, N. L., Kaushik, S. C. & Kothari, S. Role of renewable energy sources in environmental protection: A review. *Renew. Sustain. Energy Rev.* **15**, 1513–1524 (2011).

18. Fawzy, S., Osman, A. I., Doran, J. & Rooney, D. W. Strategies for mitigation of climate change: a review. *Environ. Chem. Lett.* **18**, 2069–2094 (2020).

19. World Health Organization. *Burden of disease from the joint effects of Household and Ambient Air Pollution for 2012*. *World Health Organization* vol. 35 http://www.who.int/phe/health_topics/outdoorair/databases/FINAL_HAP_AAP_BoD_24March2014.pdf (2014).

20. Falkner, R. The Paris Agreement and the new logic of international climate politics. *Int. Aff.* **92**, 1107–1125 (2016).

21. Li, J., Zhang, X., Ali, S. & Khan, Z. Eco-innovation and energy productivity: New determinants of renewable energy consumption. *J. Environ. Manage.* **271**, 111028–111034 (2020).

22. UNFCCC. *Paris Climate Agreement*. (2015).

23. Sanderson, B. M., O'Neill, B. C. & Tebaldi, C. What would it take to achieve the Paris temperature targets? *Geophys. Res. Lett.* **43**, 7133–7142 (2016).

24. Zhai, R. *et al.* Larger Drought and Flood Hazards and Adverse Impacts on Population and Economic Productivity Under 2.0 than 1.5°C Warming. *Earth's Futur.* **8**, (2020).

25. Schleussner, C.-F. *et al.* Science and policy characteristics of the Paris Agreement temperature goal. *Nat. Clim. Chang.* **6**, 827–835 (2016).

26. van Vuuren, D. P. *et al.* Alternative pathways to the 1.5 °C target reduce the need for negative emission technologies. *Nat. Clim. Chang.* **8**, 391–397 (2018).

27. Peters, G. P. *et al.* Key indicators to track current progress and future ambition of the Paris Agreement. *Nat. Clim. Chang.* **7**, 118–122 (2017).

28. Cantalloube, F. *et al.* The impact of climate change on astronomical observations. *Nat. Astron.* **4**, 826–829 (2020).

29. Eurostat. *Sustainable Development in the European Union: Monitoring report on progress towards the SDGs in an EU context - 2020 Edition*. (2020).

30. Kerr, R. A. Carbon Dioxide and a Changing Climate. *Science* **222**, 491–491 (1983).

31. Fujii, S., Kameyama, H., Yoshida, K. & Kunii, D. Chemical reaction cycles for the recovery of low-level thermal energy. *J. Chem. Eng. Japan* **10**, 224–228 (1977).

32. Bruinsma, D. & Spoelstra, S. Heat Pumps in Distillation. in *Chemical Engineering Progress* (eds. de Haan, A. B., Koojiman, H. & Górak, A.) (Technische Universiteit Eindhoven, 2010).

33. Donnellan, P., Cronin, K. & Byrne, E. Recycling waste heat energy using vapour absorption heat transformers: A review. *Renew. Sustain. Energy Rev.* **42**, 1290–1304 (2015).

34. IEA. *Energy and Air Pollution*. *World Energy Outlook* https://web.archive.org/web/20191011100229/http://www.iea.org/publications/freepublications/publication/WorldEnergyOutlookSpecialReport2016EnergyandAirPollution.pdf (2016).

35. Kapil, A., Bulatov, I., Smith, R. & Kim, J.-K. Site-wide low-grade heat recovery with a new cogeneration targeting method. *Chem. Eng. Res. Des.* **90**, 677–689 (2012).

36. Oluleye, G., Jobson, M. & Smith, R. Process integration of waste heat upgrading technologies. *Process Saf. Environ. Prot.* **103**, 315–333 (2016).

37. Agathokleous, R. *et al.* Waste heat recovery in the EU industry and proposed new technologies. in *Energy Procedia* vol. 161 489–496 (Elsevier Ltd, 2019).

38. Xia, L. *et al.* A review of low-temperature heat recovery technologies for industry processes. *Chinese J. Chem. Eng.* **27**, 2227–2237 (2019).

39. Wallerand, A. S., Kermani, M., Kantor, I. & Maréchal, F. Optimal heat pump integration in industrial processes. *Appl. Energy* **219**, 68–92 (2018).

40. Gaspillo, P. D., Abella, L. C. & Goto, S. Dehydrogenation of 2-Propanol in Reactive Distillation Column for Chemical Heat Pump. *J. Chem. Eng. Japan* **31**, 440–444 (1998).

41. Lee, H., Song, H. K. & Na, B. K. Preparation of 2-propanol dehydrogenation catalysts for chemical heat pump system. *Bull. Chem. Soc. Jpn.* **73**, 1015–1019 (2000).

42. Kapil, A., Bulatov, I., Smith, R. & Kim, J.-K. Site-wide process integration for low grade heat recovery. in *21st European Symposium on Computer Aided Process Engineering* (eds. Pistikoupolos, E. N., Georgiadis, M. C. & Kokossis, A. C.) vol. 29 1859–1863 (Elsevier B.V., 2011).

43. Cacciola, G., Anikeev, V., Recupero, V., Kirillov, V. & Parmon, V. Chemical heat pump using heat of reversible catalytic reactions. *Int. J. Energy Res.* **11**, 519–529 (1987).

44. Chen, K. S. & Hwang, W. C. On the Chemical Heat Pump System and its Second-Law Efficiency. *Energy Convers. Manag.* **28**, 123–127 (1988).

45. Chung, Y., Kim, B.-J., Yeo, Y.-K. & Song, H. K. Optimal design of a chemical heat pump using the 2-propanol/acetone/hydrogen system. *Energy* **22**, 525–536 (1997).

46. Horuz, I. & Kurt, B. Absorption heat transformers and an industrial application. *Renew. Energy* **35**, 2175–2181 (2010).

47. Ogura, H., Yasuda, S., Otsubo, Y. & Mujumdar, A. S. Continuous operation of a chemical heat pump. *Asia-Pacific J. Chem. Eng.* **2**, 118–123 (2007).

48. Paardekooper, S. *et al. Heat Roadmap Europe 4: Quantifying the Impact of Low-carbon Heating and Cooling Roadmpas*. (2018).

49. Kapil, A., Bulatov, I., Smith, R. & Kim, J.-K. Process integration of low grade heat in process industry with district heating networks. *Energy* **44**, 11–19 (2012).

50. Sayegh, M. A. *et al.* Trends of European research and development in district heating technologies. *Renew. Sustain. Energy Rev.* **68**, 1183–1192 (2017).

51. Oluleye, G., Smith, R. & Jobson, M. Modelling and screening heat pump options for the exploitation of low grade waste heat in process sites. *Appl. Energy* **169**, 267–286 (2016).

52. Yin, J., Shi, L., Zhu, M.-S. & Han, L.-Z. Performance analysis of an absorption heat transformer with different working fluid combinations. *Appl. Energy* **67**, 281–292 (2000).

53. Wang, R. Z. *et al.* Heat Pumps for Efficient Low Grade Heat Uses: From Concept to Application. *Therm. Sci. Eng.* **27**, 1–15 (2019).

54. Papapetrou, M., Kosmadakis, G., Cipollina, A., La Commare, U. & Micale, G. Industrial waste heat: Estimation of the technically available resource in the EU per industrial sector, temperature level and country. *Appl. Therm. Eng.* **138**, 207–216 (2018).

55. Kosmadakis, G. Estimating the potential of industrial (high-temperature) heat pumps for exploiting waste heat in EU industries. *Appl. Therm. Eng.* **156**, 287–298 (2019).

56. Panayiotou, G. P. *et al.* Preliminary assessment of waste heat potential in major European industries. *Energy Procedia* **123**, 335–345 (2017).

57. Bianchi, G. *et al.* Estimating the waste heat recovery in the European Union Industry. *Energy, Ecol. Environ.* **4**, 211–221 (2019).

58. Forman, C., Muritala, I. K., Pardemann, R. & Meyer, B. Estimating the global waste heat potential. *Renew. Sustain. Energy Rev.* **57**, 1568–1579 (2016).

59. Eurostat. *Energy data - 2020 edition*. (2020).

60. Karaca, F., Kincay, O. & Bolat, E. Economic analysis and comparison of chemical heat pump systems. *Appl. Therm. Eng.* **22**, 1789–1799 (2002).

61. Spoelstra, S., Haije, W. G. & Dijkstra, J. W. Techno-economic feasibility of high-temperature high-lift chemical heat pumps for upgrading industrial waste heat. *Appl. Therm. Eng.* **22**, 1619–1630 (2002).

62. Ajah, A. *et al.* On the robustness, effectiveness and reliability of chemical and mechanical heat pumps for low-temperature heat source district heating: A comparative simulation-based analysis and evaluation. *Energy* **33**, 908–929 (2008).

63. Demir, H., Agra, Ö. & Atayilmaz, S. Ö. Economical Analysis of a Chemical Heat Pump System for Waste Heat Recovery. in *Proceedings of the World Renewable Energy Congress – Sweden, 8–13 May, 2011, Linköping, Sweden* vol. 57 1545–1551 (2011).

64. Xu, M. *et al.* Technical and economic feasibility of the Isopropanol-Acetone-Hydrogen chemical heat pump based on a lab-scale prototype. *Energy* **139**, 1030–1039 (2017).

65. Deng, N. *et al.* Experimental Research of a New Steam Heat Pump System for Recovering Industrial Waste Heat. *J. Energy Eng.* **143**, 04017035 (2017).

66. Oluleye, G., Jobson, M., Smith, R. & Perry, S. J. Evaluating the potential of process sites for waste heat recovery. *Appl. Energy* **161**, 627–646 (2016).

67. Chan, C. W., Ling-Chin, J. & Roskilly, A. P. A review of chemical heat pumps, thermodynamic cycles and thermal energy storage technologies for low grade heat utilisation. *Appl. Therm. Eng.* **50**, 1257–1273 (2013).

68. Aydin, D., Casey, S. P. & Riffat, S. The latest advancements on thermochemical heat storage systems. *Renew. Sustain. Energy Rev.* **41**, 356–367 (2015).

69. Silva, L. A. P., João, I. M. & Silva, J. M. CHISA 2021 Virtually, 15-18 March. https://secure.confis.cz/chisa2021-virtually/ProgramFin/A.aspx#LBL5 (2021).

70. Silva, L. A. P., João, I. M. & Silva, J. M. Excess-heat recovery and promotion through organic chemical heat pumps (*Submitted*). *Chem. Eng. Technol.* (2021) doi:10.1002/ceat.202100242.

71. Mbaye, M., Aidoun, Z., Valkov, V. & Legault, A. Analysis of chemical heat pumps (CHPs): Basic concepts and numerical model description. *Appl. Therm. Eng.* **18**, 131–146 (1998).

72. Al-mansour, F. & Tomsic, M. Heat Pumps in Industry. *Heat Recover. Syst. CHP* **14**, 51–60 (1994).

73. Aristov, Y. I., Parmon, V. N., Cacciola, G. & Giordano, N. High-temperature chemical heat pump based on reversible catalytic reactions of cyclohexane-dehydrogenation/benzene-hydrogenation: Comparison of the potentialities of different flow diagrams. *Int. J. Energy Res.* **17**, 293–303 (1993).

74. Raldow, W. M. & Wentworth, W. E. Chemical Heat Pumps - A Basic Thermodynamic Analysis. *Sol. Energy* **23**, 75–79 (1979).

75. KlinSoda, I. & Piumsomboon, P. Isopropanol-acetone-hydrogen chemical heat pump: A demonstration unit. *Energy Convers. Manag.* **48**, 1200–1207 (2007).

76. Kitikiatsophon, W. & Piumsomboon, P. Dynamic Simulaton and Control of an Isopropanol-Acetone-Hydrogen Chemical Heat Pump. *ScienceAsia* **30**, 135–147 (2004).

77. Saito, Y., Kameyama, H. & Yoshida, K. Catalyst-assisted chemical heat pump with reaction couple of acetone hydrogenation/2–propanol dehydrogenation for upgrading low-level thermal energy: Proposal and evaluation. *Int. J. Energy Res.* **11**, 549–558 (1987).

78. Kato, Y., Honda, T. & Kanzawa, A. Kinetic measurement on the isobutene/water/tert-butanol chemical heat pump; dehydration of tert-butanol. *Int. J. Energy Res.* **20**, 681–692 (1996).

79. Kato, Y. & Pritchard, C. L. Energy performance analysis of isobutene/water/tert-butanol chemical heat pump. *Chem. Eng. Res. Des.* **78**, 184–191 (2000).

80. Kato, Y., Honda, T. & Kanzawa, A. Study of chemical heat pump with reaction system of isobutene/water/tert-butanol. *Kagaku Kogaku Ronbunshu* **17**, 135–142 (1991).

81. Wentworth, W. E. & Chen, E. Simple thermal decomposition reactions for storage of solar thermal energy. *Sol. Energy* **18**, 205–214 (1976).

82. Kim, T. G., Yeo, Y. K. & Song, H. K. Chemical heat pump based on dehydrogenation and hydrogenation ofi-propanol and acetone. *Int. J. Energy Res.* **16**, 897–916 (1992).

83. Chung, Y., Hong, S. & Song, H. K. A Chemical Reaction Heat Pump System Adopting the Reactive Distillation Process. 742–747 (1996) doi:10.1109/IECEC.1996.553790.

84. Mooksuwan, W. & Kumar, S. Study on 2-propanol/acetone/hydrogen chemical heat pump: endothermic dehydrogenation of 2-propanol. *Int. J. Energy Res.* **24**, 1109–1122 (2000).

85. Kiss, A. A., Landaeta, S. J. F. & Ferreira, C. A. I. Mastering heat pumps selection for energy efficient distillation. *Chem. Eng. Trans.* **29**, 397–402 (2012).

86. Bakhtiari, B., Fradette, L., Legros, R. & Paris, J. Opportunities for the integration of absorption heat pumps in the pulp and paper process. *Energy* **35**, 4600–4606 (2010).

87. Stitou, D., Spinner, B., Satzger, P. & Ziegler, F. Development and comparison of advanced cascading cycles coupling a solid/gas thermochemical process and a liquid/gas absorption process. *Appl. Therm. Eng.* **20**, 1237–1269 (2000).

88. Modla, G. & Lang, P. Heat pump systems with mechanical compression for batch distillation. *Energy* **62**, 403–417 (2013).

89. Sanders, Jr., R. D., Suciu, D. F., Toth, W. J. & Wikoff, P. M. *Survey and assessment of heat of reaction type chemical heat pumps*. (1984).

90. James, N. A., Braun, J. E. & Groll, E. A. The chemical looping heat pump: Thermodynamic modeling. *Int. J. Refrig.* **98**, 302–310 (2019).

91. Wongsuwan, W., Kumar, S., Neveu, P. & Meunier, F. A review of chemical heat pump technology and applications. *Appl. Therm. Eng.* **21**, 1489–1519 (2001).

92. Mert, M. S., Salt, İ., Karaca, F., Mert, H. H. & Bolat, E. Multiple Regression Analysis of Catalytic Dehydrogenation of Isopropanol in a Chemical Heat Pump System. *Chem. Eng. Technol.* **38**, 399–408 (2015).

93. Yan, T., Wang, R. Z., Li, T. X., Wang, L. W. & Fred, I. T. A review of promising candidate reactions for chemical heat storage. *Renew. Sustain. Energy Rev.* **43**, 13–31 (2015).

94. Qu, M., Abdelaziz, O. & Yin, H. New configurations of a heat recovery absorption heat pump integrated with a natural gas boiler for boiler efficiency improvement. *Energy Convers. Manag.* **87**, 175–184 (2014).

95. Tufano, V. Heat recovery in distillation by means of absorption heat pumps and heat transformers. *Appl. Therm. Eng.* **17**, 171–178 (1997).

96. Lazzarin, R. M. Heat Pumps in Industry - I. Equipment. *Heat Recover. Syst. CHP* **14**, 581–597 (1994).

97. Kohlenbach, P. & Ziegler, F. A dynamic simulation model for transient absorption chiller performance. Part I: The model. *Int. J. Refrig.* **31**, 217–225 (2008).

98. Bakhtiari, B., Fradette, L., Legros, R. & Paris, J. Retrofit of absorption heat pumps into manufacturing processes: Implementation guidelines. *Can. J. Chem. Eng.* **88**, 839–848 (2010).

99. Rivera, W., Siqueiros, J., Martínez, H. & Huicochea, A. Exergy analysis of a heat transformer for water purification increasing heat source temperature. *Appl. Therm. Eng.* **30**, 2088–2095 (2010).

100. Rivera, W. Experimental evaluation of a single-stage heat transformer used to increase solar pond's temperature. *Sol. Energy* **69**, 369–376 (2000).

101. Ma, X. *et al.* Application of absorption heat transformer to recover waste heat from a synthetic rubber plant. *Appl. Therm. Eng.* **23**, 797–806 (2003).

102. Cai, J., Li, X., Tao, Y., Huai, X. & Guo, Z. Advances in Organic Liquid-Gas Chemical Heat Pumps. *Chem. Eng. Technol.* **34**, 1603–1613 (2011).

103. Guo, J., Huai, X. & Xu, M. Study on Isopropanol-Acetone-Hydrogen chemical heat pump of storage type. *Sol. Energy* **110**, 684–690 (2014).

104. Xin, F., Xu, M., Huai, X. & Li, X. Study on isopropanol-acetone-hydrogen chemical heat pump: Liquid phase dehydrogenation of isopropanol using a reactive distillation column. *Appl. Therm. Eng.* **58**, 369–373 (2013).

105. Xin, F., Xu, M., Li, X. F. & Huai, X. L. Experimental study of isopropanol dehydrogenation over amorphous alloy raney nickel catalysts. *J. Therm. Sci.* **22**, 613–618 (2013).

106. Abella, L. C., Gaspillo, P.-A. D., Maeda, M. & Goto, S. Kinetic study on the dehydration of tert-butyl alcohol catalyzed by ion exchange resins. *Int. J. Chem. Kinet.* **31**, 854–859 (1999).

107. Knifton, J. F., Sanderson, J. R. & Stockton, M. E. Tert-butanol dehydration to isobutylene via reactive distillation. *Catal. Letters* **73**, 55–57 (2001).

108. Abella, L. C., Gaspillo, P. D., Itoh, H. & Goto, S. Dehydration of tert-Butyl Alcohol in Reactive Distillation. *J. Chem. Eng. Japan* **32**, 742–746 (1999).

109. Gastauer, P. & Prevost, M. Dehydrogenation of isopropanol at low temperatures in the vapor phase as a reaction for a chemical heat pump. *Journal of Chemical Engineering of Japan* vol. 26 580–583 (1993).

110. Xu, M. *et al.* Equilibrium model and performances of an isopropanol-acetone-hydrogen chemical heat pump with a reactive distillation column. *Ind. Eng. Chem. Res.* **52**, 4040–4048 (2013).

111. Huiyuan, W. & Songlin, X. Separation oftert-Butyl Alcohol-Water Mixtures by a Heterogeneous Azeotropic Batch Distillation Process. *Chem. Eng. Technol.* **29**, 113–118 (2006).

112. Dean, J. A. *Lange's Handbook of Chemistry*. (McGraw-Hill Professional, 1998).

113. John, S., Sarah, B. L., Samson, S. J. & Mingqiao, Z. Chemical Heat Pump (CHP) Simulation, Energy and Exergy Analysis. **4**, 53–56 (2017).

114. Guo, J., Huai, X., Li, X. & Xu, M. Performance analysis of Isopropanol-Acetone-Hydrogen chemical heat pump. *Appl. Energy* **93**, 261–267 (2012).

115. Guo, J. & Huai, X. The application of entransy theory in optimization design of Isopropanol-Acetone-Hydrogen chemical heat pump. *Energy* **43**, 355–360 (2012).

116. Guo, J., Huai, X. & Xu, M. Thermodynamic analysis of an isopropanol-acetone-hydrogen chemical heat pump. *Int. J. Energy Res.* **39**, 140–146 (2015).

117. Chen, Q., Wang, M., Pan, N. & Guo, Z. Y. Optimization principles for convective heat transfer. *Energy* **34**, 1199–1206 (2009).

118. Xu, M., Cai, J. & Huai, X. Exergy analysis and performance enhancement of isopropanol-acetone-hydrogen chemical heat pump. *Front. Energy* **11**, 510–515 (2017).

119. Hammond, G. P. & Norman, J. B. Heat recovery opportunities in UK industry. *Appl. Energy* **116**, 387–397 (2014).

120. Feng, X. & Liang, C. Strategy for total energy system retrofit of a chemical plant. *Chem. Eng. Trans.* **35**, 145–150 (2013).

121. Kemp, I. C. *Pinch Analysis and Process Integration*. *Institution of Chemical Engineers* (Elsevier, 2007).

122. Ebrahim, M. & Kawari, A. Pinch technology: an efficient tool for chemical-plant energy and capital-cost saving. *Appl. Energy* **65**, 45–49 (2000).

123. Townsend, D. W. & Linnhoff, B. Heat and power networks in process design - Part I: Criteria for Placement of Heat Engines and Heat Pumps in Process Networks. *AIChE J.* **29**, 742–748 (1983).

124. Townsend, D. W. & Linnhoff, B. Heat and power networks in process design - Part II: Design Procedure for Equipment Selection and Process Matching. *AIChE J.* **29**, 748–771 (1983).

125. Wang, M., Deng, C., Wang, Y. & Feng, X. Exergoeconomic performance comparison, selection and integration of industrial heat pumps for low grade waste heat recovery. *Energy Convers. Manag.* **207**, 112532 (2020).

126. Wallin, E. & Berntsson, T. Integration of Heat Pumps in Industrial Processes. *Heat Recover. Syst. CHP* **14**, 287–296 (1994).

127. Yang, M., Feng, X. & Chu, K. H. Graphical Analysis of the Integration of Heat Pumps in Chemical Process Systems. *Ind. Eng. Chem. Res.* **52**, 8305–8310 (2013).

128. Allen, T. T. *Introduction to engineering statistics and lean six sigma: Statistical quality control and design of experiments and systems*. (Springer, 2006).

129. Montgomery, D. C. *Introduction to Statistical Quality Control*. (John Wiley & Sons, Inc., 2012).

130. Montgomery, D. C. *Design and Analysis of Experiments*. (John Wiley & Sons, Inc., 2017).

131. Pavlov, S. Y., Kulov, N. N. & Kerimov, R. M. Improvement of chemical engineering processes using systems analysis. *Theor. Found. Chem. Eng.* **48**, 117–126 (2014).

132. Towler, G. & Sinnott, R. *Chemical Engineering Design: Principles, Practice and Economics of Plant and Process Design*. (Butterworth-Heinemann, 2008).

133. Maloney, J. O. *Perrys' chemical engineers' handbook: Conversion factors and mathematical symbols*. (McGraw-Hill Professional, 2008).

134. João, I. M. & Silva, J. M. Designing Solutions by a Student Centred Approach: Integration of Chemical Process Simulation with Statistical Tools to Improve Distillation Systems. *Int. J. Eng. Pedagog.* **7**, 4–18 (2017).

135. João, I. M. & Silva, J. M. Designing experiments with Aspen HYSYS simulation to improve distillation systems: Insights from a chemical engineering course. in *2016 2nd International Conference of the Portuguese Society for Engineering Education (CISPEE)* vol. 63 1–10 (IEEE, 2016).

136. Florindo, S. S., João, I. M. & Silva, J. M. Study of Energy Efficient Distillation Columns Usage for Multicomponent Separations through Process Simulation and Statistical Methods. in *24th European Symposium on Computer Aided Process Engineering - ESCAPE 24* (eds. Klemes, J. J., Varbanov, P. S. & Liew, P. Y.) vol. 33 145–150 (Elsevier, 2014).

137. Mendonça, M. V., João, I. M. & Silva, J. M. Azeotropic Distillation Systems: Design and Optimization through simulation with Aspen HYSYS combined with Design of Experiments. in *12th International Chemical and Biological Engineering Conference - CHEMPOR 2014* 14–21 (2014).

138. Daniel, C. Use of Half-Normal Plots in Interpreting Factorial Two-Level Experiments. *Technometrics* **1**, 311–341 (1959).

139. Xu, M., Duan, Y., Xin, F., Huai, X. & Li, X. Design of an isopropanol–acetone–hydrogen chemical heat pump with exothermic reactors in series. *Appl. Therm. Eng.* **71**, 445–449 (2014).

140. Xin, F., Xu, M., Huai, X.-L. & Li, X.-F. Characteristic and kinetic of liquid-phase isopropanol dehydrogenation over Raney nickel catalysts for chemical heat pump. *Appl. Therm. Eng.* **70**, 580–585 (2014).

141. Kato, Y., Nakagawa, N. & Kameyama, H. Study of chemical heat pump with reaction couple of acetone hydrogenation/2-propanol dehydrogenation. Kinetics of the hydrogenation of acetone. *KAGAKU KOGAKU RONBUNSHU* **13**, 714–717 (1987).

142. Duan, Y., Xu, M., Zhou, X. & Huai, X. A structured packed-bed reactor designed for exothermic hydrogenation of acetone. *Particuology* **17**, 125–130 (2014).

143. Walas, S. M., Fair, J. R., Penney, W. R. & Couper, J. R. *Chemical Process Equipment: Selection and Design*. (Butterworth-Heinemann, 1988).

144. Walas, S. M., Fair, J. R., Penney, W. R. & Couper, J. R. *Chemical Process Equipment: Selection and Design*. (Butterworth-Heinemann, 2012).

145. Eurostat. Gas prices for non-household consumers. https://ec.europa.eu/eurostat/databrowser/view/NRG_PC_203__custom_859513/default/table?lang=en (2020).

146. Eurostat. *Energy, transport and environment statistics - 2020 edition*. (2020).

147. The World Bank. *State and Trends of Carbon Pricing 2020*. https://openknowledge.worldbank.org/bitstream/handle/10986/33809/9781464815867.pdf?sequence=4&isAllowed=y (2020).

148. Asen, E. Carbon taxes in Europe. https://taxfoundation.org/carbon-taxes-in-europe-2020/ (2020).

149. The World Bank. Carbon Pricing Dashboard. https://carbonpricingdashboard.worldbank.org/map_data (2020).

150. Farris, P. W., Bendle, N. T., Pfeifer, P. E. & Reibstein, D. J. *Marketing Metrics - The Definitive Guide to Measuring Marketing Performance*. *Wharton School Publishing* (FT Press, 2010).

151. Farris, P. W., Bendle, N. T., Pfeifer, P. E. & Reibstein, D. J. *Key Marketing Metrics - The 50+ metrics every manager needs to know*. (FT Prentice Hall, 2017).

152. Magni, C. A. Average Internal Rate of Return and Investment Decisions: A New Perspective. *Eng. Econ.* **55**, 150–180 (2010).

153. Velo, E., Puigjaner, L. & Recasens, F. Inhibition by product in the liquid-phase hydration of isobutene to tert-butyl alcohol: kinetics and equilibrium studies. *Ind. Eng. Chem. Res.* **27**, 2224–2231 (1988).

154. Novita, F. J., Zou, B.-Y. & Lee, H.-Y. Design and control of a hybrid reactive extraction configuration for the production of tert-butyl alcohol. *J. Clean. Prod.* **239**, 118018 (2019).

155. Lei, Z., Yang, Y., Li, Q. & Chen, B. Catalytic distillation for the synthesis of tert-butyl alcohol with structured catalytic packing. *Catal. Today* **147**, 352–356 (2009).

156. Baiguzin, F. A., Burmistrov, D. A., Kuznetsov, V. A. & Farakhov, M. I. Theoretical description and numerical modelling of dehydration of tert-butanol via reactive distillation at concurrent flow of liquid and vapor phases. *Chem. Eng. Sci.* **200**, 73–79 (2019).

157. Gorak, A. & Olujic, Z. *Distillation: Equipment and Processes*. (Academic Press, 2014).

158. Seader, J. D., Henley, E. J. & Roper, D. K. *Separation Process Principles: Chemical and Biochemical Operations*. (John Wiley & Sons, Inc., 2010).

159. McCabe, W. L., Smith, J. C. & Harriott, P. *Unit Operations of Chemical Engineering*. (McGraw-Hill Professional, 1993).

160. Pardo, P. *et al.* A review on high temperature thermochemical heat energy storage. *Renew. Sustain. Energy Rev.* **32**, 591–610 (2014).

161. Sarbu, I. & Sebarchievici, C. A Comprehensive Review of Thermal Energy Storage. *Sustainability* **10**, 191 (2018).

162. Stengler, J. & Linder, M. Thermal energy storage combined with a temperature boost: An underestimated feature of thermochemical systems. *Appl. Energy* **262**, 114530–114543 (2020).

163. Davies, J., Dolci, F., Klassek-Bajorek, D., Cebolla Ortiz, R. & Weidner, E. *Current status of Chemical Energy Storage Technologies*. (2020) doi:10.2760/280873.

164. Guo, Z. Y., Zhu, H. Y. & Liang, X. G. Entransy-A physical quantity describing heat transfer ability. *Int. J. Heat Mass Transf.* **50**, 2545–2556 (2007).

165. Xu, M. The thermodynamic basis of entransy and entransy dissipation. *Energy* **36**, 4272–4277 (2011).

166. Chen, Q., Liang, X.-G. & Guo, Z.-Y. Entransy theory for the optimization of heat transfer – A review and update. *Int. J. Heat Mass Transf.* **63**, 65–81 (2013).

APPENDICES

Appendix A – Excess Heat Potential in Europe

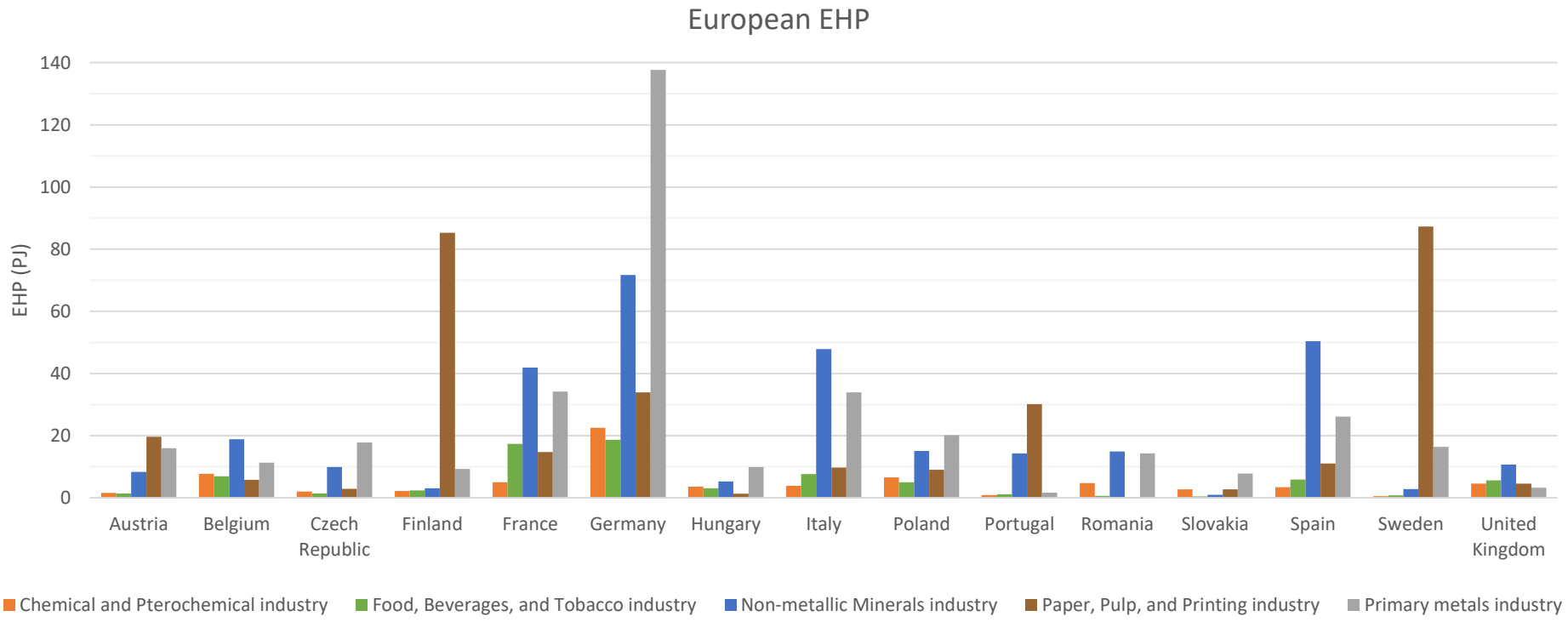

Figure 72 - EHP distribution for the largest industrial sectors in Europe's 15 major energy users

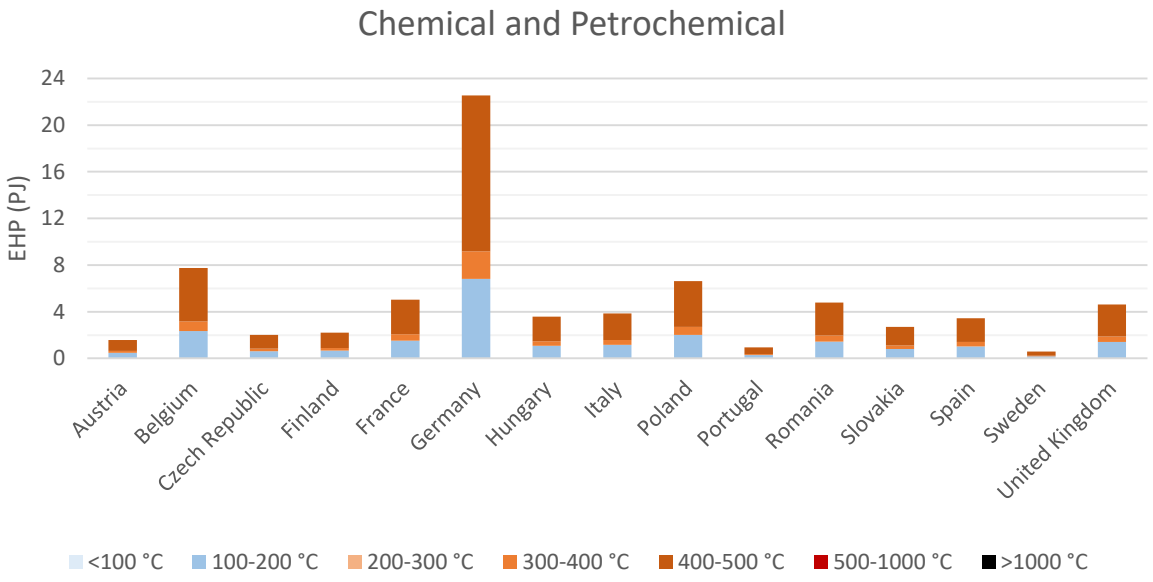

Figure 73 - EHP within the C. & P. industrial sector in Europe

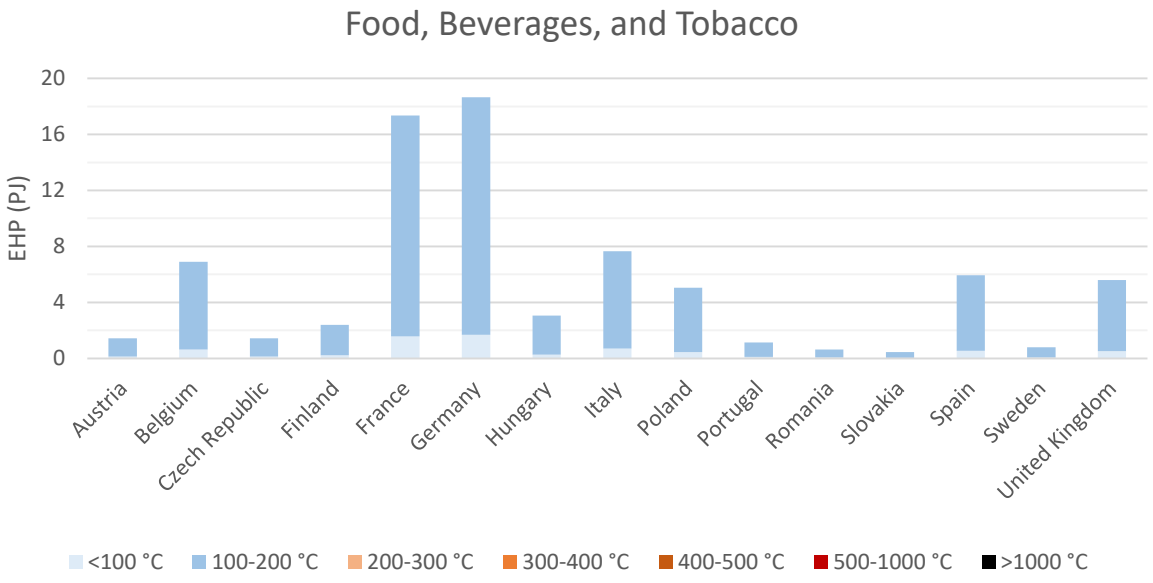

Figure 74 - EHP within the F., B. & T. industrial sector in Europe

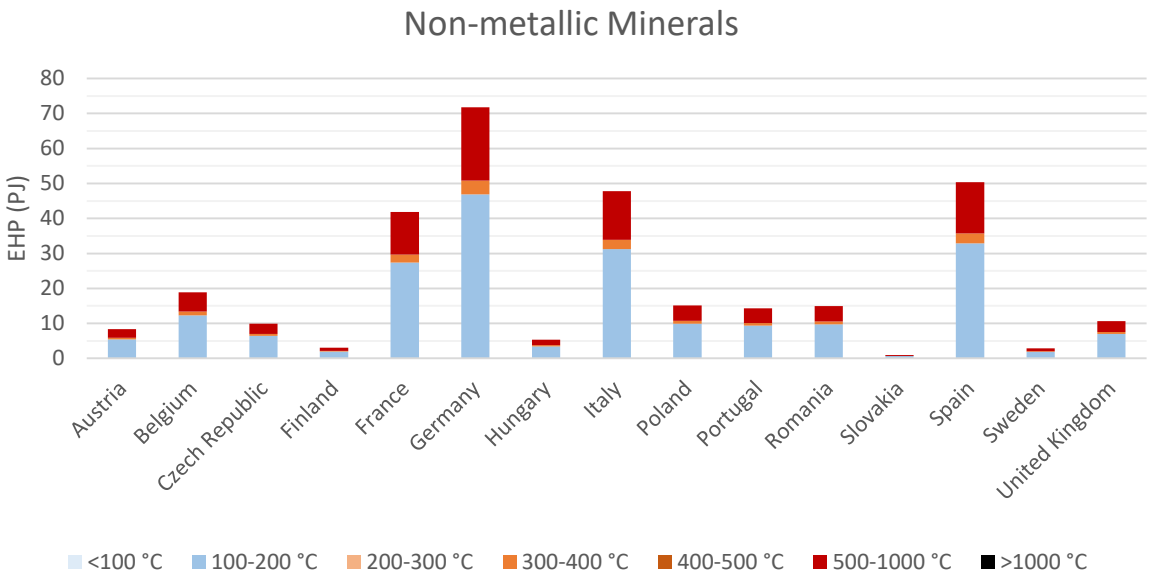

Figure 75 - EHP within the N. M. industrial sector in Europe

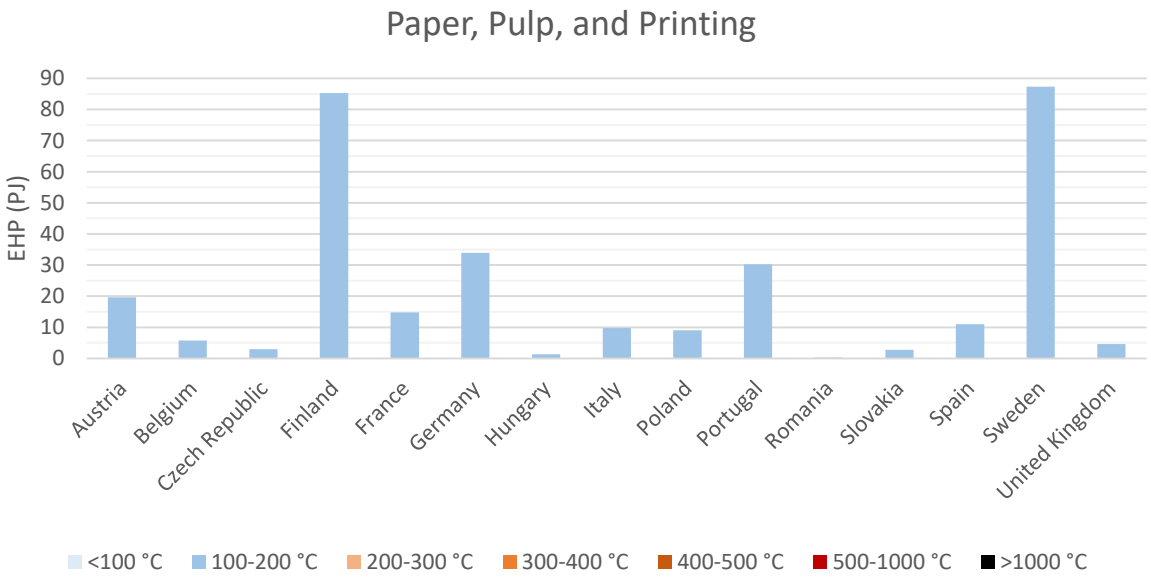

Figure 76 - EHP within the P., P. & P. industrial sector in Europe

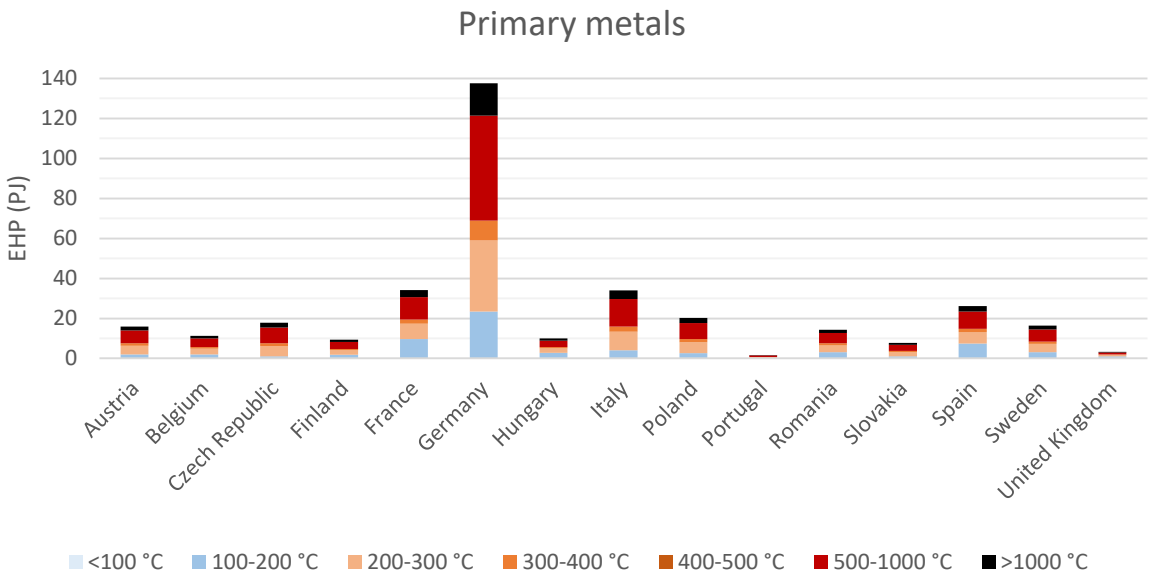

Figure 77 - EHP within the P. M. industrial sector in Europe

Appendix B – Designed Experiments matrices

Table 88 - Matrix used in the 2^2 complete factorial design experiments

		A	B
4	ab	1	1
1	**[1]**	-1	-1
3	**b**	-1	1
2	**a**	1	-1

Table 89 - Matrix used in the 2^3 complete factorial design experiments

		A	B	C
6	ac	1	-1	1
5	**c**	-1	-1	1
1	**[1]**	-1	-1	-1
2	**a**	1	-1	-1
7	bc	-1	1	1
4	ab	1	1	-1
3	**b**	-1	1	-1
8	abc	1	1	1

Table 90 - Matrix used in the 2^4 complete factorial design experiments

		A	B	C	D
9	**d**	-1	-1	-1	1
5	**c**	-1	-1	1	-1
8	abc	1	1	1	-1
2	**a**	1	-1	-1	-1
13	cd	-1	-1	1	1
11	bd	-1	1	-1	1
14	acd	1	-1	1	1
1	**[1]**	-1	-1	-1	-1
16	abcd	1	1	1	1
4	ab	1	1	-1	-1
7	bc	-1	1	1	-1
15	bcd	-1	1	1	1
10	ad	1	-1	-1	1
3	**b**	-1	1	-1	-1
6	ac	1	-1	1	-1
12	abd	1	1	-1	1

Table 91 - Matrix used in the 2^5 complete factorial design experiments

		A	B	C	D	E
30	acde	1	-1	1	1	1
22	ace	1	-1	1	-1	1
27	bde	-1	1	-1	1	1
8	abc	1	1	1	-1	-1
1	**[1]**	-1	-1	-1	-1	-1
14	acd	1	-1	1	1	-1
17	**e**	-1	-1	-1	-1	1
4	ab	1	1	-1	-1	-1
21	ce	-1	-1	1	-1	1
3	**b**	-1	1	-1	-1	-1
13	cd	-1	-1	1	1	-1
19	be	-1	1	-1	-1	1
26	ade	1	-1	-1	1	1
24	abce	1	1	1	-1	1
2	**a**	1	-1	-1	-1	-1
20	abe	1	1	-1	-1	1
29	cde	-1	-1	1	1	1
23	bce	-1	1	1	-1	1
25	de	-1	-1	-1	1	1
5	**c**	-1	-1	1	-1	-1
32	abcde	1	1	1	1	1
6	ac	1	-1	1	-1	-1
9	**d**	-1	-1	-1	1	-1
15	bcd	-1	1	1	1	-1
7	bc	-1	1	1	-1	-1
18	ae	1	-1	-1	-1	1
10	ad	1	-1	-1	1	-1
31	bcde	-1	1	1	1	1
11	bd	-1	1	-1	1	-1
28	abde	1	1	-1	1	1
16	abcd	1	1	1	1	-1
12	abd	1	1	-1	1	-1

Appendix C – Analysis of Variance and Residual Analysis for the Isopropanol/Acetone/Hydrogen system

i. First experiment

Table 92 - Aliasing relationships for a $2_{(IV)}^{8-3}$ FFD

A = BCF = BDG	***AF = BC = DEH***	***DH = BCE = AEF***
B = ACF = ADG	***AG = BD = CEH***	***EF = ADH = BGH***
C = ABF = DFG	***AH = DEF = CEG***	***EG = ACH = BFH***
D = ABG = CFG	***BE = CDH = FGH***	***EH = BCD = ADF = ACG = BFG***
F = ABC = CDG	***BH = CDE = EFG***	***FH = ADE = BEG***
G = ABD = CDF	***CD = FG = BEH***	***GH = ACE = BEF***
AB = CF = DG	***CE = BDH = AGH***	***ABE = CEF = DEG***
AC = BF = EGH	***CG = DF = AEH***	***ABH = CFH = DGH***
AD = BG = EFH	***CH = BDE = AEG***	***ACD = BDF = BCG = AFG***
AE = DFH = CGH	***DE = BCH = AFH***	

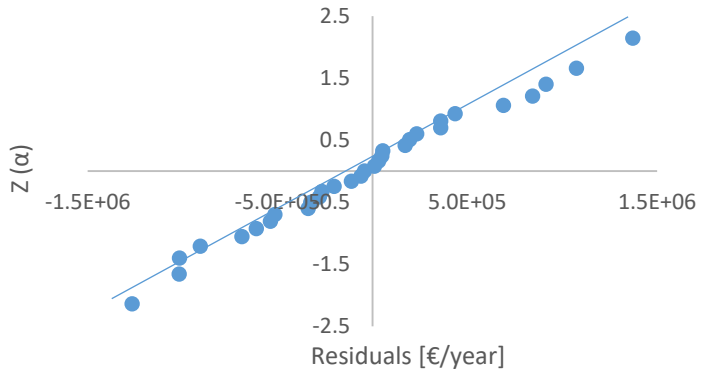

Figure 78 - Residual analysis regarding cost

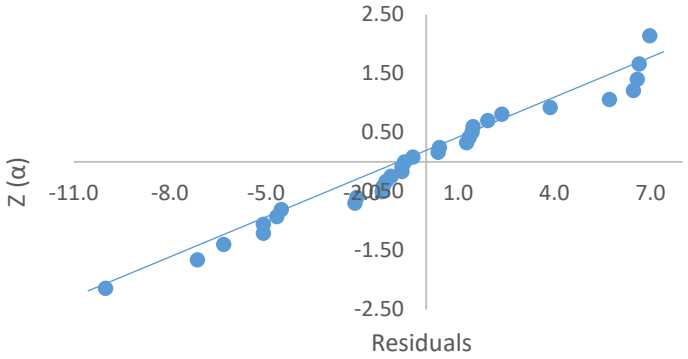

Figure 79 - Residual analysis regarding effectiveness

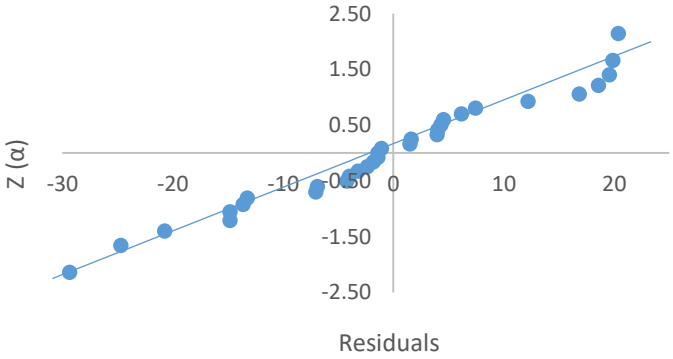

Figure 80 - Residual analysis regarding entransy efficiency

ii. Second experiment

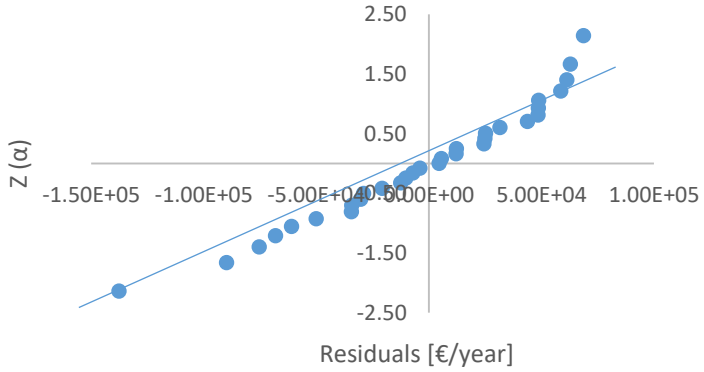

Figure 81 - Residual analysis regarding cost

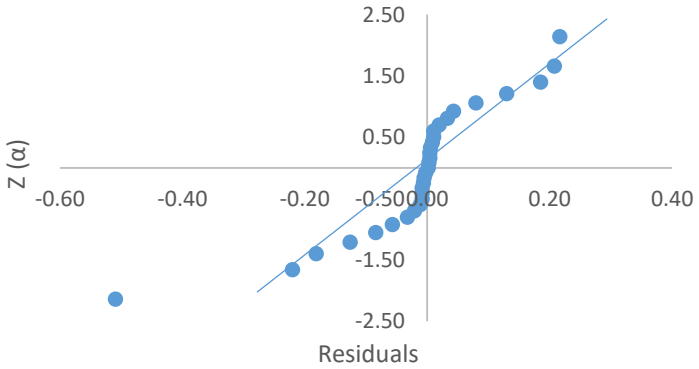

Figure 82 - Residual analysis regarding effectiveness

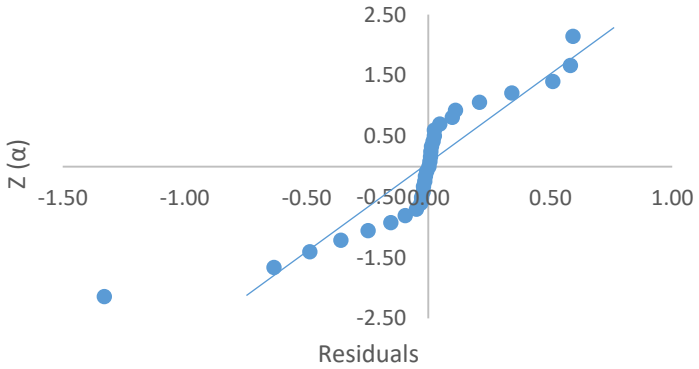

Figure 83 - Residual analysis regarding entransy efficiency

iii. Third experiment

Table 93 - ANOVA results regarding cost

	SS	DF	MS	F_0	
AB	4.60E+10	1	4.60E+10	10.75	
D	8.79E+10	1	8.79E+10	20.57	
BD	8.84E+10	1	8.84E+10	20.67	
B	2.32E+11	1	2.32E+11	54.29	
A	3.43E+11	1	3.43E+11	80.15	F. INV
Error	3.85E+10	10	4.28E+09		4.960

Table 94 - ANOVA results regarding effectiveness

	SS	DF	MS	F_0	
D	0.0012	1	0.00125	7.33	
AB	0.0023	1	0.00235	13.80	
A	0.0024	1	0.00239	14.03	
B	0.0047	1	0.00474	27.82	
C	0.0062	1	0.00620	36.39	F. INV
Error	0.0015	10	0.00017		4.960

Table 95 - ANOVA results regarding entransy efficiency

	SS	DF	MS	F_0	
D	0.007	1	0.00692	5.72	
AB	0.013	1	0.01274	10.53	
C	0.024	1	0.02382	19.70	
B	0.026	1	0.02610	21.58	F. INV
Error	0.012	11	0.00121		4.840

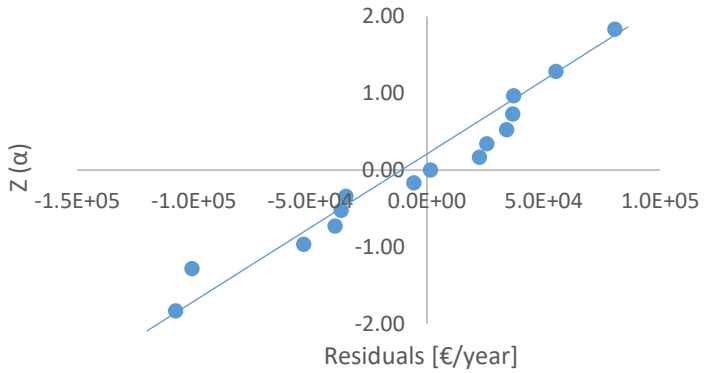

Figure 84 - Residual analysis regarding cost

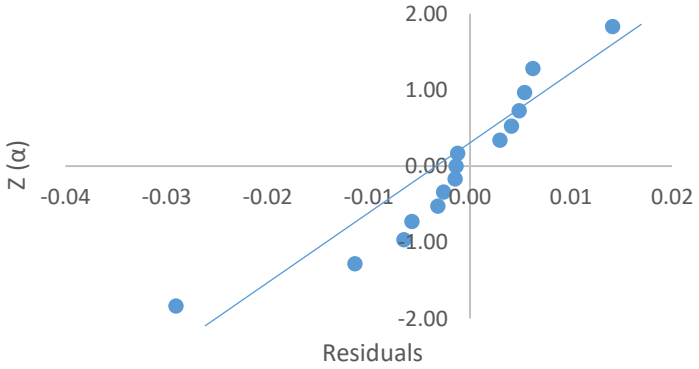

Figure 85 - Residual analysis regarding effectiveness

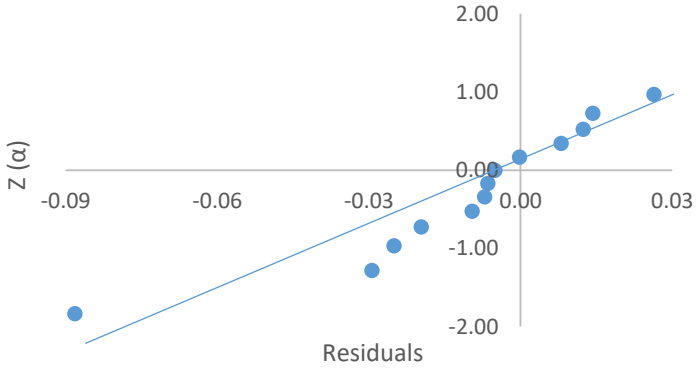

Figure 86 - Residual analysis regarding entransy efficiency

iv. Fourth experiment

Table 96 - ANOVA results regarding effectiveness

	SS	DF	MS	F_0	
B	5.57E-03	1	5.57E-03	385.40	F. INV
Error	1.44E-05	2	1.44E-05		18.51

Table 97 - ANOVA results regarding entransy efficiency

	SS	DF	MS	F_0	
B	2.96E-02	1	2.96E-02	387.08	F. INV
Error	7.66E-05	2	7.66E-05		18.51

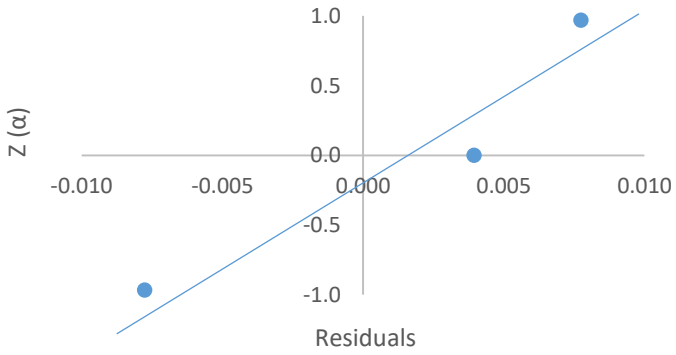

Figure 87 - Residual analysis regarding effectiveness

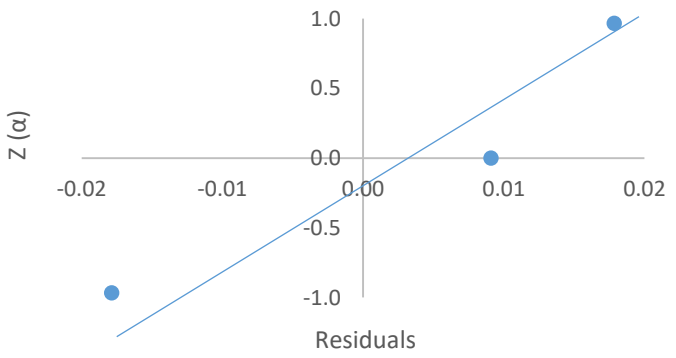

Figure 88 - Residual analysis regarding entransy efficiency

v. Fifth experiment

Table 98 - ANOVA results regarding cost

	SS	DF	MS	F_0	
B	1.11E+10	1	1.11E+10	303.68	
G	2.04E+10	1	2.04E+10	559.64	
E	7.28E+11	1	7.28E+11	19925.46	F. INV
Error	1.10E+08	4	3.65E+07		7.710

Table 99 - ANOVA results regarding effectiveness

	SS	DF	MS	F_0	
G	3.29E-04	1	3.29E-04	42.33	
B	1.12E-03	1	1.12E-03	144.25	F. INV
Error	3.11E-05	5	7.77E-06		6.610

Table 100 - ANOVA results regarding entransy efficiency

	SS	DF	MS	F_0	
G	1.77E-03	1	1.77E-03	42.09	
B	5.97E-03	1	5.97E-03	142.13	F. INV
Error	1.68E-04	5	4.20E-05		6.610

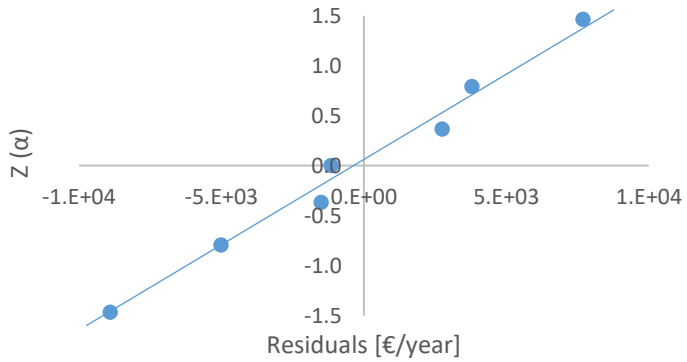

Figure 89 - Residual analysis regarding cost

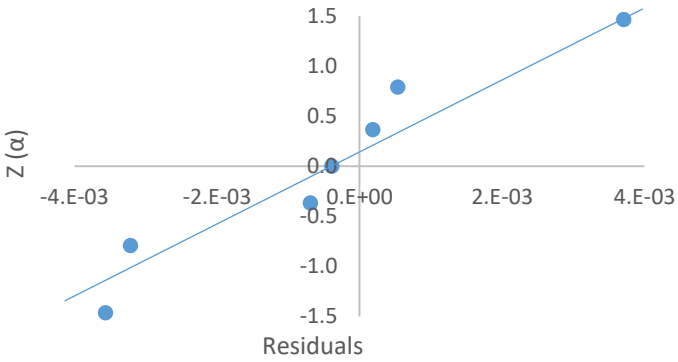

Figure 90 - Residual analysis regarding effectiveness

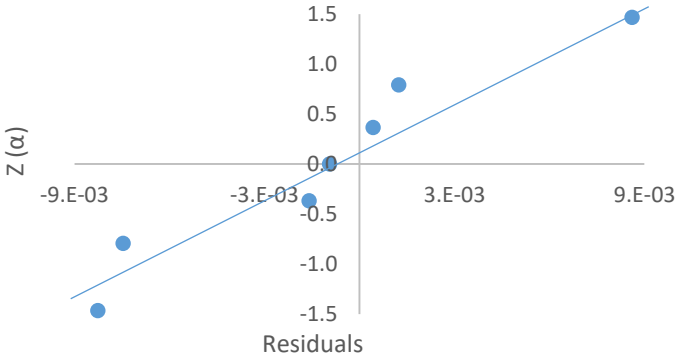

Figure 91 - Residual analysis regarding entransy efficiency

vi. Sixth experiment

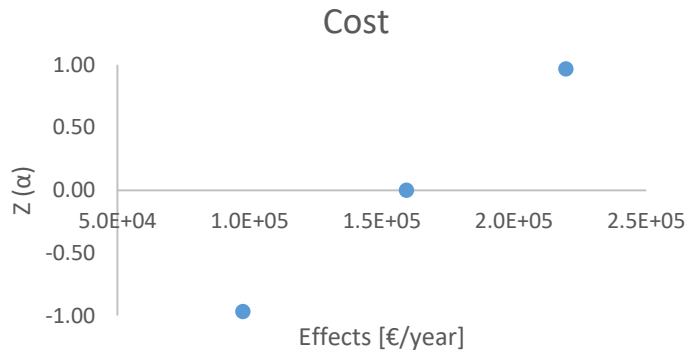

Figure 92 - Normal probability plot of effects regarding cost

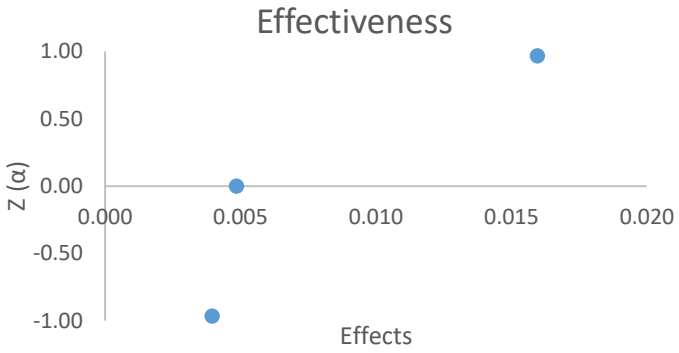

Figure 93 - Normal probability plot of effects regarding effectiveness

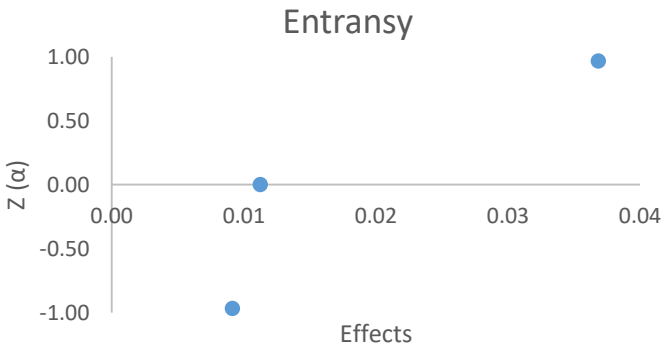

Figure 94 - Normal probability plot of effects regarding entransy efficiency

vii. Seventh experiment

Table 101 - ANOVA results regarding effectiveness

	SS	DF	MS	F_0	
F	2.08E-04	1	2.08E-04	63.86	
FH	2.25E-04	1	2.25E-04	68.97	
H	2.93E-03	1	2.93E-03	900.39	F. INV
Error	9.78E-06	4	3.26E-06		7.710

Table 102 - ANOVA results regarding entransy efficiency

	SS	DF	MS	F_0	
F	1.11E-03	1	1.11E-03	63.82	
FH	1.19E-03	1	1.19E-03	68.79	
H	1.56E-02	1	1.56E-02	900.59	F. INV
Error	5.20E-05	4	1.73E-05		7.710

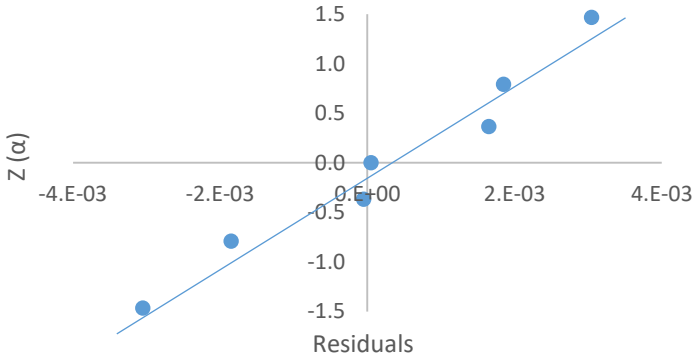

Figure 95 - Residual analysis regarding effectiveness

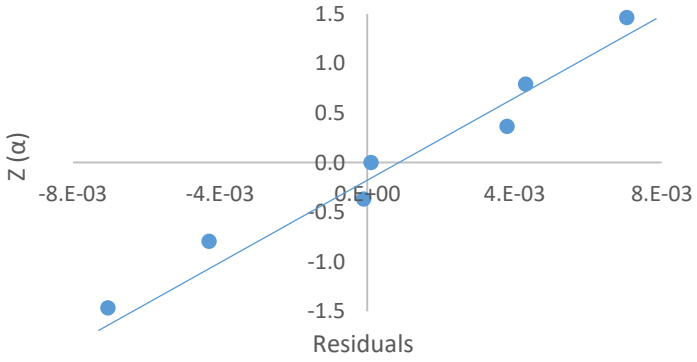

Figure 96 - Residual analysis regardinge entransy efficiency

viii. Exothermic reactors in series

Table 103 - Simulation results for two exothermic reactors in series

Experiment		**Cost [M€/year]**	**Performance**		**Heat [kW]**				**ECst**
Assay		Total	Effectiveness	Entransy	Q_L	Q_{H1}	Q_{H2}	Total	-
	Original	1.045	0.2557	0.6065	7821.00	2000.00	-	-	30.38%
2	A1	1.759	0.2758	0.6679	6603.00	1620.33	202.23	1822.57	61.73%
	A2	1.874	0.2766	0.6931	6613.33	1414.67	415.40	1830.07	63.90%
	A3	1.955	0.2516	0.6416	7879.33	1772.00	209.46	1981.46	62.74%
18	B1	1.650	0.2643	0.6572	6557.33	1427.00	295.03	1722.03	61.88%
	B2	2.184	0.2671	0.6677	7200.67	1738.67	178.66	1917.33	68.01%
	B3	1.753	0.2726	0.6777	7337.67	1641.33	353.40	1994.73	58.49%
	Original	1.306	0.3057	0.7055	8090.00	2473.00	-	-	35.69%
6	A1	2.130	0.3170	0.7661	7657.33	2056.67	367.93	2424.60	55.38%
	A2	2.274	0.3229	0.8055	7137.33	1681.67	622.83	2304.50	60.31%
	A3	2.135	0.2981	0.7587	8275.00	2101.00	366.13	2467.13	57.33%
1	B1	1.955	0.3095	0.7677	7605.33	1853.00	496.57	2349.57	60.97%
	B2	2.356	0.3148	0.7846	7401.33	2005.00	317.00	2322.00	64.59%
	B3	2.228	0.3137	0.7780	8063.00	1981.33	543.33	2524.67	47.47%

Experiment		Cost [M€/year]	Performance			Heat [kW]			ECst
Assay		Total	Effectiveness	Entransy	Q_L	Q_{H1}	Q_{H2}	Total	-
	Original	1.393	0.2915	0.6726	8660.00	2524.00	-	-	30.91%
5	A1	2.109	0.3053	0.7379	7905.67	2044.33	364.07	2408.40	58.35%
	A2	2.262	0.3108	0.7752	7457.00	1686.33	631.20	2317.53	62.60%
	A3	2.070	0.2813	0.7161	8767.33	2101.00	366.13	2467.13	57.73%
3	B1	2.004	0.2991	0.7415	7871.67	1845.33	501.07	2346.40	56.13%
	B2	2.281	0.3006	0.7493	7756.67	2005.00	317.00	2322.00	63.87%
	B3	2.156	0.2977	0.7384	8501.67	1981.33	543.33	2524.67	58.69%
	Original	1.273	0.2631	0.6071	8547.00	2248.00	-	-	33.92%
3	A1	1.844	0.2840	0.6863	7780.00	1876.00	330.30	2206.30	58.07%
	A2	1.982	0.2953	0.7381	7178.33	1587.00	533.03	2120.03	62.61%
	A3	1.949	0.2593	0.6599	8555.67	1893.00	325.43	2218.43	56.40%
12	B1	1.986	0.2790	0.6923	7660.33	1698.33	429.13	2127.47	57.08%
	B2	2.209	0.2802	0.6985	7677.33	1848.00	293.43	2141.43	62.68%
	B3	1.580	0.2794	0.6936	8176.33	1809.67	466.20	2275.87	57.31%

Experiment		**Cost [M€/year]**	**Performance**		**Heat [kW]**				**ECst**
Assay		Total	Effectiveness	Entransy	Q_L	Q_{H1}	Q_{H2}	Total	-
	Original	1.488	0.3422	0.7896	7601.00	2601.00	-	-	36.18%
7	A1	2.238	0.3699	0.8924	6927.33	2094.67	466.63	2561.30	58.08%
	A2	2.413	0.3749	0.9331	6784.33	1799.33	743.70	2543.03	61.21%
	A3	2.331	0.3499	0.8892	7773.67	2229.00	491.67	2720.67	57.34%
5	B1	2.120	0.3612	0.8944	7197.67	1976.33	619.70	2596.03	55.33%
	B2	2.514	0.3671	0.9130	7040.00	2134.33	443.50	2577.83	62.47%
	B3	2.348	0.3664	0.9073	7247.67	2012.33	638.80	2651.13	58.83%

ix. Flash separator vs Distillation column

Table 104 - Inlet temperature, total number of trays, feed tray, and pressure results for the distillation column
(T_{in} = 80 °C, Trays = 10, Feed tray = middle of the column, and Pressure = 1.00 atm, unless otherwise specified)

T_{in}	Trays	Feed Tray	Pressure	Cost [M€/year]	Performance		Heat [kW]			ECst
(°C)	-	-	(atm)	Total	Effectiveness	Entransy	Q_L	Q_r	Q_H	-
80.0				2.603	0.3119	0.5880	10010	5281	3987	44.24%
70.0				2.613	0.3055	0.5760	10010	5592	3989	44.46%
60.0				2.622	0.2992	0.5642	10010	5905	3989	44.64%
50.0				2.624	0.2911	0.5488	10010	6334	3989	44.58%
40.0				2.705	0.2378	0.4468	10010	9923	3990	46.35%
	26			2.616	0.3145	0.5954	10010	4952	3989	44.52%
	24			2.612	0.3146	0.5963	10010	4948	3989	44.43%
	22			2.609	0.3148	0.5972	10010	4946	3988	44.37%
	20			2.605	0.3149	0.5979	10010	4947	3988	44.29%
	18			2.602	0.3149	0.5983	10010	4955	3988	44.22%
	16			2.598	0.3148	0.5983	10010	4974	3987	44.13%
	14			2.595	0.3145	0.5973	10010	5015	3987	44.07%
	12			2.597	0.3138	0.5947	10010	5100	3988	44.11%
	10			2.600	0.3119	0.5880	10010	5281	3987	44.19%

T_{in}	Trays	Feed Tray	Pressure	Cost [M€/year]	Performance		Heat [kW]			ECst
(°C)	-	-	(atm)	Total	Effectiveness	Entransy	Q_L	Q_r	Q_H	-
	8			2.617	0.3082	0.5725	9986	5700	3981	44.54%
	6			2.708	0.2999	0.5350	9889	6750	3950	46.94%
	14	3		2.626	0.3073	0.5709	9959	5674	3974	44.85%
	14	5		2.602	0.3122	0.5897	9972	5192	3976	44.35%
	14	7		2.595	0.3145	0.5973	10010	5015	3987	44.07%
	14	9		2.594	0.3154	0.6001	10050	4958	3999	43.90%
	14	11		2.631	0.3089	0.5695	10070	5731	4007	44.56%
			1.00	2.603	0.3119	0.5880	10010	5281	3987	44.24%
			1.20	2.321	0.3232	0.5654	10000	5578	3988	37.48%
			1.40	1.844	0.3348	0.5442	9992	5874	3984	21.28%
			1.60	1.703	0.3473	0.5244	9980	6178	3980	14.99%
			1.80	1.496	0.3614	0.5057	9966	6488	3976	3.23%

Appendix D – Heat production using natural gas *vs* the Isopropanol/Acetone/Hydrogen chemical heat pump system's best solutions

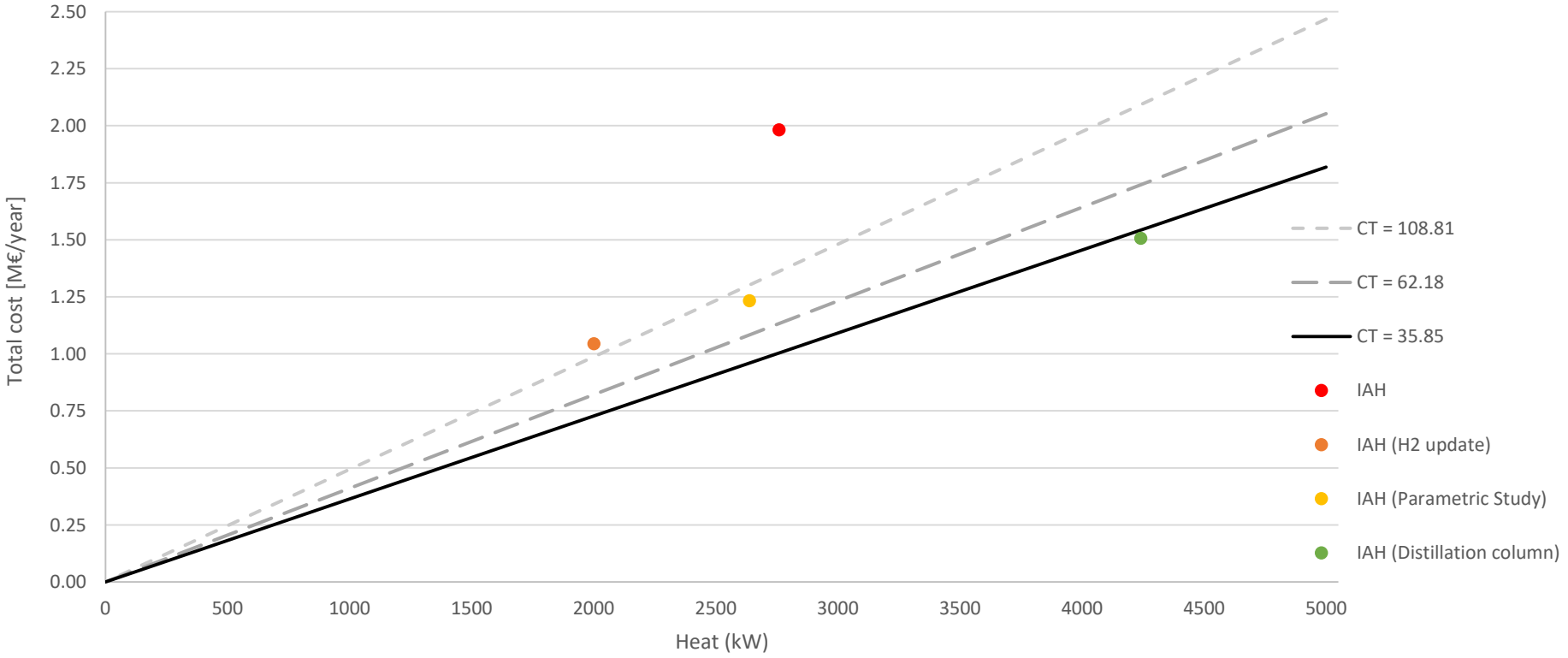

Figure 97 - Natural gas' heat production cost variation with different carbon tax values, and evolution of the IAH system's best solutions

Appendix E – Isopropanol/Acetone/Hydrogen system's schematics with 2 and 3 exothermic reactors

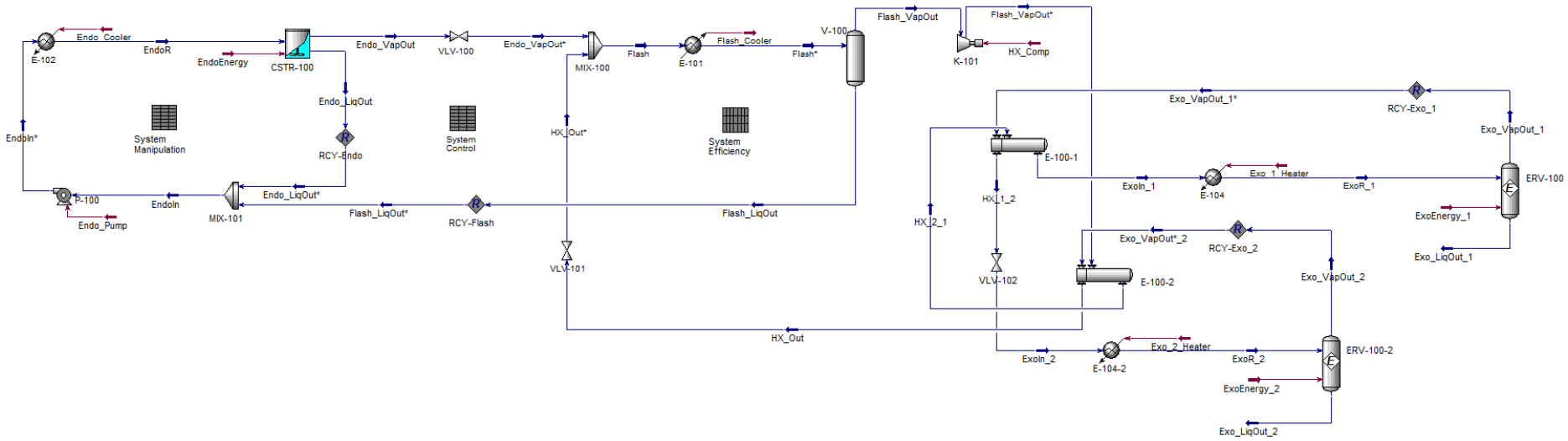

Figure 98 - IAH system with two exothermic reactors

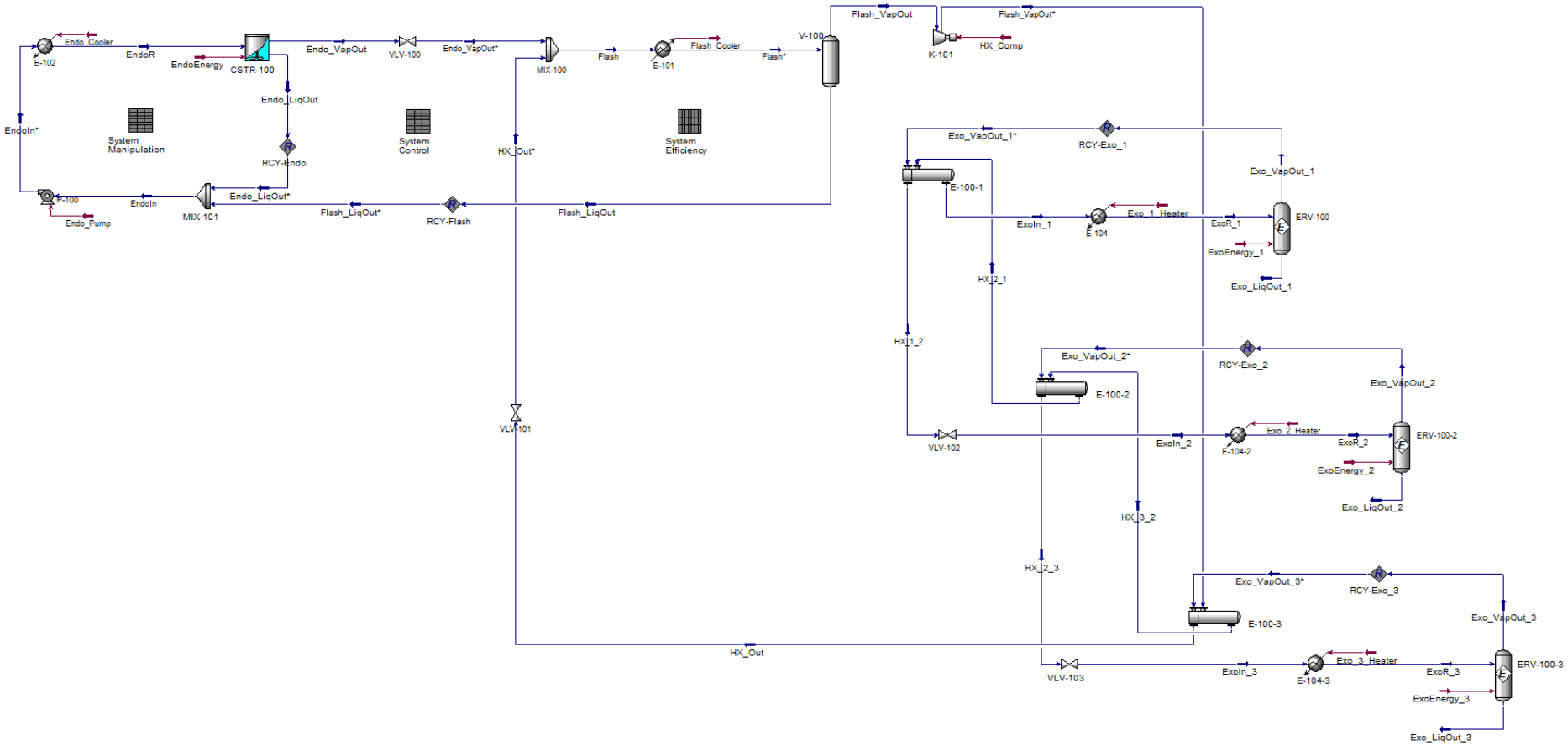

Figure 99 - IAH system with three exothermic reactors

Appendix F – Analysis of Variance and Residual Analysis for the *tert*-Butanol/Isobutene/Water system

i. First experiment

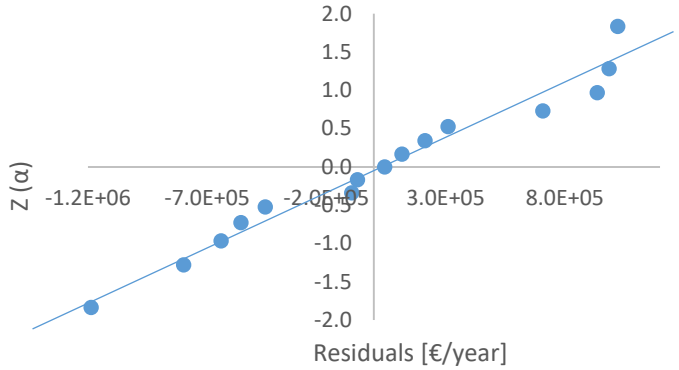

Figure 100 - Residual analysis regarding cost

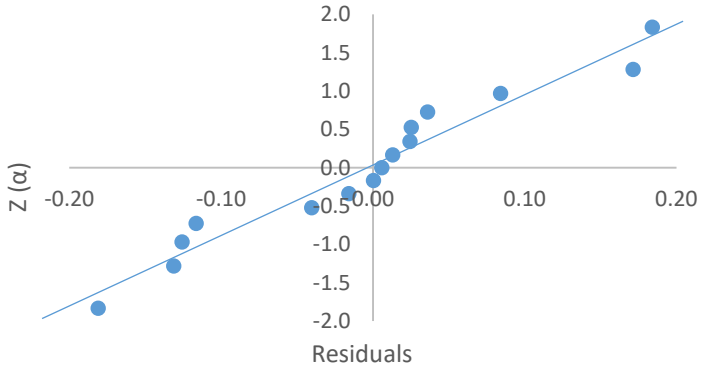

Figure 101 - Residual analysis regarding effectiveness

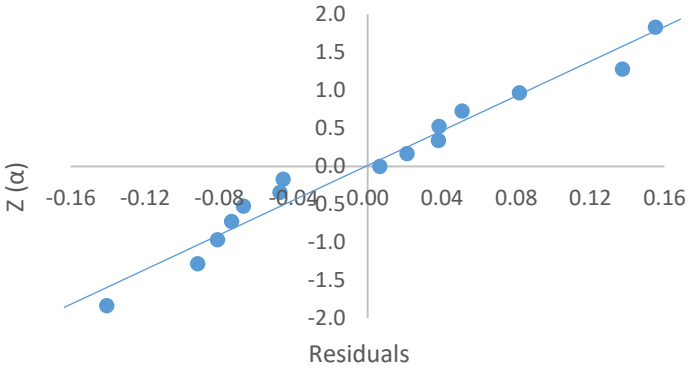

Figure 102 - Residual analysis regarding entransy efficiency

ii. Second experiment

Table 105 - Aliasing relationships for a $2_{(IV)}^{9-4}$ FFD

A = BJO = BCG = BDM	***AO = BJ = CMN = DGN***
B = AJO = ACG = ADM	***BN = GMO = CJM = DGJ = CDO***
C = ABG = GJO = MDG	***CN = AMO = BJM = BDO = ADJ***
D = ABM = JMO = CGM	***CO = AMN = GJ = BDN***
G = ABC = CJO = CDM	***DG = ANO = BJN = CM***
J = ABO = CGO = DMO	***DO = AGN = JM = BCN***
M = ABD = DJO = CDG	***DN = AGO = BGJ = BCO = ACJ***
O = ABJ = CJG = DJM	***GM = BNO = AJN = CD***
AB = JO = CG = DM	***GN = BMO = AJM = ADO = BDJ***
AC = MNO = BG = DJN	***GO= BMN = CJ = AND***
AD = GNO = BM = CJN	***JN = AGM = BCM = BDG = ACD***
AG = JMN = BC = DNO	***MN = BGO = AGJ = ACO = BCJ***
AJ = GMN = BO = CDN	***MO = BGN = ACN = DJ***
AM = GJN = CNO = BD	***NO = BGM = ACM = ADG = BCD***
AN = GJM = HMO = GJO = CDJ	***ABN = JNO = CGN = DMN***

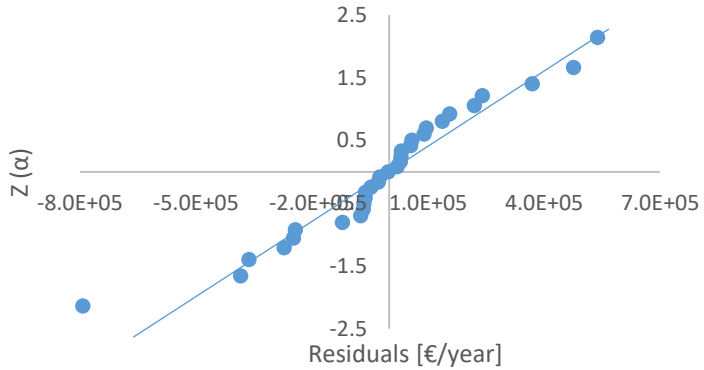

Figure 103 - Residual analysis regarding cost

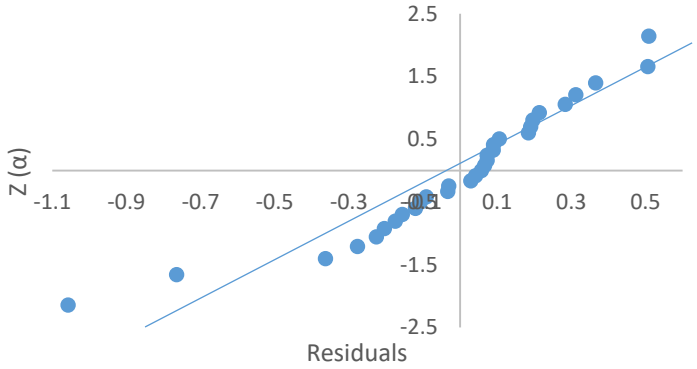

Figure 104 - Residual analysis regarding effectiveness

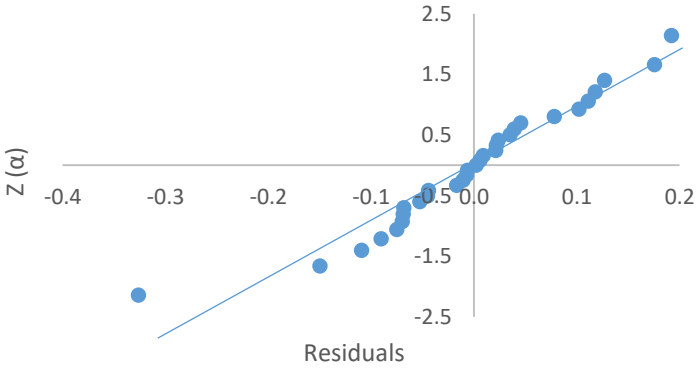

Figure 105 - Residual analysis regarding entransy efficiency

iii. Third experiment

Table 106 - ANOVA results regarding cost

	SS	DF	MS	F_0	
ON	1.518E+11	1	1.518E+11	4.735	
OGC	1.625E+11	1	1.625E+11	5.070	
N	2.964E+11	1	2.964E+11	9.247	
NC	3.148E+11	1	3.148E+11	9.821	
AN	3.329E+11	1	3.329E+11	10.387	
ANC	3.783E+11	1	3.783E+11	11.805	
OC	3.845E+11	1	3.845E+11	11.997	
GN	4.371E+11	1	4.371E+11	13.638	
AGC	5.633E+11	1	5.633E+11	17.574	
AONC	6.896E+11	1	6.896E+11	21.516	
G	1.061E+12	1	1.061E+12	33.110	F. INV
Error	6.090E+11	20	3.205E+10		4.351

Table 107 - ANOVA results regarding effectiveness

	SS	DF	MS	F_0	
AC	0.582	1	0.582	4.628	
OC	0.805	1	0.805	6.407	
NC	0.854	1	0.854	6.796	
C	1.366	1	1.366	10.869	
A	3.023	1	3.023	24.049	
G	3.459	1	3.459	27.521	
AN	6.908	1	6.908	54.957	F. INV
Error	2.891	24	0.126		4.260

Table 108 - ANOVA results regarding entransy efficiency

	SS	DF	MS	F_0	
NC	0.081	1	0.081	4.455	
AN	0.103	1	0.103	5.673	
OC	0.105	1	0.105	5.814	
G	0.268	1	0.268	14.770	
N	0.421	1	0.421	23.223	F. INV
Error	0.453	26	0.018		4.225

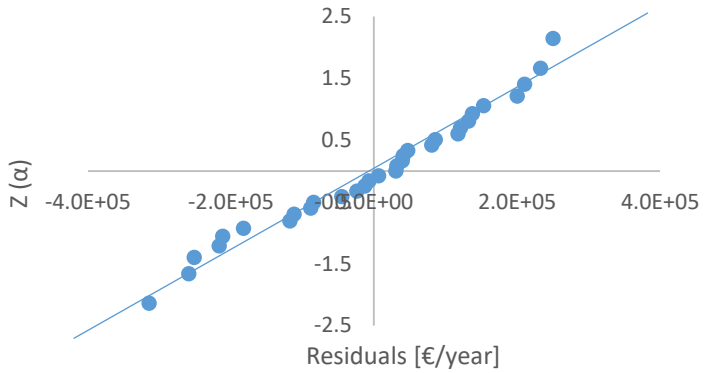

Figure 106 - Residual analysis regarding cost

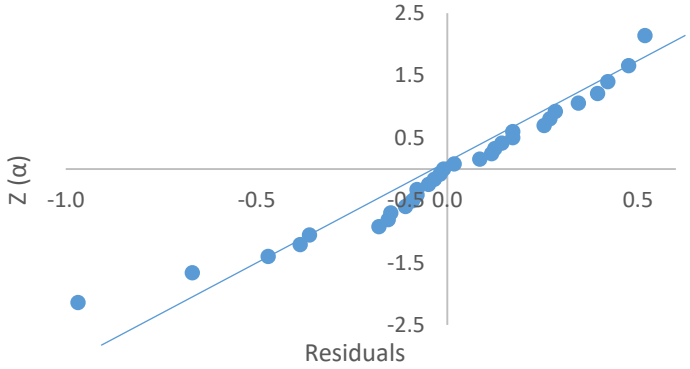

Figure 107 - Residual analysis regarding effectiveness

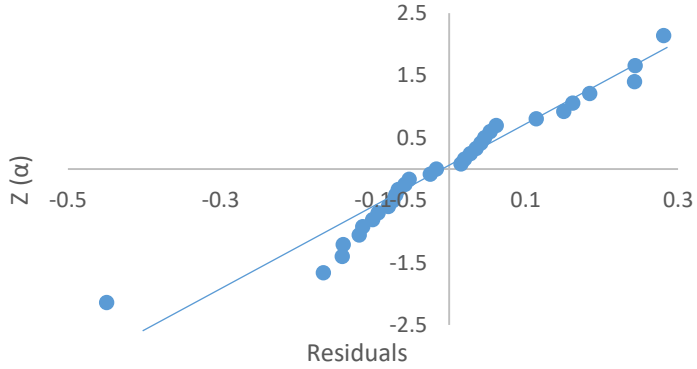

Figure 108 - Residual analysis regarding entransy efficiency

iv. Fourth experiment

Table 109 - ANOVA results regarding cost

	SS	DF	MS	F_0	
KHG	1.21E+12	1	1.21E+12	5.805	
H	3.05E+12	1	3.05E+12	14.681	
HG	3.80E+12	1	3.80E+12	18.260	
KG	4.18E+12	1	4.18E+12	20.106	
G	1.25E+13	1	1.25E+13	60.286	F. INV
Error	1.87E+12	10	2.08E+11		4.960

Table 110 - ANOVA results regarding effectiveness

	SS	DF	MS	F_0	
H	0.6217	1	0.62173	13.179	
GE	0.7491	1	0.74909	15.878	
K	0.8436	1	0.84364	17.882	
KE	0.9584	1	0.95844	20.316	
KGE	1.1578	1	1.15778	24.541	
KG	1.2023	1	1.20231	25.485	
HGE	2.5632	1	2.56320	54.331	F. INV
Error	0.3302	8	0.04718		5.320

Table 111 - ANOVA results regarding entransy efficiency

	SS	DF	MS	F_0	
H	0.0540	1	0.05397	18.371	
GE	0.0622	1	0.06221	21.175	
K	0.0850	1	0.08505	28.946	
KE	0.0861	1	0.08607	29.294	
KG	0.1053	1	0.10525	35.823	
KGE	0.1086	1	0.10855	36.947	
HGE	0.2473	1	0.24728	84.165	F. INV
Error	0.0206	8	0.00294		5.320

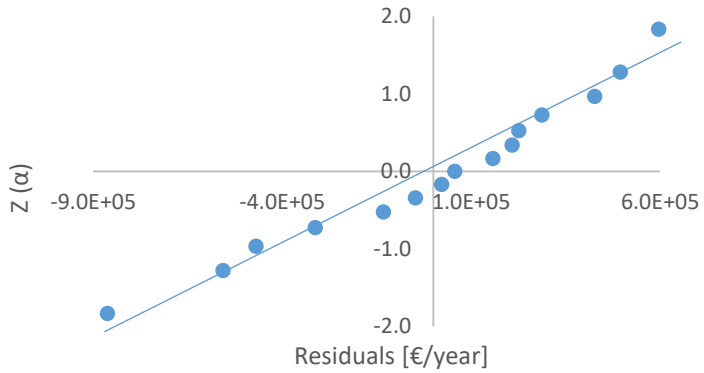

Figure 109 - Residual analysis regarding cost

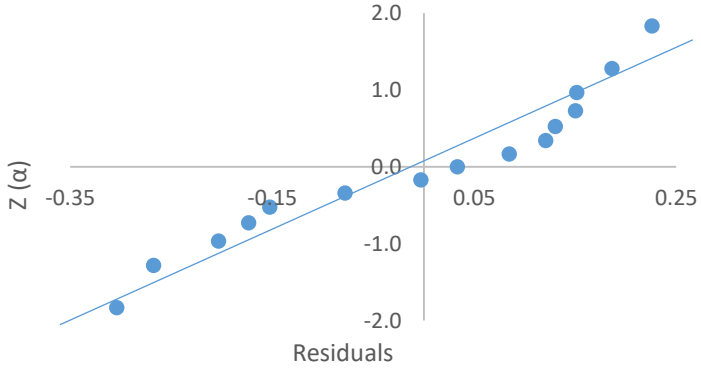

Figure 110 - Residual analysis regarding effectiveness

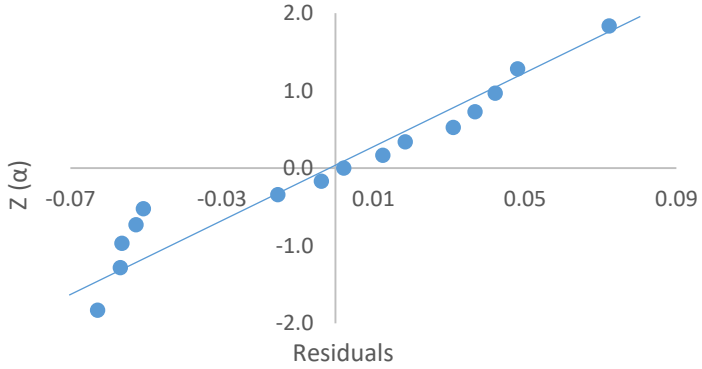

Figure 111 - Residual analysis regarding entransy efficiency

v. Fifth experiment

Table 112 - ANOVA results regarding cost

	SS	DF	MS	F_0	
JG	7.14E+11	1	7.14E+11	5.766	
JM	1.23E+12	1	1.23E+12	9.902	
G	3.36E+12	1	3.36E+12	27.107	F. INV
Error	1.36E+12	12	1.24E+11		4.750

Table 113 - ANOVA results regarding effectiveness

	SS	DF	MS	F_0	
JM	0.5027	1	0.50268	7.689	
HJM	0.6997	1	0.69973	10.703	
G	0.8940	1	0.89397	13.674	F. INV
Error	0.7192	12	0.06538		4.750

Table 114 - ANOVA results regarding entransy efficiency

	SS	DF	MS	F_0	
JGM	0.0317	1	0.03175	5.165	
JM	0.0541	1	0.05409	8.801	
HJM	0.0826	1	0.08264	13.446	
G	0.1028	1	0.10277	16.721	F. INV
Error	0.0615	11	0.00615		4.840

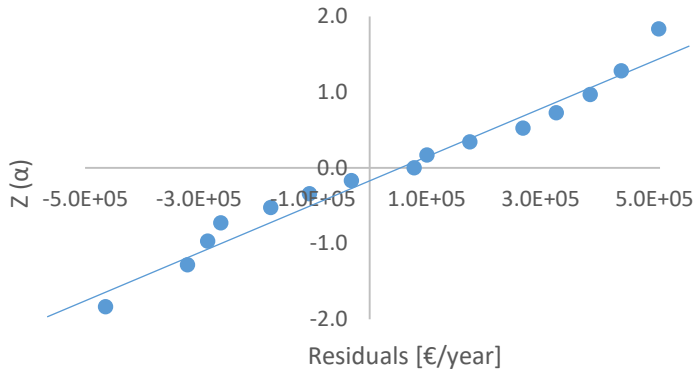

Figure 112 - Residual analysis regarding cost

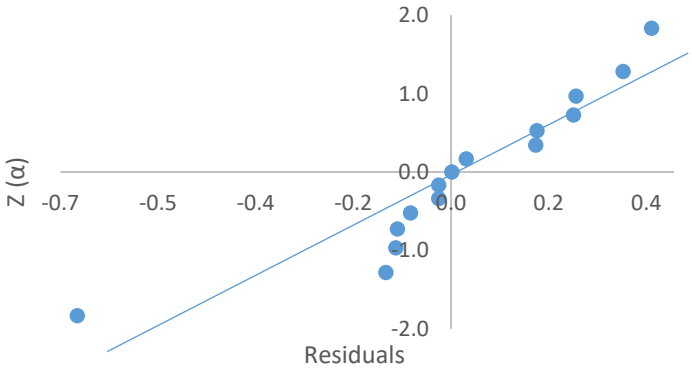

Figure 113 - Residual analysis regarding effectiveness

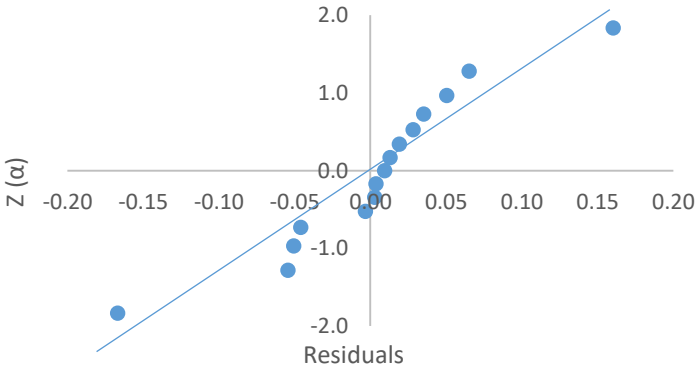

Figure 114 - Residual analysis regarding entransy efficiency

Appendix G – CHISA 2021's abstract

Excess-heat recovery and upgrade: Chemical heat pumps for a lower carbon footprint

L.A.P. Silva,[a] I.M. João,[a,b] J.M. Silva[a,c]
[a] ISEL - Instituto Superior de Engenharia de Lisboa, Instituto Politécnico de Lisboa, R. Cons. Emídio Navarro, 1959 007 Lisboa, Portugal, a40673@alunos.isel.pt
[b] CEG-IST, Instituto Superior Técnico, Universidade de Lisboa, Av. Rovisco Pais, 1049-001 Lisboa, Portugal, ijoao@deq.isel.ipl.pt
[c] CQE, Instituto Superior Técnico, Universidade de Lisboa, Av. Rovisco Pais, 1049-001 Lisboa, Portugal, jmsilva@deq.isel.ipl.pt.

The present work aims to study two distinct chemical heat pumps (CHP), utilizing different systems (isopropanol/acetone/hydrogen [IAH] and tert-butanol/isobutene/water [*t*B/iB]), in order to compare these regarding both their energetic and exergetic efficiencies, among any other relevant efficiency metrics deemed interesting and/or noteworthy. This work's importance is made clear through the understanding that the implementation of these technologies (heat recovery and upgrade) makes a 7-12% reduction in global CO2 emissions possible, solely from primary fuel consumption displacement.[1]

CHPs are a technology that enables heat recovery and upgrading by taking advantage of catalytically reversible chemical reaction systems, decreasing primary fuel consumption, which results in a carbon footprint reduction. These are sure to revolutionize the current state of the energetic world, offering advantages such as high efficiencies, without mechanical work input or electrical power consumption,[2–4] large operating conditions and temperature elevation/heat promotion capabilities, allowing for a design that fits the user's requirements and needs,[5, 6] more compact systems that do not require heavy thermal insulation, given its characteristics,[5, 7, 8] the fact that most usable reactions are very common in the existing commercial chemical industries,[5, 6] and the possibility of energy storage,[3, 7, 8] among others.

Apart from all the technical benefits associated with CHPs, the environmental advantages, such as the use of mostly harmless chemical species, for which the handling technology and expertise are extremely well-known, and the aforementioned decrease in negative atmospheric emissions, should not be disregarded as the world's present status begs for immediate action in favor of all manner of climate-change mitigation adjustments done to both our day-to-day lives and to the overall production system.[1, 2, 6, 7, 9]

In conjunction with the environmental and technical advantages listed above, the resulting economic benefits also serve as a major driving-force that firmly promotes the interest in the solution dealt with in the present work.

Given the somewhat complex nature of the systems dealt with in this work, a brief general description is not entirely uncalled for and, as such, will be provided below, as will some fundamental characteristics of the systems that shall be addressed.

Regarding the CHP schematic presented in figure 1, low-temperature (TL) excess-heat is supplied to the endothermic reactor (RL), promoting the decomposition reaction and the resulting mixture is separated in the distillation column (DC). Afterwards, the gaseous mixture is fed to the exothermic reactor (RH), where the recombination reaction yields the original reactant and releases high temperature (TH) upgraded heat. The heat exchanger (HX) present in the system is responsible for pre-heating the exothermic reactor's feed stream. The excess-

heat utilized in these systems serves two purposes, driving the endothermic reaction and the separation process, the latter being the driving-force for the continuously operating system. Recent investigation has focused its attention on the use of reactive distillation structures to obviate some catalyst deactivation observed in the simpler system.[3, 4, 8–10]

The work herein described is being developed through the use of simulation software (*e.g.* ASPEN HYSYS), which enables the study of different operating conditions, such as reactor pressure, source and sink temperatures (table 1), and even different system configurations such as the use of a reactive distillation setup. The baseline problem for the comparison at hand consists in upgrading 1 MW of excess-heat from about 60/80 °C to circa 110/130 °C. After an initial convergence was obtained utilizing the classical model and enough data was obtained, both systems were assembled according to a reactive distillation arrangement and a new round of assays, under the same conditions as the first, were carried out. With this, the optimal operating conditions were determined for each system, as well as the best possible pairing between a given excess-heat source's temperature and the system that is able to upgrade the aforementioned heat to the required temperature, under the greatest energetic and exergetic efficiencies.

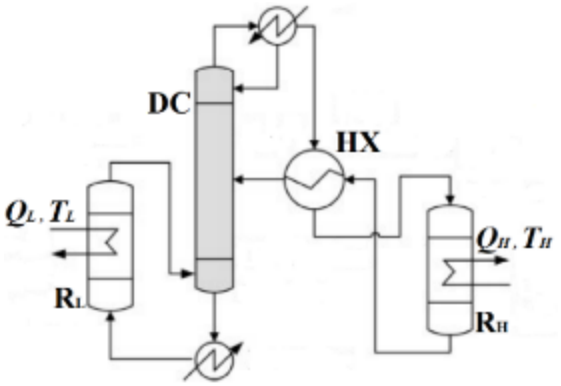

Figure 1 - Liquid-gas continuous-type CHP flow diagram[8]

Table 1 - Organic reaction systems' most relevant characteristics pertaining to the present work[8]

Reaction system		IAH	*t*B/*i*B
Endothermic reaction	Temperature [°C]	~80	~70
	Pressure [atm]	~1	~1
Exothermic reaction	Temperature [°C]	~200	~110
	Pressure [atm]	~1	~1
Reaction heat [kJ/mol]		100.4	56.6

References

1. G. Oluleye, R. Smith, M. Jobson, Appl. Energy. 169, 267–286 (2016).
2. S. Fujii, H. Kameyama, K. Yoshida, D. Kunii, J. Chem. Eng. Japan. 10, 224–228 (1977).
3. Y. Saito, H. Kameyama, K. Yoshida, Int. J. Energy Res. 11, 549–558 (1987).
4. Y. Chung, B.-J. Kim, Y.-K. Yeo, H. K. Song, Energy. 22, 525–536 (1997).
5. R. D. Sanders, Jr., D. F. Suciu, W. J. Toth, P. M. Wikoff, "Survey and assessment of heat of reaction type chemical heat pumps" (Idaho National Engineering Laboratory, 1984).
6. Y. I. Aristov, V. N. Parmon, G. Cacciola, N. Giordano, Int. J. Energy Res. 17, 293–303 (1993).
7. W. Wongsuwan, S. Kumar, P. Neveu, F. Meunier, Appl. Therm. Eng. 21, 1489–1519 (2001).
8. J. Cai, X. Li, Y. Tao, X. Huai, Z. Guo, Chem. Eng. Technol. 34, 1603–1613 (2011).
9. W. Kitikiatsophon, P. Piumsomboon, ScienceAsia. 30, 135–147 (2004).
10. I. KlinSoda, P. Piumsomboon, Energy Convers. Manag. 48, 1200–1207 (2007).